

University of Alberta

**FUNCTIONAL ANALYSES OF WEST NILE VIRUS-
HOST INTERACTIONS**

by

Zaikun Xu

A thesis submitted to the Faculty of Graduate Studies and Research in partial
fulfillment of the requirements for the degree of

Doctor of Philosophy

Department of Cell Biology

©Zaikun Xu

Fall, 2013

Edmonton, Alberta

Permission is hereby granted to the University of Alberta Libraries to reproduce single copies of this thesis and to lend or sell such copies for private, scholarly or scientific research purposes only. Where the thesis is converted to, or otherwise made available in digital form, the University of Alberta will advise potential users of the thesis of these terms.

The author reserves all other publication and other rights in association with the copyright in the thesis and, except as herein before provided, neither the thesis nor any substantial portion thereof may be printed or otherwise reproduced in any material form whatsoever without the author's prior written permission.

Abstract

West Nile virus (WNV) is a neurotropic, blood-borne flavivirus that can cause serious neurological disease in humans and animals. While significant progress has been made in identifying virus-encoded pathogenic determinants, very little is known regarding how these viral proteins interact with host cell proteins. Recent evidence suggests that in addition to its structural role in packaging genomic RNA, the WNV capsid protein plays important roles in virus host interactions and therefore, characterizing the interactions between capsid and cellular proteins should contribute to our understanding of WNV disease and may even reveal targets for antiviral therapy. Through an extensive yeast two-hybrid screen, I identified DDX56, a novel WNV capsid-interacting nucleolar RNA helicase. Experimental analyses revealed DDX56 is not required for production of viral RNA or proteins, however, WNV virions secreted from DDX56-depleted cells are 100 times less infectious than those produced in normal cells. Collectively, these data suggest that DDX56 is critical for assembly of infectious WNV virions possibly by facilitating the packaging of viral RNA.

I also investigated how WNV infection affects tight junctions in polarized cells with the goal of understanding how the virus breaches the blood-brain barrier to gain access to the central nervous system. While a number of recent studies have documented that WNV infection negatively impacts the barrier function of tight junctions, the intracellular mechanism by which this occurs is poorly understood. Using a coordinated approach to understand the direct effects of WNV infection on tight junction proteins in both epithelial and endothelial

cells, I discovered that WNV infection results in endocytosis of a specific subset of tight junction membrane proteins including claudin-1 and JAM-1 followed by microtubule-based transport to and degradation in lysosomes. Further studies into this process could lead to therapeutic treatments that block viral spread and/or design of attenuated vaccine strains.

Acknowledgements

First and foremost, I would like to offer my sincerest gratitude to my supervisor, Dr. Tom Hobman, for the continuous support of my Ph.D study and research, for his patience, motivation, enthusiasm, and immense knowledge. His valuable advice helped me in all the time of research and writing of this thesis. I could not have imagined having a better advisor and mentor for my Ph.D study. I can't say thank you enough for his tremendous support and help. Without his encouragement and guidance these projects would not have materialized.

Second, I would like to show my greatest appreciation to past and present the members of the Hobman lab, including Matt, Eileen, Valeria, Shangmei, Jae, Steven, Carolina, Justin, Jungsook, Yang, Joaquin, and Anh. Your technical support, assistance and helpful discussions were vital for the success of the projects.

Furthermore, I would like to express my warm and sincere thanks to my supervisory committee: Dr. Richard Wozniak and Dr. James Smiley for their encouragement, insightful comments, and hard questions during my Ph.D career. Their excellent scientific ideas and expertise have made a remarkable contribution to my projects. I would also like to express my gratitude for Dr. Rodney Russell and Dr. David Marchant for taking the time to read my thesis and for serving on my examining committee at the defense.

Finally, I would like to give my special thanks to my family: my wife Ran Chen and my son Shawn Zihan Xu. Words fail me to express my appreciation to Ran whose patient love, persistent confidence in me, and selfless efforts to the

family has taken the load off my shoulder. I want to thank my wife for all the support that she gave me during the years I have been working on this thesis. Without her constant help and sacrifice this thesis would not have been completed. I owe my loving thanks to my son, Shawn, who has been the most valuable gift in my life, and who has reminded me of more important things of life than work.

Table of Contents

Chapter 1: Introduction	1
1.1 History and epidemiology of West Nile virus	2
1.2 Classification and clinical importance of the family Flaviviridae	6
1.3 Genome and proteins of WNV	7
1.4 Structure of the WNV virion	13
1.5 The WNV replication cycle	14
1.6 Neuroinvasion by WNV	17
1.6.1 Breakdown of the blood-brain barrier (BBB)	17
1.6.1.1 Host proteins that alter the BBB permeability	18
1.6.1.2 Degradation of tight junction proteins	21
1.6.2 Host immune response to infection	22
1.6.3 Determinants of neuroinvasion on the viral structural proteins	23
1.7 Multifunctional capsid proteins of flaviviruses	24
1.7.1 Non-structural functions of the WNV capsid protein	34
1.7.1.1 Modulation of apoptosis	35
1.7.1.2 Modulation of signaling pathways	38
1.7.1.3 Inhibition of antiviral activity	39
1.7.1.4 Antiviral effects of host proteins that interact with capsid	40
1.8 Objectives of study	41
Chapter 2: Materials and Methods	42
2.1 Materials	43
2.1.1 Reagents	43
2.1.2 Commonly used Buffers and Solutions	46
2.1.3 Yeast strains and media	48
2.1.4 Oligonucleotides	48
2.1.5 Antibodies	52
2.1.6 Cell lines and viruses	55
2.1.6.1 Cell lines	55
2.1.6.2 Viruses	55
2.2 Methods	55
2.2.1 Molecular Biology	55
2.2.1.1 Isolation of plasmid DNA from Escherichia coli	55
2.2.1.2 Polymerase chain reaction (PCR)	56
2.2.1.3 Restriction endonuclease digestion	56
2.2.1.4 Agarose gel electrophoresis	56
2.2.1.5 Purification of DNA fragments	56
2.2.1.6 Ligation of DNA	57
2.2.1.7 Transformation of Escherichia coli	57
2.2.2 Construction of recombinant plasmids	57

2.2.2.1 Capsid expression plasmids	58
2.2.2.2 DDX56 expression plasmids	58
2.2.2.3 RNAi-resistant and DEAD box mutants of DDX56	59
2.2.2.4 DDX56 N- and C-terminal constructs	60
2.2.3 Yeast two-hybrid Screening	60
2.2.4 Cell culture and transfection	61
2.2.4.1 Cell line maintenance	61
2.2.4.2 Transient transfection of cell lines	61
2.2.5 RNA interference	62
2.2.6 Virology techniques	63
2.2.6.1 Virus infection	63
2.2.6.2 Pelleting of WNV virions by ultracentrifugation	63
2.2.6.3 WNV plaque assay	64
2.2.6.4 RV plaque assay	64
2.2.6.5 Preparation and use of lentiviruses	65
2.2.6.5.1 Production and use of lentiviruses encoding WNV capsid	65
2.2.6.5.2 Production of lentiviruses for expression of DDX56 mutants	65
2.2.6.5.3 Production of lentiviruses for knocking down DDX56	66
2.2.7 Microscopy	66
2.2.7.1 Indirect Immunofluorescence	66
2.2.8 Protein gel electrophoresis and detection	67
2.2.8.1 Preparation of protein samples	67
2.2.8.2 Sodium dodecyl-sulphate polyacrylamide gel electrophoresis (SDS-PAGE)	68
2.2.8.3 Immunoblot analysis	68
2.2.8.4 Detection of horseradish peroxidase-conjugated secondary antibodies	69
2.2.8.5 Detection of fluorophore-conjugated secondary antibodies	69
2.2.9 Biochemical analysis of protein-protein interactions	70
2.2.9.1 Co-immunoprecipitations	70
2.2.9.2 GST pull-down assay	71
2.2.10 RNA techniques	72
2.2.10.1 RNA isolation	72
2.2.10.2 Quantitative PCR analysis for viral RNA	73
2.2.10.3 Semi-quantitative PCR analysis for DDX56 mRNA	74
2.2.10.4 Quantitative PCR analysis for tight junction protein genes	74
Chapter 3: The capsid-binding nucleolar helicase DDX56 is important for infectivity of West Nile virus	77
3.1 Rationale	78
3.2 Results	83

3.2.1	The nucleolar helicase DDX56 interacts with the WNV capsid protein	83
3.2.2	WNV infection results in depletion of the nucleolar pool of DDX56	90
3.2.3	WNV infection induces proteasome-dependent degradation of DDX56	96
3.2.4	DDX56 is important for infectivity of WNV virions	103
3.2.5	Depletion of DDX56 does not affect replication of WNV RNA or protein synthesis	108
3.2.6	DDX56 is important for assembly of infectious WNV particles	110
3.3	Summary	113
Chapter 4: The helicase activity of DDX56 is required for its role in assembly of infectious West Nile virus particles		114
4.1	Rationale	115
4.2	Results	116
4.2.1	Construction of RNAi-resistant forms of DDX56 mutants	116
4.2.2	DEAD box mutants are correctly targeted to the nucleolus	121
4.2.3	Helicase activity of DDX56 is important for infectivity of WNV	123
4.2.4	Helicase activity of DDX56 is important for packaging viral RNA into virions	127
4.2.5	Over-expression of the capsid-binding region of DDX56 reduces infectivity of WNV	129
4.3	Summary	138
Chapter 5: West Nile virus infection causes endocytosis of a specific subset of tight junction membrane proteins		139
5.1	Rationale	140
5.2	Results	141
5.2.1	WNV infection results in degradation of the tight junction membrane proteins claudin-1 and JAM-1	141
5.2.2	Dynamin and microtubules are required for WNV-induced degradation of claudin-1 and JAM-1	147
5.2.3	Dengue virus infection does not affect tight junction membrane proteins	154
5.2.4	Expression of WNV capsid protein does not cause degradation of tight junction membrane proteins	157
5.3	Summary	162
Chapter 6: Discussion		163
6.1	Overview	164
6.2	Cellular helicases as antiviral targets	165

6.2.1	A role for DDX56 in assembly of infectious WNV virions	165
6.2.2	DDX56 as an antiviral target for WNV or other flaviviruses	172
6.2.2.1	Examples of host RNA helicases that have been considered for antiviral therapy	174
6.2.2.2	DDX56, a potential antiviral target for WNV and/or other flaviviruses?	177
6.3	Mechanism by which WNV causes failure of tight junctions	179
6.4	Future Directions	186
	References	187

List of Tables

Table 1.1 Host cell proteins that have been reported to interact with flavivirus capsid proteins	26
Table 2.1 Commercial sources of materials, chemicals, and reagents	43
Table 2.2 Molecular size standards	45
Table 2.3 DNA/RNA modifying enzymes	45
Table 2.4 Multi-component systems	45
Table 2.5 Detection systems	45
Table 2.6 Buffers and Solutions	46
Table 2.7 Oligonucleotides	48
Table 2.8 Primary antibodies	52
Table 2.9 Secondary antibodies	54
Table 3.1 22 host proteins that have been identified to interact with the WNV capsid protein by yeast two-hybrid screen	80

List of Figures

Figure 1.1 Schematic representation of WNV genome organization and polyprotein processing	12
Figure 1.2 The WNV replication cycle	16
Figure 3.1 Nucleolar helicase DDX56 was identified as a binding partner of WNV capsid by yeast two-hybrid screen	84
Figure 3.2 The WNV capsid protein interacts with DDX56 in mammalian cells	86
Figure 3.3 WNV capsid protein forms a stable complex with endogenous DDX56	88
Figure 3.4 The WNV capsid colocalizes with DDX56 in the nucleoli	91
Figure 3.5 WNV infection results in depletion of the nucleolar pool of DDX56	93
Figure 3.6 Rubella and Dengue viruses do not induce loss of nucleolar DDX56	95
Figure 3.7 WNV infection induces proteasome-dependent degradation of DDX56	98
Figure 3.8 WNV infection causes relocalization of DDX56 from the nucleus to cytoplasm	101
Figure 3.9 siRNA-mediated depletion of DDX56 affects infectivity of WNV virions	104
Figure 3.10 shRNA-mediated depletion of DDX56 decreases WNV titers	107
Figure 3.11 Depletion of DDX56 does not affect WNV viral RNA and protein production	109
Figure 3.12 DDX56 is important for assembly of infectious WNV particles	111
Figure 3.13 DDX56 is not required for replication of Rubella virus	112

or assembly of infectious virions

Figure 4.1 Construction of RNAi-resistant forms of DDX56 with mutations in the DEAD box motif	117
Figure 4.2 Expression of RNAi-resistant DDX56 mutants in stable cell lines depleted of endogenous DDX56	119
Figure 4.3 Mutations in the DEAD box site of DDX56 do not affect targeting to the nucleolus	121
Figure 4.4 Absence of DDX56 helicase activity does not affect WNV replication	124
Figure 4.5 Helicase activity of DDX56 is important for WNV infectivity	127
Figure 4.6 Helicase activity of DDX56 is important for packaging genomic RNA into WNV particles	128
Figure 4.7 The C-terminus of DDX56 binds to the WNV capsid protein in transfected cells	130
Figure 4.8 The C-terminus of DDX56 binds to the WNV capsid protein in infected cells	133
Figure 4.9 Nucleolar targeting information of DDX56 is contained in the C-terminal 329 amino acid residues	134
Figure 4.10 Expression of the capsid-binding region of DDX56 reduces infectivity of WNV	136
Figure 5.1 WNV infection results in loss of claudin-1 and JAM-1 proteins in epithelial and endothelial cells	144
Figure 5.2 WNV infection leads to increased transcription of multiple tight junction genes	146
Figure 5.3 WNV-induced degradation of claudin-1 and JAM-1 requires dynamin and microtubules	149
Figure 5.4 Internalization of claudin-1 is blocked by disrupting microtubules or inhibiting dynamin function	152
Figure 5.5 Internalization of JAM-1 is blocked by disrupting microtubules or inhibiting dynamin function	153

Figure 5.6 DENV infection does not affect tight junctions	155
Figure 5.7 Expression of capsid in the absence of other WNV proteins does not cause degradation of tight junction proteins	158
Figure 5.8 WNV capsid expression does not affect localization of claudin-1 or JAM-1	160

List of Nomenclature and Abbreviations

μ	micro ($\times 10^{-6}$)
A	amperes
A549	human alveolar basal epithelial 549 cells
AP-1	activator protein-1
ATP	adenosine triphosphate
ATPase	adenosine triphosphatase
BAF	bafilomycin A
BBB	blood-brain barrier
BHK-21	baby hamster kidney-21 cells
bp	base pair
BSA	bovine serum albumin
C	capsid
CACO-2	human colon carcinoma cells
cDNA	complementary deoxyribonucleic acid
CNS	central nervous system
CSI	conserved sequence I
Ct	threshold cycle
CT	C-terminus
DAPI	4',6-diamidino-2-phenylindole
DAXX	death associated protein 6
DCs	dendritic cells

DENV	dengue virus
DMEM	Dulbecco's modified Eagle's medium
DMSO	dimethyl sulphoxide
DNA	deoxyribonucleic acid
DNase	deoxyribonuclease
dNTPs	deoxyribonucleotide triphosphate
DOX	doxycycline
Drak2	death-associated protein kinase-related apoptosis-inducing kinase 2
dsRNA	double-stranded ribonucleic acid
DTT	dithiothreitol
E	envelope
EDTA	ethylenediaminetetraacetic acid
EF1 α	elongation factor α
ER	endoplasmic reticulum
FBS	fetal bovine serum
fH	complement regulatory protein factor H
g	gram
<i>g</i>	gravitational force
GFP	green fluorescent protein
GP	glycine– proline
GST	glutathione-S-transferase
HBV	hepatitis B virus
HCV	hepatitis C virus

HEK293T	human embryonic kidney 293T cells
HEPES	4-(2-hydroxyethyl)-1-piperazineethanesulphonic acid
HIV-1	human immunodeficiency virus 1
HRP	horseradish peroxidase
HUVEC	human umbilical vein endothelial cells
ICAM-1	intercellular adhesion molecule 1
IgG	immunoglobulin G
IF	immunofluorescence
IP	immunoprecipitation
IP-10	IFN- γ -inducible protein 10
JAM	junctional adhesion molecules
JEV	japanese encephalitis virus
kDa	kilo ($\times 10^3$) Daltons
LDs	lipid droplets
LMB	leptomycin B
m	milli ($\times 10^{-3}$)
M	moles per litre
MCP-5	monocyte chemoattractant protein 5
MDA-5	melanoma differentiation-associated gene 5
MDCK	Madin-Darby canine kidney cells
MIF	macrophage migration inhibitory factor
MIG	monokine induced by IFN- γ

MMPs	matrix metalloproteinases
MOI	multiplicity of infection
mRNA	messenger RNA
n	nano ($\times 10^{-9}$)
NLS	nuclear localization signal
NP40	nonidet-P40
NS	nonsilencing control cell line
nt	nucleotide
NT	N-terminus
°C	degrees Celsius
ORF	open reading frame
P body	processing body
PB	processing body
PBS	phosphate buffered saline
PBS-T	phosphate buffered saline, tween 20
PCR	polymerase chain reaction
pH	power hydrogenii
PI3K	phosphatidylinositol 3-kinase
PKC	protein kinase C
Poly(A)	poly(adenosine)
PP2A	phosphatase 2A
prM	precursor membrane protein
PVDF	polyvinylidene difluoride

RHA	ribonucleic acid helicase A
RIG-I	retinoic-acid-inducible gene I
RNA	ribonucleic acid
RNAi	RNA interference
RNase	ribonuclease
ROX	5-carboxy-X-rhodamine
RT	room temperature
RT-PCR	reverse transcriptase-PCR
SDS-PAGE	sodium dodecyl-sulphate polyacrylamide gel
siRNA	short interfering RNA
SGs	stress granules
SLEV	St Louis encephalitis virus
SP	signal peptidase
SPP	signal peptide peptidase
TBEV	tick-borne encephalitis virus
TEMED	N,N,N',N'-tetramethylethylenediamine
TLR3	toll-like receptor 3
TNF- α	tumor necrosis factor α
U	enzymatic units
v	volts
VSV	vesicular stomatitis virus
VSV-G	vesicular stomatitis virus glycoprotein
v/v	volume per volume
WNV	west nile virus

WT	wild type
w/v	weight per volume
WB	western blot
YFV	yellow fever virus

CHAPTER 1

Introduction

1.1 History and epidemiology of West Nile virus

West Nile virus (WNV) is a mosquito-transmitted virus that is found in temperate and tropical regions of the world. It was first isolated in 1937 from a feverish woman in the West Nile region of Uganda (Smithburn et al., 1940). Prior to the mid-1990s, WNV disease occurred only occasionally and was not considered a major risk for humans. However, this perception changed after a large outbreak in Romania in 1996 in which a high number of patients with neuroinvasive disease were reported (Savage et al., 1999; Tsai et al., 1998). Since then, the virus is endemic through Europe, Asia, Australia, the Middle East and Africa and notably, incidences of WNV-associated outbreaks of severe neurological disease including meningitis and encephalitis have dramatically increased (Gubler, 2007; Hayes, 2001; Zeller and Schuffenecker, 2004). In 1999, WNV was introduced into the Western Hemisphere following an outbreak in the New York City that resulted in at least seven human fatalities as well a large number of avian and equine deaths (Nash et al., 2001). Over the next five years, the virus has rapidly spread across the continental United States, north into Canada, as well as southward into the Caribbean Islands and Latin America. In 2012, WNV infections resulted in at least 286 deaths in the United States, the majority of which occurred in Texas (<http://www.cdc.gov/ncidod/dvbid/westnile/index.htm>). WNV is now the leading cause of viral encephalitis in the United States.

WNV is maintained in an enzootic cycle between *Culex* mosquitoes, birds and some mammals, primarily horses and humans. Birds are the most commonly

infected animal and serve as the primary reservoir host. Approximately 80% of WNV infections in humans are subclinical, and among clinical cases, many develop a self-limiting non-neuroinvasive illness termed WNV fever, which is characterized by fever, headaches, fatigue, muscle pain, nausea, vomiting, and rash (Davis et al., 2006b; Hayes et al., 2005). A subset of the symptomatic cases (~1%) progress to a severe neuroinvasive form of WNV disease where the central nervous system (CNS) is affected. The symptoms of WNV-induced neurological disease include acute flaccid paralysis, encephalitis, meningitis, and ocular manifestations (Hayes et al., 2005; Lanciotti et al., 1999). According to a 2012 report from the CDC (<http://www.cdc.gov/ncidod/dvbid/westnile/index.htm>), approximately 51% of clinically diagnosed WNV cases in the United States were associated with neuroinvasive disease, which has a 10% mortality rate.

Severe disease is more often observed with infections of young children, the elderly, transplant patients and immunocompromized individuals, but in recent years, neurological disease is commonly being reported in healthy young adults that contract WNV (DeBiasi et al., 2005; Emig and Apple, 2004; Fischer, 2008). This suggests an increase in virulence that can occur independently of immune senescence or immune deficiencies.

Currently, there is no approved vaccine for human use, but there are several ongoing clinical trials with vaccine candidates (reviewed in (Rossi et al., 2010)). There are several strategies being pursued for WNV vaccine development. The first one is inoculation of multiple doses of formalin-inactivated whole virus (Ng et al., 2003). The vaccine (Innovator) developed by Fort Dodge Animal Health has been approved for use in horses since 2003. Although the Innovator vaccine

appears safe and effective for horses, mice and hamsters, assessment of its use to protect birds from WNV disease have been less encouraging because the vaccine failed to induce detectable neutralizing antibody response (Nusbaum et al., 2003). The second strategy involves the production of WNV antigens from a heterologous virus backbone. The vectors being used are canarypox (Recombitek), yellow fever virus (ChimeriVax), and dengue 4 (WNV-DEN4). The Recombitek vaccine (Meril) has been licensed for use in horses. A chimeric WNV vaccine, named ChimeriVax-WNV, is also under development. This technology involves splicing the structural genes (prM and E) of WNV into a DNA infectious clone of the attenuated 17D vaccine strain of yellow fever virus. The resulting hybrid virus contains the viral replicative machinery (non-structural genes and untranslated regions of the genome) and the capsid protein (C) derived from 17D host virus, whereas the immunogenic virion surface proteins (E and prM/M) are derived from WNV virus. In 2011, a vaccine candidate called ChimeriVax-WN02 began undergone phase II clinical trials (Arroyo et al., 2004; Biedenbender et al., 2011). ChimeriVax-WN02 is highly immunogenic in both younger and older adults and was well tolerated at all dose levels and in all age groups. Further clinical studies to define vaccine safety and immunogenicity are warranted. Using a similar technology, a chimeric virus containing an attenuated Dengue virus type 4 genetic background, and the WNV proteins prM and E has been shown to induce neutralizing antibody responses to WNV and protect mice and monkeys (Pletnev et al., 2003). It is currently undergoing phase II clinical trials in human (<http://www.clinicaltrials.gov/>). The third approach is DNA vaccination in which WNV structural antigens (prM-E) are expressed from

plasmids. Some of these vaccine candidates were found to be protective in mice, horses and birds (Davis et al., 2001; Turell et al., 2003). Finally, inoculation with purified recombinant viral proteins produced in mammalian cell culture, bacteria, or yeast is being considered (Chu et al., 2007; Ledizet et al., 2005; Lieberman et al., 2007; Qiao et al., 2004). Most of these vaccine candidates are still at the preclinical stage.

Studies from cell culture and animal models have resulting in some promising leads. For example, AMD3100, which had been considered as an antiviral drug for HIV, has shown promise against WNV-caused encephalitis (McCandless et al., 2008). Inhibition of CXCR4 (a protein located at the blood-brain barrier (BBB)) by AMD3100 allows WNV-specific CD8 (+) T cells to cross the BBB to combat the virus infecting the brain. Compared with placebo control, AMD3100 improved survival in mice infected with WNV by 50 percent (McCandless et al., 2008). Morpholino antisense oligonucleotides conjugated to cell penetrating peptides partially protect mice from WNV disease by targeting the conserved 3' conserved sequence I (CSI) RNA element of the viral genome (Deas et al., 2007). Ribavirin, intravenous immunoglobulin, or alpha interferon have also been used to treat WNV infections (reviewed in (Diamond, 2009)). Moreover, it was found that blocking angiotensin II can enhance recovery from WNV encephalitis as well as other viruses (Moskowitz and Johnson, 2004). However, at present, no specific therapy against WNV has been approved for use in humans. The development of therapeutics that treat WNV disease is challenging because most patients with severe symptoms often show immune deficits and present to clinical attention relatively late (Granwehr et al., 2004;

Jackson, 2004). Even with the discovery of new anti-WNV drugs, a major obstacle remains as to whether they can be administered in a timely manner before serious and irreversible neuronal degeneration occurs. Additional technical challenges will include developing inhibitors that can efficiently cross into the CNS and control WNV replication within neurons.

1.2 Classification and clinical importance of the family Flaviviridae

WNV belongs to the family Flaviviridae, a group of small, enveloped, positive-sense, and single-stranded RNA viruses (Calisher and Gould, 2003). These pathogens are primarily spread through arthropod vectors (ticks and mosquitoes). The family name Flaviviridae derives from Yellow Fever virus (flavus means yellow in Latin).

The family Flaviviridae comprises a diverse group of animal viruses and is divided into three genera: Flavivirus, Hepacivirus, and Pestivirus (Calisher and Gould, 2003). The Flavivirus genus is composed of more than 70 viruses, 40 of which are associated with human disease (reviewed in (Diamond, 2009)). Within this genus, members can be further classified into tick-borne and mosquito-borne virus groups. The mosquito-borne viruses may be largely grouped into the encephalitic clade, or the JE serocomplex, which includes WNV and Japanese encephalitis virus (JEV), and the nonencephalitic or hemorrhagic fever clade, which includes dengue virus (DENV) and yellow fever virus (YFV) (Heinz and Stiasny, 2012; Kuno et al., 1998; Shi, 2012). Hepacivirus includes the type virus -hepatitis C virus (HCV), which is the cause of hepatitis

C in humans. Pestiviruses are a group of viruses that mainly infect hoofed mammals.

Flavivirus infections have a significant public health impact on a global level as they result in extensive morbidity and mortality. Major human diseases caused by this family include: Dengue fever, Yellow fever, Japanese encephalitis, West Nile encephalitis, tick-borne encephalitis, and hepatitis C virus infection (Turtle et al., 2012). JEV is endemic in large areas of Asia and similar to WNV, can infect the CNS and has a high mortality rate. Dengue virus is an extremely important pathogen that infects more than 100 million people each year (Wilder-Smith and Schwartz, 2005). It is the most common cause of arboviral disease in the world and there are no specific treatments for this disease. HCV is the major etiological agent of non-A, non-B hepatitis. Current estimates suggest that 130–200 million people worldwide are infected with HCV (Gravitz, 2011). In approximately 85% of cases, infection becomes chronic where the virus can persist for decades. Patients chronically infected with HCV account for approximately 30–40% of all liver transplants. As such, HCV has been the focus of much research in an attempt to understand the mechanisms by which the virus causes and maintains a disease state.

1.3 Genome and proteins of WNV

The WNV genome consists of a ~11-kb positive-sense single-stranded RNA which is flanked by 5' and 3' untranslated regions. The RNA genome has no polyadenylation tail at the 3' end (reviewed in (Brinton, 2002)). Both the 5' and

3' noncoding regions of the genome form stem-loop structures that aid in viral RNA translation, replication, and packaging (Friebe and Harris, 2010; Khromykh et al., 2001a; Shi et al., 1996). The viral RNA contains a single open reading frame (ORF) and is translated as a single polyprotein that is post-cleaved by cellular and viral proteases, resulting in three structural and seven nonstructural proteins (Figure 1.1). The three structural proteins include a capsid protein (C) that binds viral RNA to form nucleocapsids, an envelope protein (E) that mediates cell surface attachment, membrane fusion, and virus entry, and a transmembrane protein (prM) that aids in proper folding and function of the E protein (reviewed in (Lindenbach and Rice, 2003)).

The nonstructural proteins have a diversity of functions that are necessary for genome replication and immune evasion. NS1 functions as a cofactor for viral RNA replication (Westaway et al., 2002). It colocalizes with the double-stranded RNA replicative form and mutations attenuate viral RNA accumulation (Khromykh et al., 1999; Westaway et al., 1999). NS1 exists as both cellular and secreted form. High levels of secreted NS1 accumulate in the serum of WNV-infected patients and correlate with the development of severe disease (Macdonald et al., 2005). NS1 interferes with the immune response by decreasing complement recognition of infected cells. Chung *et al.* demonstrated soluble NS1 binds to the complement regulatory protein factor H (fH) and promotes the fH-mediated cleavage of C3b, resulting in decreased complement activation in solution. Cell-surface-associated NS1 attenuates the deposition of C3b and C5b-9 membrane attack complexes on cell surfaces (Chung et al., 2006). NS3, in

conjunction with the NS2B protein, functions as a serine protease that cleaves the viral polyprotein to release structural and non-structural viral proteins. Disruption of this protease activity abrogates virus replication (Chambers et al., 1990). The NS3 protein has other enzyme activities (helicase, nucleoside triphosphatase, RNA triphosphatase) (Gorbalenya et al., 1989; Wengler and Wengler, 1991), all of which are tightly regulated through localization to distinct membranous compartments in the infected cell (Westaway et al., 1997b). NS3 has also been implicated in other stages of the flavivirus replication cycle, including virion budding and membrane reorganization (Chua et al., 2004; Lobigs, 1993; Yamshchikov and Compans, 1993). This protein is linked to neurovirulence possibly through induction of apoptosis (McMinn, 1997). NS5 is a large, well-conserved, multifunctional protein that is critical for viral RNA replication as it possesses polymerase activity as well as a methyltransferase domain (Lindenbach and Rice, 2003). Mutagenesis of the Kunjin virus polymerase active site motif confirmed that it is essential for virus replication and that polymerase activity can function in *trans* from a Kunjin replicon (Khromykh et al., 1998). However, in cells only expressing NS5, *trans* complementation of this defect was not efficient, suggesting that expression of additional viral proteins are required for the polymerase to associate with other replicase components (Khromykh et al., 1999). Indeed, NS5 forms a complex with NS3 (Kapoor et al., 1995) and can stimulate NS3 NTPase activity (Cui et al., 1998).

The other nonstructural proteins including NS2A, NS2B, NS4A, and NS4B are small, hydrophobic proteins that contain no functional motifs/domains

characteristic of known enzymes. Some or all of those proteins may facilitate the assembly of viral replication complexes and/or their localization on cytoplasmic membranes. For example, NS2A is part of the replication complex and mutation of the hydrophobic residue at codon 59 blocks the production of secreted virus particles, suggesting that NS2A plays a role in the biogenesis of virus-induced membranes in virus assembly (Leung et al., 2008). NS2B functions as the cofactor for the viral serine protease NS3 (Chambers et al., 1993; Falgout et al., 1993). NS4A is a membrane-bound protein involved in the viral replication complex and it is responsible for a rapid expansion and modification of the endoplasmic reticulum (ER) that helps establish replication domains (Egloff et al., 2002; Khromykh et al., 1998; Mackenzie et al., 1998; Speight et al., 1988). Specifically, the C-terminal transmembrane domain 2K of NS4A that is cleaved from NS4A during the polyprotein processing, is important for the induction of membrane alterations and the localization of NS4B in the lumen of the ER (Roosendaal et al., 2006).

As mentioned above, WNV non-structural proteins have immune escape functions. For example, using subgenomic replicons of the Kunjin subtype of WNV, Liu *et al.* demonstrated that NS2A is a major inhibitor of IFN- β -driven transcription and that a single amino acid substitution in NS2A (Ala30 to Pro [A30P]) dramatically reduced its inhibitory effect (Liu et al., 2004). Moreover, a mutant virus with the incorporation of the A30P mutation into the genome results in more rapid induction and higher levels of IFN- α/β than that detected following wild-type virus infection. Accordingly, replication of the NS2A/A30P mutant

virus in cells producing high levels of IFN- α/β was ineffective. Furthermore, the mutant virus was highly attenuated in neuroinvasiveness and also attenuated in neurovirulence in mice. Intriguingly, the mutant virus was also partially attenuated in IFN receptor knockout mice, indicating that the A30P mutation could also be involved in other antiviral pathways in addition to the IFN response (Liu et al., 2006). NS4B was reported to partially block activation of STAT1 and play a role in the inhibition of the IFN- α/β -stimulated JAK-STAT signaling pathway (Evans and Seeger, 2007; Munoz-Jordan et al., 2005). Furthermore, NS2A, NS2B, NS3, NS4A and NS4B have all been implicated in the inhibition of the IFN signaling pathway by preventing STAT1 and STAT2 phosphorylation (Liu et al., 2005).

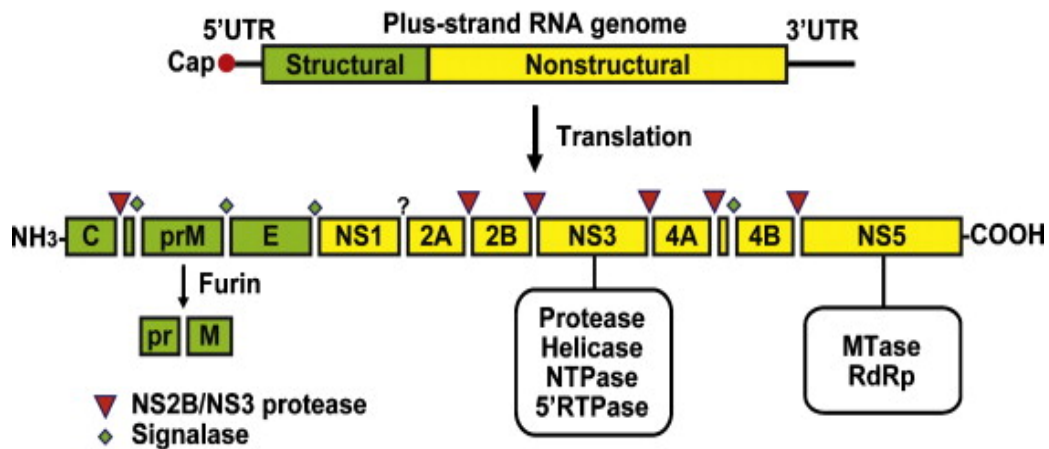


Figure 1.1 Schematic representation of WNV genome organization and polyprotein processing. The 11 kb positive-sense, single-stranded RNA genome contains a single open reading frame which encodes 3 structural proteins (capsid (C), precursor membrane (prM) and envelope (E)) and 7 non-structural proteins (NS1, NS2A, NS2B, NS3, NS4A, NS4B, NS5). The open reading frame is flanked by untranslated regions. Sites of polyprotein cleavage mediated by the viral NS2B-NS3 and by host signalase and furin are shown, and the enzymatic activities of NS3 and NS5 are also indicated. (Modified from (Sampath and Padmanabhan, 2009). Permitted by Elsevier, license number: 3212630840121)

1.4 Structure of the WNV virion

WNV virions are small (~50 nm in diameter), spherical, enveloped particles with a buoyant density of ~1.2 g/cm³ (reviewed in (Brinton, 2002)). The spherical nucleocapsid is ~25 nm in diameter and is composed of multiple copies of the capsid protein and a single molecule of genomic RNA. Three dimensional reconstruction images from cryoelectron microscopy demonstrate that the WNV virion has a well-organized outer protein shell, a 40Å lipid membrane bilayer, and a less-defined inner nucleocapsid core (Mukhopadhyay et al., 2003). Two transmembrane proteins are inserted into a host-derived lipid membrane, the major envelope glycoprotein E and the membrane protein M. The M protein, is derived by proteolytic processing of its precursor form, prM. In mature virions, the icosahedral scaffold consists of 180 E and M proteins arranged in a repeating herringbone pattern (Kuhn et al., 2002; Zhang et al., 2003a). Structural analysis of the soluble ectodomain of WNV E protein displays three distinct domains (DI, DII, DIII) (Kanai et al., 2006; Nybakken et al., 2006), which are consistent with previous studies on related flaviviruses (Modis et al., 2003; Rey, 2003; Rey et al., 1995). The 180 E monomers lay relatively flat along the virion surface as sets of three anti-parallel homodimers. Neither E nor M interacts with the nucleocapsid in mature virions. In infected cells, budding at the ER results in immature virions whose structural organization is distinct from secreted virions. In the immature virus particles, E glycoprotein is associated with the glycoprotein prM and three of these heterodimers form one viral spike (Kuhn et al., 2002; Zhang et al., 2003b). Virus particle maturation occurs during viral egress (details in section

1.5).

1.5 The WNV replication cycle

The WNV replication cycle primarily consists of four stages: virion entry, translation, replication, and virion assembly/egress (Rossi et al., 2010). WNV enters cells through receptor-mediated endocytosis after attachment to the cell surface, which requires the formation of clathrin-coated pits (Chu and Ng, 2004a; Krishnan et al., 2007) and cholesterol-rich lipid rafts (Medigeshi et al., 2008). Although several molecules have been implicated as potential receptors for WNV (DC-SIGN, $\alpha\beta 3$ integrin, and several glycosaminoglycans (Chu and Ng, 2004a, b; Davis et al., 2006a; Lee et al., 2004)), the receptors that function in infection of physiologically relevant cell types such as neurons or macrophages are not known. Indeed, more recent studies suggest that WNV entry occurs independently of the $\alpha\beta 3$ integrin (Medigeshi et al., 2008). Following endocytosis, WNV is transported into endosomes. Within endosomes, a low pH-catalyzed conformational change in the E protein (Modis et al., 2004; Zhang et al., 2004) facilitates fusion of the viral and endosomal membranes and release of the virus nucleocapsid into the cytoplasm (Allison et al., 1995; Gollins and Porterfield, 1986). After capsid disassociation, the viral RNA associates with ER membranes and is translated as a polyprotein, which is then processed into 10 individual proteins by viral and host proteases. Viral RNA replication is carried out in specific sites called vesicle packets which are established by the rough ER and Golgi-derived membranes (Chu and Westaway, 1992; Mackenzie, 2005). RNA

translation is a prerequisite for generating a negative-strand RNA intermediate that primes synthesis of nascent positive-strand genomic RNA (Mackenzie and Westaway, 2001). RNA synthesis of WNV is semi-conservative and asymmetric since positive-strand RNA genome production is approximately ten times more efficiently than negative-strand RNA synthesis (reviewed in (Brinton, 2002)). Positive-strand RNA is either packaged within progeny virions or used to translate additional viral proteins. The virus assembles and buds into the ER to form enveloped immature particles containing the prM protein. Maturation of virus particles occurs through the ER-Golgi secretion pathway in which a host furin-like protease cleaves off prM (Elshuber et al., 2003; Stadler et al., 1997), resulting in the release of infectious mature virus from the cell surface by exocytosis (Figure 1.2).

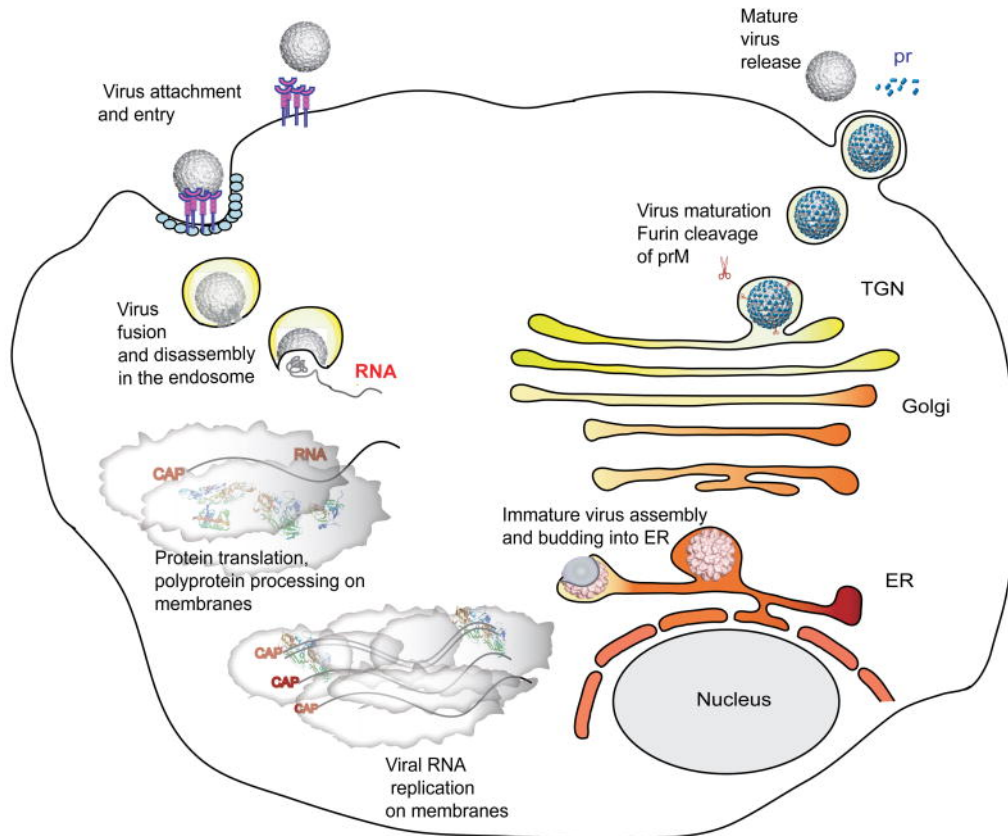


Figure 1.2 The WNV replication cycle. Virion entry is initiated after the envelope protein (E) binds to an unknown cellular receptor (or receptors), followed by receptor-mediated endocytosis of the virus. The low-pH environment within the endosomes triggers viral fusion with the endosomal membrane, leading to virion uncoating and release of the viral genomic RNA into the cytoplasm. The viral RNA is translated into a single polyprotein at the ER and cleaved into mature proteins by viral and cellular proteases. Viral non-structural proteins then replicate the genomic RNA. The viral capsid protein (C) is responsible for encapsidating viral genomic RNA, with assembly occurring on rough ER membranes. Immature virions are transported through the host secretory pathway, resulting in glycosylation of the viral E protein and host cell furin mediated-cleavage of the protein prM to the mature membrane protein, M. Mature virions are transported to the plasma membrane and released by exocytosis. (Modified from (Sampath and Padmanabhan, 2009). Permitted by Elsevier, license number: 3212630840121)

1.6 Neuroinvasion by WNV

The pathogenesis of WNV encephalitis in humans is poorly understood. However, studies using animal models of infection have contributed to our understanding of the mechanism. In the mouse model, three distinct phases of WNV pathogenesis have been identified, including the initial infection and spread phase, the peripheral viral amplification phase and neuroinvasion phase (Samuel and Diamond, 2006). These processes are thought to represent what occurs in humans following WNV infection.

Following a mosquito bite, WNV is transmitted to the host and an initial replication is presumed to occur in the local dendritic cells in the skin. Infected cells then transport the virus to the draining lymph node and after replication at these sites, a transient, low-level viremia occurs (Byrne et al., 2001; Johnston et al., 2000). Then, the virus disseminates systemically and infects multiple peripheral organs, including the spleen, liver, and kidney.

WNV neuropathogenesis depends on the ability of the virus to enter the CNS and replicate efficiently within target cells, including neurons and glia cells. Although the exact mechanism through which WNV gains entry to the CNS is not completely understood, a combination of mechanisms that facilitates viral neuroinvasion as described below has been implicated.

1.6.1 Breakdown of the blood-brain barrier (BBB)

The BBB is a dynamic interface that regulates the paracellular movement of small molecules (nutrients and toxins) and large particles (cells) in and out of the

CNS. To gain access to the brain following mosquito bite, WNV virions need to cross multiple polarized epithelial and endothelial cell layers including the BBB. A previous study showed that high viremia in mice can easily lead to an infection of the brain if the BBB is disrupted, and it was correlated with severity of disease in experimentally infected mice (Samuel and Diamond, 2005). In contrast, high viremia and high viral titers in the periphery alone (the BBB remains intact) do not predict neuroinvasion.

Disruption of the BBB can be triggered by changes in capillary endothelial cell permeability during WNV infection, which is regulated by host proteins that alter BBB permeability and degradation of tight junction proteins.

1.6.1.1 Host proteins that alter the BBB permeability

The macrophage migration inhibitory factor (MIF), which is an upstream mediator of innate immunity, has been implicated in altering the BBB permeability during WNV infection (Arjona et al., 2007). It was found that the MIF expression was increased in patients suffering from acute WNV infection and in WNV-infected mice. Remarkably, abrogation of MIF action rendered mice more resistant to WNV lethality. Moreover, *Mif*(*-/-*) mice showed a reduced viral load and inflammatory response in the brain when compared with wild-type (WT) mice. To directly evaluate the role of MIF in BBB permeability, poly(I:C)-challenged WT and *Mif*(*-/-*) mice were injected with Evans blue, a dye that binds to the albumin present in the sera and forms a complex that does not reach the CNS when the BBB is intact. Twenty-four hours after poly(I:C) challenge, BBB

leakiness was evident in WT but not in *Mif(-/-)* mice, based on the macroscopic observation of Evans blue staining of the brain. Importantly, *Mif(-/-)* mice also presented with reduced BBB permeability during WNV infection. It was further confirmed that the reduced viral load observed in the brain and the enhanced survival of *Mif(-/-)* mice was exclusively due to decreased WNV neuroinvasion. This was because of the fact that there was no significant difference in survival between WT and *Mif(-/-)* mice when the same amount of virus were directly injected into the brains. These data (Arjona et al., 2007) collectively supported the conclusion that MIF promotes WNV neuroinvasion by compromising the integrity of the BBB.

Intercellular adhesion molecule 1 (ICAM-1), one molecule locating on vascular endothelial cells and leukocytes, has been shown to play important roles in leukocyte traffic into the brain (Dietrich, 2002; Greenwood et al., 2002). It was reported that upregulation of ICAM-1, leukocyte-mediated disruption of the BBB, and followed leukocyte recruitment into the CNS occur in brain inflammation (Dietrich, 2002; Lossinsky and Shivers, 2004). Like MIF, *ICAM-1(-/-)* mice are more resistant than WT mice to lethal WNV encephalitis (Dai et al., 2008). Infection of these knockout mice results in lower viral loads, reduced leukocyte infiltration, less BBB leakage and diminished neuronal damage in the brain compared to control animals.

Death-associated protein kinase-related apoptosis-inducing kinase-2 (Drak2), a member of the death-associated protein family, is specifically expressed in B and T cells (Kogel et al., 2001; McGargill et al., 2004). It

functions to negatively modulate signals involved in T cell activation (Friedrich et al., 2007). It has been shown that, in the absence of Drak2, mice are remarkably resistant to experimental autoimmune encephalomyelitis due in part to a reduction of infiltrating cells into the CNS (McGargill et al., 2004). It was reported that *Drak2(-/-)* mice are also more resistant to lethal WNV challenge than WT mice (Wang et al., 2008b). Although *Drak2(-/-)* mice exhibited increased number of IFN- γ -producing T cells in the spleen after infection, viral load in the peripheral tissues was not significantly different from control mice. In contrast, viral loads in the brains of *Drak2(-/-)* mice were lower, which corresponded with a decrease in the number of *Drak2(-/-)* CD4(+) and CD8(+) T cells in the brain. Moreover, viral antigens were detected in T cells isolated from the spleen or brain of WNV-infected mice. These results (Wang et al., 2008b) suggest that following a systemic infection, WNV may cross the BBB and enter the CNS via infected infiltrating T cells.

Another host factor, matrix metalloproteinase 9 (MMP9) has also been implicated in WNV entry into the brain by enhancing BBB permeability (Wang et al., 2008a). In mice, WNV infection induces MMP9 expression and levels of activity are observed in the blood and brain. Cerebrospinal fluid from patients infected with WNV reportedly contains increased MMP9. Moreover, without showing significant difference in the peripheral viremia and expression of host cytokines, *MMP9(-/-)* mice were more resistant to lethal WNV challenge than WT mice. This resistance was associated with an intact BBB as IgG, Evans blue leakage into brain, and type IV collagen degradation (three methods used for

measuring BBB permeability) were remarkably decreased in the *MMP9(-/-)* mice compared with the levels in controls. Furthermore, levels of viral loads, selected inflammatory cytokines, and infiltrating leukocytes were significantly reduced in *MMP9(-/-)* mice compared to their levels in WT mice. These data suggest that MMP9 plays an important role in facilitating WNV entry into the CNS.

1.6.1.2 Degradation of tight junction proteins

Tight junctions that form between adjacent cells form the basic structure of the BBB, which limits paracellular permeability. Tight junction complexes are composed of transmembrane proteins including claudins, occludins and junctional adhesion molecules (JAM). These membrane proteins interact with cytosolic components such as ZO-1, ZO-2, ZO-3 and the actin cytoskeleton (reviewed in (Shen et al., 2011)). Homotypic interactions between claudins, occludins and JAMs on apposing cells constitute the main barrier to intercellular passage of macromolecules and pathogens. A number of studies have reported that WNV infection disrupts the integrity of the tight junctions (Medigeshi et al., 2009; Verma et al., 2010; Verma et al., 2009), however, the collective findings do not agree with respect to the underlying mechanism. One study reported that expression of capsid protein inhibits the barrier function of tight junctions by inducing degradation of claudin proteins in lysosomes (Medigeshi et al., 2009). In contrast, Verma *et al.* report that infection of endothelial cells by WNV *per se* does not reduce levels of tight junction components, but rather, matrix metalloproteases that are secreted from infected astrocytes cause breakdown of

these structures (Verma et al., 2010; Verma et al., 2009). The discrepancies observed regarding tight junction compromise suggest that further research is required to determine whether or not WNV directly affects the expression and/or degradation of tight junction proteins.

1.6.2 Host immune response to infection

The host response to infection may also contribute to WNV neuropathogenesis. Studies from experimentally infected mice suggest that the innate immune sensing molecule toll-like receptor 3 (TLR3) that recognizes viral double-stranded (ds) RNA may play a critical role in WNV invasion of the CNS (Wang et al., 2004). It was shown that increased peripheral viremia (virus load) and impaired production of cytokines (IFN- β , IL-6, and TNF- α) in TLR3-deficient (*TLR3(-/-)*) mice did not result in decreased survival rate after WNV infection compared to WT mice. In contrast, *TLR3(-/-)* mice were resistant to lethal WNV challenge and showed markedly decreased levels of CNS inflammatory cytokines, viral loads, infiltrating leukocytes, and neuropathology. Further experiments demonstrated that TNF- α receptor 1 signaling is vital for BBB compromise upon TLR3 stimulation by dsRNA or WNV. Therefore, TLR3 appears to be necessary for altering BBB permeability and allowing the virus to gain entry into the brain.

In addition to TNF- α , other proinflammatory chemokines/cytokines including MIF, IFN- γ , IFN- γ -inducible protein 10 (IP-10), monokine induced by IFN- γ (MIG) and monocyte chemoattractant protein 5 (MCP-5) are reportedly

upregulated in the brains of experimentally infected mice (Arjona et al., 2007; Garcia-Tapia et al., 2007). These studies suggest that the host immune response is at least partially responsible for neurologic symptoms of WNV disease.

1.6.3 Determinants of neuroinvasion on the viral structural proteins

The neuroinvasive potential of WNV is governed, in part, strain dependent (Beasley et al., 2002). By comparing genetic and neurovirulence properties of 19 strains of WNV, it was possible to link neuroinvasive phenotypes with gene-specific polymorphisms. In particular, virus isolates from North America were found to be more neuroinvasive with a lack of age-related resistance to infection in mice (Beasley et al., 2002). To elucidate the basis for these differences, genetic sequencing of ETH76a (an attenuated strain for mouse neuroinvasion) showed five amino acid differences in the E protein gene compared with NY99 (highly virulent strain for neuroinvasion). Moreover, substitution of prM and E genes of ETH76a into a NY99 infectious clone backbone yielded a virus with altered *in vitro* growth characteristics and a mouse virulence phenotype comparable to ETH76a. Further mutagenesis studies revealed that the altered phenotype was due primarily to loss of glycosylation of *N*-linked glycan on domain I of the E protein and that this was associated with altered stability of the virion at mildly acidic pH (Beasley et al., 2005). The mechanism by which these determinants mediate neuroinvasion is unknown, but it is possible that they enhance binding to and penetration of the brain endothelial cells (Verma et al., 2009), thereby increasing viral infection and entry into the CNS.

Additional proposed mechanisms of CNS entry include direct axonal retrograde transport from infected peripheral neurons (Samuel et al., 2007b), Trojan Horse mechanism by which virus is transported to the CNS by infected immune cells (Bai et al., 2010), and infection of olfactory neurons and spread from the olfactory bulb (Getts et al., 2008)

1.7 Multifunctional capsid proteins of flaviviruses

Like other RNA viruses, flaviviruses are gene poor and only encode a small number of proteins (reviewed in (Ahlquist et al., 2003)). Therefore, manipulation of multiple host cell factors by a relatively small number of viral proteins is critical for virus replication and spread. In addition, due to the limited coding capacity of the flavivirus genome, its protein products must be multifunctional in order to counter host cell antiviral defenses.

Flavivirus capsid proteins are internal structural components whose primary function is to package viral genomic RNA into nucleocapsids (reviewed in (Sampath and Padmanabhan, 2009)). However, increasing evidence suggests that in addition to their well-defined roles in virus assembly, flavivirus capsid proteins have important nonstructural functions (Bulich and Aaskov, 1992; Hunt et al., 2007; Makino et al., 1989; Mori et al., 2005; Tadano et al., 1989; Urbanowski and Hobman, 2013; Westaway et al., 1997a; Xu et al., 2011; Xu and Hobman, 2012). Capsid is the first viral protein synthesized in an infected cell, however it is not required as a structural component until late in the assembly pathway. Furthermore, during viral entry it is the first viral protein to contact host cell

proteins in the cytoplasm. Temporally and spatially, this places the flavivirus capsid protein in a strategic position to act as a modulator of the host cell environment. Second, even though flavivirus replication is confined to the cytoplasm of host cells and assembly of nascent virions occurs on the ER, large pools of WNV, JEV, and DENV capsid proteins are localized to the nuclei of infected cells (Hunt et al., 2007; Mori et al., 2005; Tadano et al., 1989; Westaway et al., 1997a; Xu et al., 2011; Xu and Hobman, 2012). As there is no obvious role for nuclear localized capsid in virus assembly, the nuclear cohort of capsid is thought to engage in nonstructural functions, presumably in modifying the host cell environment in such a way that virus replication and/or dissemination is benefited. Notably, interactions between capsids and host cell proteins contribute to this process. A partial list summarizing flavivirus capsid-interacting host proteins is shown in Table 1.1. Of note, the best-characterized examples comprise capsid proteins that modulate apoptosis or regulate viral genome transcription and/or translation. Together, these studies are consistent with the idea that flavivirus capsids serve as important modulators that function at the virus-host cell interface. Importantly, evidence presented below suggests that flavivirus capsids perform these multiple functions by interacting with host cell proteins.

Table 1.1 Host cell proteins that have been reported to interact with flavivirus capsid proteins

Virus	Host protein	Function	Reference
DENV	DAXX	Apoptosis	(Limjindaporn et al., 2007; Netsawang et al., 2010)
	Core histones: H2A, H2B, H3 and H4 Sec3	Nucleosome formation Secretory pathway and vesicular trafficking	(Colpitts et al., 2011) (Bhuvanakantham et al., 2010b; Raghavan and Ng, 2013)
	hnRNP K	Transcriptional regulation	(Chang et al., 2001)
HCV	ACY3	Disease development	(Chen et al., 2009)
	AP2M1	Virus assembly	(Neveu et al., 2012)
	Apolipoprotein AII	Lipid metabolism	(Sabile et al., 1999; Shi et al., 2002)
	Cap-Rf	RNA helicase	(You et al., 1999b)
	Complement Receptor gC1qR	T-cell response	(Kittlesen et al., 2000)
	Cyclin dependent kinase 7	Cell cycle regulation	(Ohkawa et al., 2004)
	C14orf166	Microtubule organization	(Lee et al., 2011)
	DEAD-box protein DBX	RNA helicase	(Mamiya and Worman, 1999)
	DEAD-box protein 3	RNA helicase	(Owsianka and Patel, 1999)
	DDX3X	RNA helicase	(Sun et al., 2010)
	fibrinogen- β	Acute-phase response	(Ait-Goughoulte et al., 2010)
	Heterogeneous nuclear ribonucleoprotein K	Transcriptional control	(Hsieh et al., 1998)
	hnRNPH1	mRNA metabolism	(Lee et al., 2011)
	HSC90	regulation of protein stability	(Kubota et al., 2012)
Hsp60	Molecular chaperon	(Kang et al., 2009)	
JAK1/2	Signal transduction	(Hosui et al., 2003)	
Lymphotoxin- β receptor	Apoptosis	(Chen et al., 1997)	
MAPKAPK3	Signal transduction	(Ngo et al., 2013)	

Table 1.1 (Continued)

Virus	Host protein	Function	Reference
	Mcl-1	Apoptosis	(Mohd-Ismail et al., 2009)
	p53	Transcriptional control	(Otsuka et al., 2000)
	p73	Transcriptional control	(Alisi et al., 2003)
	Proteasome activator PA28 γ	Protein degradation	(Moriishi et al., 2003)
	Retinoid X receptor α	Transcriptional control	(Tsutsumi et al., 2002)
	Smad3	Transcriptional control	(Cheng et al., 2004)
	sp110b	Transcriptional control	(Watashi et al., 2003)
	STAT3	Cell transformation	(Yoshida et al., 2002)
	TAFII28	Transcriptional control	(Otsuka et al., 2000)
	Tumor necrosis factor receptor I	Apoptosis	(Zhu et al., 2001)
	14-3-3 protein	Regulate activity and transport of various cellular proteins	(Aoki et al., 2000)
WNV	DDX56	RNA helicase	(Xu et al., 2011; Xu and Hobman, 2012)
	HDM2	Cell cycle, regulation of protein stability	(Bhuvanakantham et al., 2010a; Yang et al., 2008)
	Hsp70	Molecular chaperon	(Oh and Song, 2006)
	I ^{2PP2A}	Signal transduction	(Hunt et al., 2007)
	Importin α/β	Nuclear import	(Bhuvanakantham et al., 2010a; Bhuvanakantham et al., 2009)
	Jab1	Transcriptional control, regulation of protein stability	(Oh et al., 2006)
	MKRN1	E3 ligase	(Ko et al., 2010)
	Sec3	Secretory pathway and vesicular trafficking	(Bhuvanakantham et al., 2010b; Raghavan and Ng, 2013)

The most commonly known functions of each host cell protein are listed.

HCV core

The HCV capsid, also known as core protein, is by far the best studied of the flavivirus capsids. There are two forms of the HCV core protein that exist during the virus life cycle. One is the immature form, which is generated from the polyprotein by a host signal peptidase (SP) cleavage at the C-terminus of a signal peptide that lies between core and the E1 glycoprotein (Santolini et al., 1994). The other one is the mature form. Maturation of core requires further processing by another host signal peptide peptidase (SPP) to remove the signal peptide present at the C-terminus of the immature core (McLauchlan et al., 2002).

Before the availability of a cell culture system for producing infectious HCV, different localizations of the core protein were reported in the context of heterologous expression systems or HCV replicons. For example, core was found attached to the ER and at the surface of lipid droplets (LDs) (Dubuisson et al., 2002; McLauchlan, 2000). In some conditions, a minor proportion of the core protein was located in the nucleus (Yasui et al., 1998). More recently, the core protein has been found to colocalize with mitochondrial markers in Huh-7 cells containing a full-length HCV replicon (Schwer et al., 2004). However, studies with an infectious HCV system demonstrated that the core protein associates primarily with LDs (Rouille et al., 2006). Maturation of the core protein modulates the trafficking between rough ER membranes, the site of core protein synthesis, and LDs (McLauchlan et al., 2002). It is worth noting that only the mature form of core associates with LDs. Rouille *et al.* showed that core initially attached to a punctate site on droplets after processing by SPP and then

progressively coated the entire organelle (Rouille et al., 2006). The ability of core to coat the entire surface of LDs appears to be important for virus production as mutations that impair this process negatively impact the production of infectious virions (Boulant et al., 2007). Similarly, blocking LD localization of core by disrupting maturation of the protein by SPP almost completely abrogates release/production of infectious virus (Targett-Adams et al., 2008).

LDs are intracellular structures that store neutral lipids. They are typically located throughout the cytoplasm of cells and are associated with the ER membrane. Interestingly, attachment of core changes the intracellular distribution of droplets such that they have a tendency to aggregate towards the periphery of the nucleus (Boulant et al., 2008). This aggregation can be blocked by either disrupting the microtubule network or impairing the function of the dynein motor protein (Boulant et al., 2008). Hence, it is thought that core protein modifies the microtubule-dependent mobility of LDs. The ability of core to modify the distribution of droplets appears to be important for virus production since disrupting the microtubule network reduces virus production.

HCV core protein has long been implicated in disease development through its roles in apoptotic pathways (Benali-Furet et al., 2005) as well as regulating the innate immune response (Miller et al., 2004). Data from many research groups indicate that the HCV core protein interacts with at least 30 different host cell proteins (Table 1.1) in transfected and/or infected cells. In addition, microarray analyses revealed that it directly and/or indirectly regulates the expression of more than 400 human genes (Dominguez-Villar et al., 2007; Nguyen et al., 2006).

Although HCV core protein has been proposed to be involved in apoptosis, tumorigenesis, cell signaling, and lipid metabolism, in most cases, it is not known whether these interactions truly occur in a normal virus infection or are artifacts of ectopic protein overexpression. Further studies with the developed cell culture system for HCV (Lindenbach et al., 2005; Wakita et al., 2005; Zhong et al., 2005) should help clarify whether all the functions identified for HCV core protein can be observed in the context of infected cells.

DENV capsid

A large pool of DENV capsid protein localizes to the nucleus and nucleolus of many infected cell lines (Tadano et al., 1989; Wang et al., 2002). Three putative nuclear localization signal (NLS) motifs are proposed to be present on the capsid protein: ⁶KKAR⁹, ⁷³KKSK⁷⁶, and the bipartite signal ⁸⁵RK⁸⁵egrmlnlnRRRR¹⁰⁰ (Bulich and Aaskov, 1992). Using recombinant DENV capsid proteins expressed in HeLa cells, it was reported that capsid nuclear localization is predominantly due to the bipartite sequence at aa 85-100 (Wang et al., 2002). In contrast, Sangiambut *et al.* demonstrated that at least two NLS regions (⁷³KKSK⁷⁶ and the bipartite sequence ⁸⁵RK⁸⁵egrmlnlnRRRR¹⁰⁰) in DENV capsid protein contribute to nuclear localization during virus infection. Double alanine-substitution mutations in the capsid protein ((K73A, K74A) and (R85A, K86A)) resulted in an elimination of nuclear localization in two mammalian cell lines (Sangiambut et al., 2008). Moreover, both mutants displayed reduced replication in mammalian and mosquito cell lines, but interestingly, there was no

correlation between nuclear localization and viral replication (Sangiambut et al., 2008).

Expression of DENV capsid protein has been reported to sensitize liver HepG2 cells to Fas-dependent apoptosis possibly by a mechanism that involves binding to DAXX in the nucleus (Limjindaporn et al., 2007). DAXX is a Fas-associated pro-apoptotic protein and functions in the Fas-dependent pathway (Yang et al., 1997). It was found that DENV capsid and DAXX were predominantly co-localized in the nucleus of infected HepG2 cells (Limjindaporn et al., 2007) and the loss of nuclear localization of DENV capsid resulted in the disruption of its interaction with DAXX and induction of apoptosis (Netsawang et al., 2010). Based on these observations, the authors proposed that the interaction of DENV capsid and DAXX was critical for apoptosis of DENV infected liver cells. However, there is no direct evidence to suggest that the interaction between capsid and DAXX is directly involved in this process (Limjindaporn et al., 2007; Netsawang et al., 2010). Given that liver damage as a result of virus-induced apoptosis may be a key component of dengue hemorrhagic fever and dengue shock syndrome (Marianneau et al., 1997), the capsid protein may be viewed as an important pathogenic determinant.

DENV capsid protein interacts with several cellular proteins, including histones to inhibit nucleosome formation (Colpitts et al., 2011), hnRNP K to regulate gene transcription (Chang et al., 2001), and Sec3 to nullify the antiviral activity of Sec3 by accelerating its degradation (Bhuvanakantham et al., 2010b; Raghavan and Ng, 2013). The mature form of the DENV capsid protein also

associates with hepatic LDs, and disruption of this process by site-directed mutagenesis of the capsid gene negatively affects the virus replication cycle (Carvalho et al., 2012; Samsa et al., 2009). These results suggest early in the infection pathways, LDs may provide a scaffold for genome encapsidation.

JEV Capsid

Nuclear localization of the JEV capsid protein also appears to be important for viral replication and pathogenesis (Mori et al., 2005). A conserved glycine–proline (GP) motif in the central region of the capsid is essential for nuclear localization of capsid. Recombinant JEV strains with alanine substitution mutations in this motif exhibited reduced replication in mammalian and insect cells. Interestingly, mutations in the GP motif also attenuated the neuroinvasiveness in mice. This study suggested that nuclear localization of the capsid protein was important for pathogenesis of encephalitis, possibly by allowing the virus to breach the BBB. While it is clear that the GP motif is required for neuroinvasion, it remains to be determined if nuclear localization of capsid *per se* is required for neuropathogenesis. The GP motif does not resemble any known nuclear localization signals and it is possible that mutagenesis of the GP codons results in a conformational change that prevents the capsid from exposing the nuclear localization signal and/or potentially activating signaling pathways that result in secretion of neuroinflammatory cytokines such as TNF- α . Recently, a nucleolar phosphoprotein B23 has been reported to interact with the capsid protein of JEV (Tsuda et al., 2006). During JEV infection, a fraction of

B23 translocates from the nucleoli to the cytoplasm and colocalizes with the WT capsid but not with GP-motif mutant capsid at the cytoplasm. Furthermore, overexpression of dominant negative forms of B23 reduced JEV replication (Tsuda et al., 2006). These results suggest that B23 plays an important role in the intracellular localization of the capsid protein and replication of JEV.

Recently, a smaller isoform of capsid protein has been reported in JEV-infected cells, but not in the viral particles (Mori et al., 2007). Generation of this capsid isoform requires the host cysteine protease cathepsin L, which cleaves between amino acid residues Lys18 and Arg19 of capsid protein. It was demonstrated that the replication of the mutant virus resistant to the cleavage of the capsid protein by cathepsin L was impaired in mouse macrophage and neuroblastoma cells. Furthermore, the neurovirulence and neuroinvasiveness of the mutant JEV to mice were lower than those of the WT JEV (Mori et al., 2007). These data suggest that the processing of the JEV capsid protein by cathepsin L is required for robust replication of JEV in both neural and macrophage cells, which leads to the JEV pathogenesis. More recently, it has also been reported that JEV capsid protein inhibits stress granules (SGs) formation through an interaction with Caprin-1, an SG-associated cellular factor (Kato et al., 2013). Knockdown of Caprin-1 abrogates SG inhibition during JEV infection and suppresses viral propagation. Moreover, interaction of the JEV capsid protein with Caprin-1 is important in the pathogenesis in mice through the suppression of SG formation.

1.7.1 Non-structural functions of the WNV capsid protein

The mature capsid protein of WNV is composed of 105 amino acid residues, whereas its precursor, designated immature capsid, contains an additional 18-amino-acid hydrophobic region at its C-terminus (Hunt et al., 2007). This hydrophobic domain serves as a signal peptide for ER translocation of prM and is cleaved by the viral serine protease NS2B/NS3 during the polyprotein processing. In addition to its structural role in nucleocapsid formation, previous studies have indicated that the WNV capsid protein plays various non-structural functions during the virus life cycle. For example, a number of studies have documented that expression of the full-length immature capsid in the absence of other viral proteins results in induction of apoptosis both *in vitro* and *in vivo* through different mechanisms (Bhuvanakantham et al., 2010a; Ko et al., 2010; Oh et al., 2006; van Marle et al., 2007; Yang et al., 2002; Yang et al., 2008) . However, Urbanowski *et al.* recently showed that only the mature capsid was detected in WNV infected cells and expression of the mature capsid blocked apoptosis (Urbanowski and Hobman, 2013). Like other flaviviruses, although WNV replication and assembly occur in the cytoplasm, a large pool of capsid is present in the nuclei of infected cells, which suggests that nuclear targeting of capsid proteins is of fundamental importance to WNV (Westaway et al., 1997a). It has been suggested that nuclear localization of capsids may serve to sequester host factors or disrupt nuclear/cytoplasmic trafficking in a way that benefits virus replication (Bhuvanakantham et al., 2010a; Bhuvanakantham et al., 2009; Hiscox, 2003). Recently, WNV capsid protein has been implicated in induction of

degradation of tight junction membrane components, which facilitates viral neuroinvasion (Medigeshi et al., 2009). Moreover, it is interesting to note that some of the known WNV capsid-binding proteins, I₂^{PP2A}, Jab1, MKRN1 and Sec3 are nuclear proteins and their interactions with capsid have different effects on viral replication (Bhuvanakantham et al., 2010b; Hunt et al., 2007; Ko et al., 2010; Oh et al., 2006; Raghavan and Ng, 2013). The detailed aspects of non-structural functions of the WNV capsid protein are summarized below.

1.7.1.1 Modulation of apoptosis

Infection of WNV in many mammalian cell lines and primary cells has been reported to cause apoptosis (Kleinschmidt et al., 2007; Kobayashi et al., 2012; Medigeshi et al., 2007; Parquet et al., 2001; Smith et al., 2012). Interestingly, numerous studies have implicated the capsid protein is involved in this process (Bhuvanakantham et al., 2010a; Ko et al., 2010; Oh et al., 2006; van Marle et al., 2007; Yang et al., 2002; Yang et al., 2008). Specifically, expression of the capsid in the absence of other viral proteins induces apoptosis or cell cycle arrest in a number of different *in vitro* and *in vivo* systems. For example, transient expression of capsid protein in HeLa cells results in mitochondrial dysfunction and activation of caspase-9 and caspase-3 (Yang et al., 2002). *In vivo*, expression of capsid in the brains and interskeletal muscles of laboratory mice causes local inflammation and apoptotic cell death (Yang et al., 2002). One report identified the nuclear protein HDM2 as a capsid-binding protein (Yang et al., 2008). HDM2 is an E3 ubiquitin ligase that regulates levels of the transcription factor p53.

Inhibition of the E3 ligase activity of HDM2 by capsid results in accumulation of p53 and consequent transcriptional upregulation of Bax and subsequent loss of mitochondrial membrane potential (Yang et al., 2008). In addition, phosphorylation of the capsid protein by protein kinase C (PKC) was demonstrated to enhance its binding to HDM2 and then subsequently induce p53-dependent apoptosis (Bhuvanakantham et al., 2010a). However, all of the studies described above are not biologically relevant because they employed the uncleaved immature form of WNV capsid which does not appear to exist in infected cells (Urbanowski and Hobman, 2013). Mapping studies revealed that the mature capsid lacking the carboxyl-terminal 18 amino acid residues do not bind HDM2 (Yang et al., 2008), which coincidentally, is a region shown to be critical for induction of apoptosis (Oh et al., 2006; Yang et al., 2002; Yang et al., 2008). Together, all the evidence so far supporting that capsid possesses apoptotic ability is not convincing.

The idea that WNV capsid is a pro-apoptotic protein actually conflicts with what is known about the biology of this virus (Bhuvanakantham et al., 2010a; Oh et al., 2006; Yang et al., 2002; Yang et al., 2008). In contrast to other RNA viruses, such as vesicular stomatitis virus (VSV) and Sindbis virus, which replicate rapidly and induce apoptotic cell death much earlier than flaviviruses (Gadaleta et al., 2005; Lopez-Herrera et al., 2009; Pearce and Lyles, 2009), WNV propagates relatively slow and triggers cell death after several rounds of replication, often days after infection. Therefore, it is seemingly detrimental to the virus if the first viral protein generated in cells induces apoptotic cell death. In

fact, a signaling process that involves activation of the pro-survival kinase Akt has been implicated to inhibit apoptosis during the early stages of flavivirus infection (Das et al., 2010; Lee et al., 2005; Scherbik and Brinton, 2010; Yang et al., 2012). Specifically, infection of WNV, DENV, or JEV can enhance the Akt activity within an hour or even minutes. It was further demonstrated that prevention of Akt phosphorylation by blocking the upstream kinase phosphatidylinositol 3-kinase (PI3K) leads to increased activation of caspase-3 and decreased viral titers. Moreover, caspase-3 activation does not occur until later in infection, after the activation of PI3K/Akt has subsided.

In apparent contrast to the previous findings that WNV capsid possesses apoptotic activity, (Bhuvanakantham et al., 2010a; Ko et al., 2010; Oh et al., 2006; Yang et al., 2002; Yang et al., 2008), it was reported that this protein can be stably expressed in mammalian cells (Medigeschi et al., 2009). With respect to the work of Medigeschi *et al.*, the mature WNV capsid (105-amino-acid-residue isoform) was utilized. On the contrary, in studies where capsid was found to induce apoptosis, a full-length capsid (123-amino-acid-residue isoform), which contains the C-terminal 18-amino-acid-residue signal peptide of prM was used for those experiments. However, as the result of coordinated cleavage of the polyprotein between capsid and prM by the NS2B/3 protease, the mature WNV capsid is in fact 105 amino acid residues in size in the context of infection (Amberg and Rice, 1999; Lobigs et al., 2010; Stocks and Lobigs, 1998).

Recently, our laboratory discovered that expression of the mature 105-amino-acid-residue isoform of the WNV capsid blocks apoptosis (Urbanowski

and Hobman, 2013). In this report, only the mature isoform of WNV capsid was detected in infected cells, which is supported by previous studies of flavivirus polyprotein processing kinetics (Amberg and Rice, 1999; Lobigs et al., 2010; Stocks and Lobigs, 1998). The study revealed that the anti-apoptotic activity of capsids is PI3K-dependent, a situation that is consistent with previous studies reporting that elevated activation of Akt occurs shortly after cells are infected with flaviviruses (Das et al., 2010; Lee et al., 2005; Yang et al., 2012). These results strongly suggest that the WNV capsid protein plays an important role in activating pro-survival signaling pathway during virus infection. Moreover, given the fact that only the mature form of WNV capsid protein can be detected in infected cells, it explains why our findings (Urbanowski and Hobman, 2013) differ from those of other studies reporting that the full-length WNV capsid protein induces apoptosis (Bhuvanankantham et al., 2010a; Ko et al., 2010; Oh et al., 2006; Yang et al., 2002; Yang et al., 2008) .

1.7.1.2 Modulation of signaling pathways

In addition to its roles in apoptosis, the WNV capsid protein has also been implicated in other signaling pathways. For example, our laboratory found that WNV capsid expression upregulates phosphatase 2A (PP2A) activity through interaction with I^{2PP2A} , which is an inhibitor of PP2A that is concentrated in the nucleus (Hunt et al., 2007). To our knowledge, this is the first study showing that expression of a flavivirus capsid protein in the absence of other viral proteins is sufficient to increase the PP2A activity. Mapping studies revealed that the capsid-binding site overlaps with the region of I^{2PP2A} that is required for inhibition of

PP2A activity. PP2A has been shown to suppress the transcriptional activity of activator protein-1 (AP-1) (Al-Murrani et al., 1999), a transcription factor that upregulates expression of type I interferon genes (Ludwig et al., 2001). Therefore, it is hypothesized that WNV capsid-mediated downregulation of AP-1 serves to dampen or delay the innate immune response. Moreover, enhanced PP2A activity has also been found in HCV-infected cells (Duong et al., 2004), and is purportedly critical for blocking interferon response.

1.7.1.3 Inhibition of antiviral activity

Recently, it has been reported that WNV and DENV capsid protein negates the antiviral activity of a capsid-interacting cellular protein human Sec3 through the proteasome pathway (Raghavan and Ng, 2013). The Sec3 protein is a component of the human Sec6/8 exocyst complex (Lipschutz and Mostov, 2002). The exocyst complex functions in the secretory pathway and vesicular trafficking, specifically in the tethering and targeting of vesicles to the plasma membrane prior to vesicle fusion (Hsu et al., 1999; TerBush et al., 1996). It has been implicated in many cellular processes such as exocytosis and cell migration and growth (Yeaman et al., 2001; Zhang et al., 2008). Human Sec3 protein is a novel transcriptional and translational repressor of flavivirus and modulates virus production by affecting viral RNA transcription and translation through the sequestration of elongation factor α (EF1 α) (Bhuvanakantham et al., 2010b). WNV and DENV capsid proteins reportedly reduce human Sec3 levels by activation of a chymotrypsin-like proteolytic function of the 20S proteasome.

Physical interaction between capsid proteins and Sec3 was essential to induce Sec3 degradation and the Sec3-binding motif and degradation motif on capsid protein must be intact for efficient flavivirus production (Raghavan and Ng, 2013). These studies not only shed light on the protective role of Sec3 during flavivirus infection, but also indicate that the nonstructural functions of capsid proteins allow flaviviruses to nullify the antiviral activity of Sec3 by accelerating its degradation and facilitating efficient binding of EF1 α with flaviviral RNA genome.

1.7.1.4 Antiviral effects of host proteins that interact with capsid

Cellular mechanisms protective against cytotoxic effect induced by the immature WNV capsid protein have been implicated. For example, one study showed that a WNV capsid-interacting nuclear protein, Jab1, mediates cytoplasmic localization of the mature and immature WNV capsid protein (Oh et al., 2006). They revealed that overexpressed mature or immature WNV capsid was translocated from the nucleolus to the cytoplasm upon its co-expression with Jab1 and Jab1-facilitated nuclear export of both capsids is CRM1 complex dependent. However, Jab1 only promoted the degradation of the immature WNV capsid in a proteasome-dependent way. Recently, another study from the same group has reported that a novel nuclear protein, MKRN1, interacts with and induces degradation of both mature and immature forms of WNV capsid protein by functioning as an E3 ubiquitin ligase (Ko et al., 2010). MKRN1 induces ubiquitination of capsid protein followed by degradation in a proteasome-dependent manner. Finally, overexpression of MKRN1 significantly reduces

WNV titers whereas depletion of this host protein increases virus titers.

Other nonstructural functions of WNV capsid by interacting with host factors have also been implicated. For example, one study showed that importin- α plays an important role in nuclear transport of WNV capsid protein through their direct association (Bhuvanakantham et al., 2009). This interplay is mediated by the consensus sequences of bipartite nuclear localization signal located within the capsid protein. The binding efficiency of the importin- α /capsid interaction influenced the nuclear entry of capsid and virus production (Bhuvanakantham et al., 2009). The other function of WNV capsid such as inducing degradation of tight junction proteins has been described in section 1.6.1.2.

1.8 Objectives of study

Compared with HCV core protein which binds at least 30 host proteins, the list of known WNV capsid interacting proteins is likely incomplete. The main objective of this thesis was to identify novel WNV capsid interacting partners and to investigate the significance of these interactions in virus biology. The first study focused on examining the role of the WNV capsid and the host encoded nucleolar RNA helicase DDX56 interaction in virus assembly/infectivity. The second study was undertaken to investigate the mechanism by which the nucleolar helicase DDX56 functions in morphogenesis of WNV virions. The final study was carried out to study the effect of WNV infection on tight junction membrane proteins that would provide implications for understanding the molecular basis for neuroinvasion.

CHAPTER 2

Materials and Methods

2.1 Materials

2.1.1 Reagents

The following reagents and supplies were purchased from the indicated suppliers and utilized according to the manufacturers' recommendations unless otherwise stated.

Table 2.1 Commercial sources of materials, chemicals, and reagents

<i>Name</i>	<i>Source</i>
40% Acrylamide/Bis-acrylamide solution	Bio-Rad
Acetone (Certified ACS)	Thermo Fisher Scientific
Acid washed glass beads (425-600 micron)	Sigma-Aldrich
Adenine hemisulfate salt	Sigma-Aldrich
Agar	Difco
Agarose, ultrapure, electrophoresis grade	Invitrogen
Amino acid dropout -Leu	BIO 101
Amino acid dropout -Trp	BIO 101
Amino acid dropout -Leu/-Trp	BIO 101
Amino acid dropout -His/-Leu/-Trp	BIO 101
Amino acid dropout -Ade/-His/-Leu/-Trp	BIO 101
Ammonium acetate	Invitrogen
Ammonium chloride	Sigma-Aldrich
Ammonium persulphate	Sigma-Aldrich
Ammonium sulfate	Thermo Fisher Scientific
Ampicillin	Sigma-Aldrich
Bacto-tryptone	Difco
Bacto-yeast extract	Difco
Bafilomycin A	Sigma-Aldrich
Bovine serum albumin (BSA)	Sigma-Aldrich
1-Bromo 3-chloropropane	Sigma-Aldrich
Bromophenol blue	Sigma-Aldrich
Chloroform	Thermo Fisher Scientific
Complete ¹ ™ EDTA-free protease inhibitors	Roche
Crystal violet	Sigma-Aldrich
4',6-diamidino-2-phenylindole (DAPI)	Sigma-Aldrich
DDX56 cDNA	Open Biosystems
DDX56-specific shRNAmir	Open Biosystems
Dimethyl sulphoxide (DMSO)	Sigma-Aldrich
Dithiothreitol (DTT)	Sigma-Aldrich
Doxycycline	Sigma-Aldrich
Dulbecco's modified Eagle's medium	Invitrogen
Dynasore	Sigma-Aldrich
Ethanol	Commercial Alcohols
Ethidium bromide solution	Sigma-Aldrich
Ethylenediaminetetraacetic acid (EDTA)	EMD Chemicals
Fetal bovine serum (FBS)	Invitrogen

Table 2.1 (Continued)

<i>Reagents</i>	<i>Source</i>
Formaldehyde, 37% (v/v)	Sigma-Aldrich
G418 (Geneticin)	Sigma-Aldrich
Glacial acetic acid	Thermo Fisher
Glucose	Thermo Fisher Scientific
Glutathione sepharose 4 fast flow	GE Healthcare
Glycerol	Thermo Fisher Scientific
Glycine	EM Science
Guanidine hydrochloride	Thermo Fisher Scientific
Hydrochloric acid	Thermo Fisher Scientific
Isopropanol	Commercial Alcohols
Isopropanol, molecular biology grade	Sigma-Aldrich
Kanamycin	Sigma-Aldrich
Latrunculin B	Sigma-Aldrich
Lauria broth base	Invitrogen
LB agar	Invitrogen
Leptomycin B	Sigma-Aldrich
L-Glutamine	Invitrogen
L-Histidine	Sigma-Aldrich
Lipofectamine 2000	Invitrogen
L-Leucine	Sigma-Aldrich
Magnesium chloride	EMD Chemicals
2-Mercaptoethanol	Thermo Fisher Scientific
Methanol	Thermo Fisher Scientific
Methylcellulose	Sigma-Aldrich
MG132	Sigma-Aldrich
N,N,N',N',-tetramethylenediamine (TEMED)	Sigma-Aldrich
Nocodazole	Sigma-Aldrich
Non-silencing shRNAmir	Open Biosystems
Nonidet P-40 (NP40)/IGEPAL CA-630	Sigma-Aldrich
OptiMEM	Invitrogen
Paclitaxel	Sigma-Aldrich
Paraformaldehyde	Thermo Fisher Scientific
Penicillin-streptomycin solution (100X)	Invitrogen
Phenol, buffer saturated	Sigma-Aldrich
Phenol: Chloroform: Isoamyl Alcohol	Sigma-Aldrich
Poly-L-lysine	Sigma-Aldrich
Potassium acetate	Anachemia
Potassium chloride	Becton, Dickinson & Company
ProLong Gold Antifade reagent with DAPI	Invitrogen
Protein A-sepharose	GE Healthcare
Protein G-sepharose	GE Healthcare
Puromycin	Sigma-Aldrich
Restore TM Western Blot Stripping Buffer	Pierce
siRNAs Alexa Fluor 488	Qiagen-Xeragon
Skim milk powder	Carnation

Table 2.1 (Continued)

<i>Reagents</i>	<i>Source</i>
SMARTpool [®] siRNA against DDX56	Dharmacon
Sodium azide	Sigma-Aldrich
Sodium chloride	Sigma-Aldrich
Sodium dodecyl sulphate (SDS)	Bio-Rad
Sodium hydroxide	Sigma-Aldrich
Sucrose	EMD Chemicals
Tetracycline-free FBS	Clontech
TRI Reagent or TRIzol	Invitrogen
Tris base	VWR
Triton X-100	VWR International
0.25% Trypsin-EDTA	Invitrogen
Tween 20 (polyoxyethylenesorbitan monolaureate)	Thermo Fisher Scientific
UltraPure distilled water	Invitrogen
X-alpha-Gal	Clontech
Yeast extract	Difco

Table 2.2 Molecular size standards

<i>Marker</i>	<i>Source</i>
GeneRuler 1 kb DNA Ladder	Fermentas
PageRuler Pre-stained Protein Ladder (10-170 kDa)	Fermentas

Table 2.3 DNA/RNA modifying enzymes

<i>Enzyme</i>	<i>Source</i>
Calf intestinal alkaline phosphatase	Invitrogen
DNase I, amplification grade	Invitrogen
Restriction endonucleases	New England BioLabs/ Invitrogen
RNase A	Invitrogen
RNase Out	Invitrogen
T4 DNA ligase	Invitrogen

Table 2.4 Multi-component systems

<i>System</i>	<i>Source</i>
Expand High Fidelity PCR system	Roche
Expand Long Template PCR System	Roche
Fast SYBR Green Master Mix	Applied Biosystems
FuGENE 6 Transfection reagent	Roche
High Capacity RNA-to-cDNA Master Mix	Applied Biosystems
Lipofectamine 2000 Transfection reagent	Invitrogen
Matchmaker pretransformed human cDNA library	Clontech
PerfeCTa SYBR Green SuperMix, UNG, Low Rox	Quanta Biosciences
PerFectin Transfection reagent	Genlantis
Pierce BCA Protein Assay kit	Thermo Scientific
Platinum Taq PCR System	Invitrogen

Table 2.4 (Continued)

<i>System</i>	<i>Source</i>
QIAEX II gel extraction kit	QIAGEN
QIAGEN plasmid maxi kit	QIAGEN
QIAGEN plasmid midi kit	QIAGEN
QIAprep spin miniprep kit	QIAGEN
QIAquick PCR Purification kit	QIAGEN
qScript One-Step SYBR Green qRT-PCR Kit	Quanta Biosciences
SuperScript III Reverse Transcriptase system	Invitrogen
TransIT-293 Transfection reagent	MirusBio

Table 2.5 Detection systems

<i>System</i>	<i>Source</i>
Axioskop2 plus with AxioCam MRC	ZEISS
Axioskop2 with CoolSNAP HQ Photometrics	ZEISS
CFX96	BIO-RAD
Leica TCS SP5	Leica microsystems
Molecular Imager GelDoc™ XR+ imaging system	BIO-RAD
MX3005P	Stratagene
NanoDrop ND-1000 Spectrophotometer	Thermo Scientific
Odyssey Infrared Imaging System	LiCor
PVDF membrane (0.45 μM)	Millipore
Rx film	Fuji
Supersignal West Pico chemiluminescent substrate	Thermo Scientific
Ultraviolet gel transilluminator	Thermo Fisher Scientific
XO-MAT Developer	Kodak

2.1.2 Commonly used Buffers and Solutions

Table 2.6 Buffers and Solutions

<i>Name</i>	<i>Composition</i>
4x SDS Laemmli loading buffer	0.01% bromophenol blue, 40% glycerol, 3.34% (v/v) β-mercaptoethanol, 8% SDS, 200 mM Tris- HCl (pH 6.8)
5x Protein sample buffer	62.5 mM Tris-HCl (pH 6.8), 25% (v/v) glycerol, 2% (w/v) SDS, 0.01% (w/v) bromophenol blue, 5% (v/v) β-mercaptoethanol
5x First strand buffer	250 mM Tris-Cl (pH 8.3), 375 mM KCl, 15 mM MgCl ₂
6 x DNA gel loading buffer	40% (w/v) sucrose, 0.25% (w/v) bromophenol blue, 0.25% (w/v) xylene cyanol FF

Table 2.6 (Continued)

<i>Name</i>	<i>Ingredients</i>
Alkaline lysis buffer	200 mM NaOH, 1% (w/v) SDS
Bacteria resuspension buffer	50 mM Tris-HCl (pH 8.0), 10 mM EDTA, 100 µg/mL RNase A
Cracking buffer	8 M Urea, 5% (w/v) SDS, 40 mM Tris-HCl (pH 6.8), 0.1 mM EDTA, 0.4 mg/ml bromophenol blue
Hepes buffered saline (HEBS)	137 mM NaCl, 5 mM KCl, 6 mM dextrose, 0.7 mM Na ₂ HPO ₄ , 20 mM Hepes, pH 7.0
LB growth media	1% (w/v) Bacto-tryptone, 0.5% (w/v) Bacto-yeast extract, 0.5% (w/v) NaCl, 0.1% (v/v) 1 M NaOH
Neutralization buffer	3.0 M Potassium acetate (pH 5.5)
NP-40 lysis buffer	50 mM Tris-HCl (pH 7.2), 150 mM NaCl, 2 mM EDTA, 1% (v/v) NP-40, 1 mM fresh DTT
Phosphate buffered saline (PBS)	137 mM NaCl, 2.7 mM KCl, 8 mM Na ₂ HPO ₄ (pH 7.4)
PBSCM	137 mM NaCl, 2.7 mM KCl, 8 mM Na ₂ HPO ₄ , 0.5 mM CaCl ₂ , 1mM MgCl ₂ , pH 7.4
PBS-T	137 mM NaCl, 2.7 mM KCl, 8 mM Na ₂ HPO ₄ (pH 7.4), 0.05% (v/v) Tween-20
RIPA buffer	50 mM Tris-HCl (pH 7.5), 150 mM NaCl, 0.1% SDS, 1% Triton X-100, 1% sodium deoxycholate, 5 mM EDTA
SDS-PAGE resolving gel buffer	0.1% SDS, 374 mM Tris-HCl (pH 8.8)
SDS-PAGE running buffer	250 mM glycine, 0.1% SDS, 100 mM Tris Base (pH 8.3)
SDS-PAGE stacking gel buffer	0.1% SDS, 250 mM Tris-HCl (pH 6.8)
TAE	40 mM Tris acetate, 1 mM EDTA (pH 8.0)

Table 2.6 (Continued)

<i>Name</i>	<i>Ingredients</i>
Tris-buffered saline (TBS)	137 mM NaCl, 2.7 mM KCl, 24 mM Tris-HCl (pH 7.4)
TBS-T	137 mM NaCl, 2.7 mM KCl, 24 mM Tris-HCl (pH 7.4), 0.05% (v/v) Tween 20
TE	1 mM EDTA, 10 mM Tris-HCl, pH 7.5
Transfer buffer	200 mM glycine, 25 mM Tris base (pH 8.3), 20% (v/v) methanol, 0.1% (w/v) SDS

2.1.3 Yeast strains and media

Saccharomyces cerevisiae strains AH109 and Y187 were purchased from Clontech. Yeast liquid and solid media used for two-hybrid screening are described in Matchmaker™ Pretransformed Libraries User Manual. (www.clontech.com/xxclt_ibcGetAttachment.jsp?cItemId=17603)

2.1.4 Oligonucleotides

Table 2.7 Oligonucleotides

<i>Primer name</i>	<i>Sequence (5'-3')</i>	<i>Engineered sites*</i>	<i>Usage</i>
DNA-BD-Capsid-F	GAAGGAATTCATGTCTAAGAA ACCAG	EcoRI	Cloning
DNA-BD-Capsid-R	CGGTCTGCAGCTATCTTTTCTT TTG	PstI	Cloning
DDX56-myc-F	CTATGAATTCGCCACCATGG AGGACTCTGAAGCACTG	EcoRI	Cloning
DDX56-myc-R	GCGTGGATCCGGAGGGCTTGG CTGTGGGTCTG	BamHI	Cloning
WNV-env F	TCAGCGATCTCTCCACCAAAG		qRT-PCR

Table 2.7 (Continued)

<i>Primer name</i>	<i>Sequence (5'-3')</i>	<i>Engineered sites*</i>	<i>Usage</i>
WNV-env R	GGGTCAGCACGTTTGTTCATTG		qRT-PCR
Cyclophilin F	TCCAAAGACAGCAGAAA TTCG		qRT-PCR
Cyclophilin R	TCTTCTTGCTGGTCTTGCCATT CC		qRT-PCR
GAPDH F	ACCACAGTCCATGCCATCAC		Semi qRT-PCR
GAPDH R	TCCACCACCCTGTTGCTGTA		Semi qRT-PCR
DDX56 F	CTATGAATTCGCCACCATGGA GGACTCTGAAGCACTG		Semi qRT-PCR
DDX56 R	GCGTGGATCCAAGGGTAACC GGGTTATGTAA		Semi qRT-PCR
NotI-F	ACTCGAGCGGCCGCACT GTGCTGGATATC	Not I	Cloning
MluI-R	GCGTACGCGTTCACAGATCCT CTTCTGAGATGAG	Mlu I	Cloning
RNAi resistant-F	GCTGATATTACATAACCCAGT AACGCTCAAATTGCAGGA GTCCCAGCTGCCTG		Cloning
RNAi resistant-R	CAGGCAGCTGGGACTCCTGCA ATTTGAGCGTACTGGGT ATGTAATATCAGC		Cloning
D166N-F	GCTTTTGGTGGTGAACGAAGC TGACC		Cloning
D166N-R	GGTCAGCTTCGTTACCACCA AAAGC		Cloning
E167Q-F	CTTTTGGTGGTGGACCAAGCT GACCTTC		Cloning
E167Q-R	GAAGGTCAGCTTGGTCCACCA CCAAAAG		Cloning
SpeI-F	CTATACTAGTCCGCCACCATG GAGGACTCTG	Spe I	Cloning

Table 2.7 (Continued)

<i>Primer name</i>	<i>Sequence (5'-3')</i>	<i>Engineered sites*</i>	<i>Usage</i>
XhoI-R	CGGTCTCGAGTCACAGATC CTCTTCTGAG	Xho I	Cloning
SpeI-EcoRV-F	CTATACTAGTACTGTGCTG GATATCTGCAG	SpeI, EcoRV	Cloning
DDX56-F	CTATGAATTCGCCACCATGGA GGACTCTGAAGCACTG	EcoR I	Cloning
DDX56-R	GCGTGGATCCGGAGGGCTTGG CTGTGGGTCTG	BamH I	Cloning
NT-R	GCGTGGATCCAAGGGTAAC CGGGTTATGTAA	BamH I	Cloning
CT-F	CTATGAATTCGCCACCATGAA GTTACAGGAGTCCCAG	EcoR I	Cloning
WNV-env-F	TCAGCGATCTCTCCACCAAAG		qRT-PCR
WNV-env-R	GGGTCAGCACGTTTGTTCATTG		qRT-PCR
Cyclophilin-F	TCCAAAGACAGCAGAAAA CTTTCG		qRT-PCR
Cyclophilin-R	TCTTCTTGCTGG TCTTGC CATTCC		qRT-PCR
Claudin-1 Forward	CCAACGCGGGGCTGCAGCT		qRT-PCR
Claudin-1 Reverse	TTGTTTTTCGGGGACAGGA		qRT-PCR
Claudin-3 Forward	CTGCTCTGCTGCTCGTGTCC		qRT-PCR
Claudin-3 Reverse	TTAGACGTAGTCCTTGCGGTC GTAG		qRT-PCR
Claudin-4 Forward	GGCTGCTTTGCTGCAACTGTC		qRT-PCR
Claudin-4 Reverse	GAGCCGTGGCACCTTACACG		qRT-PCR
Occludin Forward	TCAAACCGAATCATTATGCAC CA		qRT-PCR

Table 2.7 (Continued)

<i>Primer name</i>	<i>Sequence (5'-3')</i>	<i>Engineered sites*</i>	<i>Usage</i>
Occludin Reverse	AGATGGCAATGCACATCACA A		qRT-PCR
JAM1 Forward	ACCAAGGAGACACCACCAGA C		qRT-PCR
JAM1 Reverse	GAGGCACAAGCACGATGAGC		qRT-PCR
ZO-1 Forward	CAAGATAGTTTGGCAGCAAG AGATG		qRT-PCR
ZO-1 Reverse	ATCAGGGACATTCAATAGCGT AGC		qRT-PCR
GAPDH Forward	GAAATCCCATCACCATCTTCC AGG		qRT-PCR
GAPDH Reverse	GAGCCCCAGCCTTCTCCATG		qRT-PCR
WNV Forward	TCTGCGGAGAGTGCAGTCTGC GAT		qRT-PCR
WNV Reverse	TCAGCGATCTCTCTC CACCAAAG		qRT-PCR

* Restriction sites in the sequences are underlined.

2.1.5 Antibodies

Table 2.8 Primary antibodies

<i>Antibody</i>	<i>Dilution</i>	<i>Application*</i>	<i>Source</i>
Mouse anti-DDX56	1:3000, 1:500,1:500	WB, IF, IP	PROGEN Biotechnik
Human anti-DV2	1:2500	IF	Dr. Robert Anderson, Dalhousie University
Mouse anti-WNV NS3	1:3000, 1:1000	WB, IF	R&D systems
Mouse anti-WNV NS3/2b	1:500	IF	R&D systems
Rabbit anti-nucleolin	1:1000	IF	Abcam
Mouse anti- β -actin	1:4000	WB	Abcam
Mouse anti-RNA helicase A	1:2000	WB	Abcam
Rabbit anti-GAPDH	1:3000	WB	Abcam
Mouse anti-GST	1:5000	WB	Sigma-Aldrich
Rabbit anti-GST	1:3000	WB	Abcam
Rabbit anti-WNV capsid	1:3000, 1:300,1:500	WB, IF, IP	This laboratory
Guinea pig anti-WNV capsid	1:4000, 1:1000	WB, IF	This laboratory
Guinea pig anti-DV2 capsid	1:4000, 1:1000	WB, IF	Pocono Rabbit Farm & Laboratory
Rabbit anti-RV capsid	1:1000, 1:300	WB, IF	This laboratory
Mouse anti-myc (9E10)	1:3000, 1:800,1:500	WB, IF, IP	ATCC
Mouse anti-claudin-1	1:3000, 1:500	WB, IP	Invitrogen
Mouse anti-claudin-1	1:300	IF	Santa Cruz Biotechnology
Mouse anti-occludin	1:3000, 1:300	WB, IF	Invitrogen

Table 2.8 (Continued)

<i>Antibody</i>	<i>Dilution</i>	<i>Application*</i>	<i>Source</i>
Rabbit anti-JAM-1	1:2500, 1:300,1:500	WB, IF, IP	Invitrogen
Mouse anti-HA	1:1000	WB	Abcam
Rabbit anti-GFP	1:20000	WB	Dr. L.G. Berthiaume, University of Alberta

* WB: Westernblot; IP: immunoprecipitation; IF: immunofluorescence

Table 2.9 Secondary antibodies

<i>Antibody::Conjugate</i>	<i>Dilution</i>	<i>Application*</i>	<i>Source</i>
Goat anti-mouse::HRP	1:5000	WB	Jackson ImmunoResearch Laboratories
Goat anti-rabbit::HRP	1:5000	WB	Jackson ImmunoResearch Laboratories
Donkey anti-mouse::Alexa680	1:10000	WB	Invitrogen
Donkey anti-rabbit::Alexa800	1:10000	WB	Invitrogen
Donkey anti-rabbit::Alexa647	1: 500	IF	Invitrogen
Chicken anti-mouse::Alexa594	1: 500	IF	Invitrogen
Goat anti-mouse::Alexa647	1: 500	IF	Invitrogen
Donkey anti-mouse::Alexa488	1: 500	IF	Invitrogen
Donkey anti-rabbit::Alexa488	1: 500	IF	Invitrogen
Donkey anti-mouse::Alexa546	1: 500	IF	Invitrogen
Goat anti-guinea pig::Alexa488	1: 500	IF	Invitrogen
Goat anti-guinea pig::Alexa546	1: 500	IF	Invitrogen
Donkey anti-human::TexasRed	1: 500	IF	Jackson ImmunoResearch Laboratories

* WB: Westernblot, IF: immunofluorescence

2.1.6 Cell lines and viruses

2.1.6.1 Cell lines

A549 (human alveolar basal epithelial), BHK-21 (baby hamster kidney), CACO-2 (human colon carcinoma), HEK293T (human embryonic kidney) and MDCK (Madin-Darby canine kidney) cells were purchased from the American Type Culture Collection (Manassas, VA). Primary HUVEC (human umbilical vein endothelial) cells were obtained from Dr. Denise Hemmings (Obstetrics & Gynaecology, University of Alberta).

2.1.6.2 Viruses

WNV strain NY99 and DENV-2 were provided by Dr. Mike Drebot (Public Health Agency of Canada, Winnipeg, MB). The M33 strain of Rubella virus was obtained from Dr. S. Gillam (University of British Columbia, Vancouver, BC).

2.2 Methods

2.2.1 Molecular Biology

2.2.1.1 Isolation of plasmid DNA from *Escherichia coli*

Small scale and large-scale isolation of plasmid DNA were performed using QIAprep spin mini prep kit and QIAGEN plasmid midi/maxi kits (Table 2.4) respectively following manufacturer's recommendations. The concentrations of the plasmid DNAs were determined using a NanoDrop ND-1000 Spectrophotometer (Table 2.5). When not in use, DNA samples were stored at -20°C.

2.2.1.2 Polymerase chain reaction (PCR)

DNA was amplified using the Expand High Fidelity PCR system (Table 2.4), Platinum *Taq* (Table 2.4) or the Expand Long Template PCR system (Table 2.4). A typical reaction (50 μ L) contained 50-200 ng of plasmid DNA template, 200 nM of forward and reverse primers, 200 nM of each dNTP and 2.5-5 U of polymerase. Reactions were performed for 30 to 35 cycles in a TC-312 thermocycler (Techne).

2.2.1.3 Restriction endonuclease digestion

Reactions were typically performed in a volume of 20 μ L containing 0.5 - 3 μ g of plasmid DNA and 2 - 10 U of restriction endonuclease in the appropriate reaction buffer (Table 2.3).

2.2.1.4 Agarose gel electrophoresis

Electrophoresis grade agarose [0.8%-1.5% (w/v)] was dissolved by heating in TAE buffer (Table 2.6). Prior to pouring the gel into the casting tray, ethidium bromide was added to a final concentration of 0.5 μ g/mL. After setting, the gel was immersed in TAE and the DNA samples were mixed with 6x DNA gel loading buffer (Table 2.6) and then separated in the agarose gel. DNA fragments were visualized using an Ultra-violet gel transilluminator (Table 2.5) or images captured using a Molecular Imager GelDoc XR+ imaging system (Table 2.5).

2.2.1.5 Purification of DNA fragments

A QIAquick PCR purification kit (Table 2.4) was used to purify PCR products for subsequent endonuclease digestion. Following endonuclease

digestion, DNA fragments were separated by agarose gel electrophoresis and the bands of interest were excised from the gel with a clean razor blade. DNA fragments were then eluted from the agarose gel using the QIAEX II gel extraction kit (Table 2.4).

2.2.1.6 Ligation of DNA

DNA inserts and vectors were combined in molar ratios ranging from 3:1-6:1, typically using a minimum of 20 ng of vector DNA and 1–5 U of T4 DNA ligase (Table 2.3). Reaction volumes were kept minimal, typically not exceeding 15 μ L, and performed for at least 30 minutes at room temperature (for cohesive-end ligations) or overnight at 16°C (for blunt-end ligations). To reduce occurrences of vector self-ligation, vector DNA was dephosphorylated using calf intestinal alkaline phosphatase (Table 2.3) according to manufacturer's recommendations.

2.2.1.7 Transformation of *Escherichia coli*

SubCloning Efficiency DH5 α competent (Invitrogen) *E. coli* was used during the course of this work. Chemically competent cells were transformed and cultured following the manufacturer's recommendations.

2.2.2 Construction of recombinant plasmids

Recombinant plasmids as described below were constructed using PCR and standard subcloning techniques. All primers used for the construction of the plasmids are listed in Table 2.7. The authenticity of all plasmid constructs was verified by DNA sequencing at The Applied Genomics Centre (TAGC,

Department of Medical Genetics, University of Alberta).

2.2.2.1 Capsid expression plasmids

To construct the bait plasmid pGBKT7-Capsid, which was used for yeast two-hybrid screening, the cDNA for the mature WNV capsid protein (amino acid [aa] residues 1 to 105) was amplified by PCR with primers DNA-BD-Capsid-F and DNA-BD-Capsid-R (Table 2.7) using the template plasmid pBR-5'Eg101, which encodes the 5' region of the Eg101 WNV genome (Hunt et al., 2007). The resulting PCR product was digested with EcoRI and PstI and then subcloned into the bait vector pGBKT7 (Clontech). To construct lentiviral plasmid encoding WNV capsid, a PCR-generated WNV capsid cDNA was subcloned into the SpeI and XhoI sites of the plasmid pTRIP-CMV-MCS-IRES-AcGFP; which was derived by replacing the red fluorescent protein cassette of pTRIP-CMV-IRES-tagRFP (Schoggins et al., 2011) with AcGFP using NheI and SacII. The resulting plasmid pTRIP-IRES-AcGFP-Cap (Urbanowski and Hobman, 2013), directs independent expression of AcGFP and capsid. Other WNV capsid expression plasmids in mammalian cells including pCMV5-Capsid and pEBG-GST-Capsid have been described previously (Hunt et al., 2007).

2.2.2.2 DDX56 expression plasmids

The cDNA encoding full-length human DDX56 (aa 1 to 547) was amplified by PCR using pCMV-SPORT6-DDX56 (clone ID 345647; Open Biosystems) as a template and the primer pair DDX56-myc-F and DDX56-myc-R (Table 2.7). The resulting product was digested with EcoRI and BamHI and then subcloned into the vector pcDNA3.1(-)-myc-His A (Invitrogen) to yield

pcDNA3.1(-)/DDX56-myc.

2.2.2.3 RNAi-resistant and DEAD box mutants of DDX56

Constructs encoding myc-tagged RNAi resistant forms of DDX56 were generated using the overlap extension PCR method. For the first PCR, the plasmid pcDNA3.1(-)-DDX56-myc served as the template. Primer pairs used for the first PCR were NotI-F and RNAi-resistant-R and MluI-R and RNAi-resistant-F (Table 2.7). The RNAi-resistant mutations were designed based on the target sequence recognized by the DDX56-specific shRNAmir-353980 targeting sequence as shown in Figure 4.1. The product of the overlap PCR which was amplified using primers NotI-F and MluI-R was subcloned into the NotI and MluI sites of pLVX-Tight-Puro (Clontech) to produce pLVX-DDX56-wt-RNAi-R. To generate RNAi-resistant DEAD box mutants of DDX56, the wild type RNAi resistant DDX56 cDNA produced as described above was subjected to PCR using the primer pair NotI-F/MluI-R together with primers that introduce mutations into the DEAD box motif (D166N-F and D166N-R; E167Q-F and E167Q-R) (Table 2.7). The resulting cDNAs (D166N and E167Q) were then subcloned into the NotI and MluI sites of pLVX-Tight-Puro to produce pLVX-DDX56-D166N-RNAi-R and pLVX-DDX56-E167Q-RNAi-R, respectively. The cDNAs encoding RNAi-resistant wild type, D166N and E167Q DDX56 were excised from the pLVX plasmids and sub-cloned into the SpeI and XhoI sites of the lentiviral vector pTRIP-CMV-MCS-IRES-AcGFP (Section 2.2.2.1). The resulting plasmids pTRIP-AcGFP-DDX56-wt, D166N, and E167Q-RNAi-R, respectively, direct independent expression of AcGFP and DDX56 wild type and mutants. The

plasmid pTRIP-AcGFP-DDX56-wt-RNAi-S (sensitive) was created by ligation of a cDNA encoding wild type myc-tagged DDX56 into the SpeI and XhoI sites of pTRIP-IRES-AcGFP.

2.2.2.4 DDX56 N- and C-terminal constructs

DNA fragments encoding myc-tagged amino acid residues 1–218 and 219–547 of DDX56 were generated by PCR with primers pairs DDX56-F/DDX56-NT-R and DDX56-CT-F/DDX56-R, respectively using the plasmid pcDNA3.1(-)-DDX56-myc (Section 2.2.2.2) as template. The resulting cDNAs were ligated into the EcoRI and BamHI sites of the mammalian expression vector pcDNA3.1(-)-myc (Invitrogen). Myc-tagged DDX56-NT and DDX56-CT cDNAs produced by PCR using primers SpeI-EcoRV-F and XhoI-R were also ligated into the SpeI and XhoI sites of the lentiviral vector pTRIP-CMV-MCS-IRES-AcGFP (Section 2.2.2.1).

2.2.3 Yeast two-hybrid Screening

Yeast two-hybrid screening was performed with the Matchmaker™ GAL4 Yeast Two-Hybrid System 3 using a pre-transformed normalized human universal cDNA library (Clontech). In brief, the bait plasmid pGBKT7-Capsid was transformed into yeast strain AH109 and transformants were mated with Y187 that had been pre-transformed with the human universal cDNA library. Candidates for two-hybrid interaction were initially selected on medium-stringency selection SD medium (-His, -Leu, and -Trp) and further confirmed on high-stringency selection SD medium (-Ade, -His, -Leu, and -Trp) containing X-alpha-gal (4 mg/mL). The prey plasmids were isolated from positive blue clones

and then retransformed with or without pGBKT7-Capsid into AH109 for further interaction confirmation. Clones that grew on the high-stringency selection SD plate (-Ade, -His, -Leu, and -Trp) containing X-alpha-gal only in the presence of pGBKT7-Capsid were characterized by restriction endonuclease digestion and DNA sequencing using the 5'-T7 Sequencing Primer (5-TAATACGACTCACTATAGGGC-3). Sequences were compared to those in the GenBank database. Detailed yeast two-hybrid screening techniques are described in Matchmaker™ Pretransformed Libraries User Manual. (www.clontech.com/xxclt_ibcGetAttachment.jsp?cItemId=17603)

2.2.4 Cell culture and transfection

2.2.4.1 Cell line maintenance

A549, BHK21, CACO-2, HEK293T and MDCK cells were cultured in Dulbecco's modified Eagle's medium (DMEM) containing 10% heat-inactivated FBS, 4.5 g/L D-glucose, 2 mM glutamine, 25 mM HEPES (pH 7.4), 110 mg/L sodium pyruvate, 1% penicillin-streptomycin. HUVECs were cultured in M199 containing Earle's salts, 10% heat-inactivated FBS, L-glutamine, NaHCO₃, 1% penicillin-streptomycin plus 1% of endothelial cell growth supplement. HUVEC were passaged in 0.2% gelatin-coated flasks. Cells were incubated at 37°C in a humidified atmosphere with 5% CO₂.

2.2.4.2 Transient transfection of cell lines

HEK293T cells were transiently transfected with plasmid DNA using PerFectin or TransIT®-293 transfection reagent as described by the manufacturers. A549 cells were transiently transfected using Lipofectamine 2000.

Twenty-four hours prior to transfection, cells (1.5×10^5) were seeded in 35mm dishes. Cells were then transfected with 1 μ g of plasmid DNA and 2.5 μ L of Lipofectamine 2000 in 1 mL of OptiMEM per dish. Cells were incubated with the DNA-lipocomplexes for 4 hours, after which the medium was replaced with fresh culture medium without antibiotics. When experiments were performed in other culture dish formats, the amounts of plasmid DNA and Lipofectamine 2000 were scaled up or down according to the surface area of the dish. Transfected cells were processed for experimental analysis 24-72 hours post-transfection as indicated.

2.2.5 RNA interference

To transiently knock down of DDX56, A549 or HEK 293T cells were transfected with ON-TARGET plus SMARTpool[®] siRNA specific for human DDX56 mRNA (Table 2.1) or non-silencing control siRNAs Alexa Fluor 488 (Table 2.1). The siRNAs (200 nM, final concentration) were mixed with Lipofectamine reagent prior to addition to cells. Cells were then processed for immunoblot analysis 24-96 hours post-transfection as indicated.

Stable cells lines with reduced levels of DDX56 were constructed by transduction with lentiviruses encoding a DDX56-specific shRNAmir (clone Id V3LHS_353977, Table 2.1). A negative control cell line was established by transducing with a lentivirus encoding a non-silencing shRNAmir (Cat. # RHS4346, Table 2.1). The pGIPZ plasmid containing shRNAmir constructs was co-transfected together with psPAX2 and pMD2.G into HEK 293T cells. The psPAX2 and pMD2.G plasmids encode retroviral packaging components and the

vesicular stomatitis G protein respectively. They were developed in the laboratory of Dr. Didier Trono (École Polytechnique Fédérale De Lausanne) and are distributed by Addgene Inc. After 48 hours, virus-containing supernatants were used to transduce HEK 293T or A549 cells. Puromycin (1 µg/mL) was added to the transduced cells after 48 hours. Puromycin-resistant cells were maintained in 0.25 µg/mL of puromycin.

2.2.6 Virology techniques

2.2.6.1 Virus infection

WNV and DENV-2 infection: WNV (strain NY99) manipulation was performed in the Glaxo CL-3 facility (University of Alberta) and DENV-2 was handled under CL-2 conditions. WNV or DENV-2 stocks were diluted with cell culture media without FBS and antibiotics and then added to cells that had been washed with PBS. Cells were incubated with the virus for 2-4 hours at 37°C after which time the inoculum was replaced with normal growth media. Infected cultures were kept at 37°C until experimental analyses. Cells were infected with viruses at multiplicity of infection (MOI) of 2-5.

Rubella virus (RV) infection: For experiments involving infection with RV, cells in 35 mm dishes were grown to 80% confluence and then infected with 1 mL of the diluted virus at a MOI of 2 for 4 hours at 35°C after which time the inoculum was replaced with normal growth media. Infected cultures were kept at 35°C until experimental analyses.

2.2.6.2 Pelleting of WNV virions by ultracentrifugation

To recover WNV particles from infected cells, media from infected cells

were pre-cleared of cell debris by centrifugation for 10 min at $2,500 \times g$ after which the resulting supernatants were passed through 0.45- μm filters. Virus was inactivated by exposure to ultraviolet light in the biosafety cabinet for 1 h to allow transport of the material out of the level 3 facility. WNV virions were then recovered from the clarified media by centrifugation at $100,000 \times g$ for 1 hour.

2.2.6.3 WNV plaque assay

The day before infection, BHK21 cells (2×10^5 per well) were seeded into six-well plates. Culture supernatants from WNV-infected A549 or HEK293T cells were 10-fold serially diluted in serum-free DMEM on ice. To each well, 200 μL of virus-containing dilution was added, and plates were placed in a 37°C with 5% CO_2 incubator for 1 h with occasionally mixing. After 1 h, 2.5 mL of DMEM containing 2% methylcellulose and 2% FBS was added to each well. After 5 days, cells were fixed with 50% v/v methanol for 4 hours, and then stained with 1% w/v crystal violet in 20% v/v methanol for 2 hours. The cells were then rinsed with water and the number of plaques in each well was counted.

2.2.6.4 RV plaque assay

BHK21 cells (4×10^5 cells/well) were infected with serial dilutions of virus stocks in six-well plates for 4 hours. Cells were then washed and overlaid with warm 0.5% (w/v) agarose in culture medium and incubated at 35°C in a 5% CO_2 atmosphere for 6 days. Viral plaques were visualized by staining with 0.05% (w/v) crystal violet in 17% (v/v) methanol for 2 hours at room temperature (RT).

2.2.6.5 Preparation and use of lentiviruses

2.2.6.5.1 Production and use of lentiviruses encoding WNV capsid

To produce infectious lentiviral pseudoparticles, HEK293T cells (2.5×10^6) grown in 100 mm-diameter dishes were co-transfected with pTRIP-IRES-AcGFP-Cap (5.6 μ g, section 2.2.2.1) or pTRIP-IRES-AcGFP (5.6 μ g, section 2.2.2.1), pGag-Pol (5.6 μ g) and pHCMV-VSVG (1.6 μ g) (Schoggins et al., 2011) using Fugene 6 transfection reagent. Forty eight hours later, polybrene (4 μ g/mL) and HEPES (20 mM, pH 7.4) were added to harvested lentivirus-containing cell culture supernatants which were then passed through 0.45 μ m filter, aliquotted and then stored at -80°C or used to transduce CACO-2 or MDCK cells in 6 well dishes. Typically, lentiviral stocks were diluted 1:10 in DMEM containing 3% FBS, polybrene (4 μ g/mL polybrene) and HEPES (20 mM). Cells were then spinoculated by centrifugation at 1200 rpm in an Eppendorf A-4-62 rotor for 1 h at 37°C after which the plates were transferred to a 37°C incubator. After 6 h, the media were replaced with DMEM containing 10% FBS. Unless otherwise indicated, transduced cells were analyzed 48 h post-transduction.

2.2.6.5.2 Production of lentiviruses for expression of DDX56 mutants

HEK293T cells (2.5×10^6) in 100 mm dishes were co-transfected with pTRIP-AcGFP plasmids encoding myc-tagged DDX56 cDNAs (WT, D166N, E167Q, NT or CT, sections 2.2.2.2-2.2.2.4), pGag-Pol (5.6 μ g) and pHCMV-VSVG (1.6 μ g) using TransIT®-293 transfection reagent. Forty-eight hours later, polybrene (4 μ g/mL) and HEPES (20 mM) were added to the lentivirus-

containing culture supernatants which were then passed through 0.45 μm filter before aliquotting. Stocks were stored at -80°C or used immediately to transduce HEK293T or A549 cells. Typically, lentiviral stocks were diluted 1:10 in DMEM containing 3% FBS, polybrene (4 $\mu\text{g}/\text{mL}$) and HEPES (20 mM). Cells were then spinoculated by centrifugation at 1200 rpm for 1 h at 37°C after which the plates were transferred to a 37°C incubator. Six hour later, the media was replaced with DMEM containing 10% FBS. Transduced cells were analyzed 48 h post-transduction.

2.2.6.5.3 Production of lentiviruses for knocking down DDX56

To construct stable cells lines with reduced levels of DDX56, lentiviruses encoding a DDX56-specific shRNAmir were produced as described in section 2.2.5.

2.2.7 Microscopy

2.2.7.1 Indirect Immunofluorescence

A549, CACO-2 and MDCK cells cultured on glass coverslips were processed for indirect immunofluorescence microscopy after 24, 48, or 72 hours post-infection, post-transfection or post-transduction as indicated. Cells were washed twice with PBS containing 0.5 mM Ca^{2+} and 1.0 mM Mg^{2+} (PBSCM) (Table 2.6) and then fixed in 4% (w/v) paraformaldehyde for 20 minutes, followed by quenching with PBS containing 50 mM ammonium chloride. Fixed cells were rinsed with PBSCM three more times prior to permeabilization with PBS containing 0.2% (v/v) TritonX-100 for 5 minutes. Following permeabilization, coverslips were rinsed three times with

PBSCM and then blocked for 30 minutes in PBSCM solution containing 1% BSA at RT. For samples that were to be incubated with rabbit anti-JAM-1, cells were fixed with ethanol at 4°C for 30 minutes followed by treatment with cold acetone for 5 minutes at RT. Primary antibody (diluted as indicated in Table 2.8) incubations were performed in PBSCM containing 1% BSA for 2 hours at RT or overnight at 4°C. Following primary antibody incubation, coverslips were washed three times in PBSCM while rocking for a total of 1 hour. Secondary antibody (Table 2.9) incubations were performed in PBSCM for 1 hour at RT followed by three additional PBSCM washes, for a total of one hour. Coverslips were mounted onto microscope slides using ProLong Gold anti-fade reagent with DAPI. Samples were then examined using Leica TCS SP5 confocal microscope or a Zeiss Axioskop2 microscope equipped with a CoolSNAP HQ digital camera (Photometries). Captured images were processed using Image-Pro MC5.1, Image J, and LAS AF Lite software.

2.2.8 Protein gel electrophoresis and detection

2.2.8.1 Preparation of protein samples

Virus-infected or lentivirus-transduced cells were washed twice with cold PBS on ice, and then lysed in RIPA buffer (Table 2.6) containing a cocktail of protease inhibitors. Cell lysates were incubated on ice for 30 min and then centrifuged at 12,000 x g for 15 min at 4°C after which protein concentrations in the supernatants were quantified by BCA protein assay according to the manufacturer's recommendation. Equivalent amounts of proteins (20 µg/sample) were resolved by SDS-PAGE, transferred to immobilon-polyvinylidene fluoride

(PVDF) membranes and then detected by immunoblotting as described below.

2.2.8.2 Sodium dodecyl-sulphate polyacrylamide gel electrophoresis (SDS-PAGE)

Proteins were separated by discontinuous gel electrophoresis (5% stacking gel and 8%, 10% or 12% resolving gels). Stacking gels were prepared by adding acrylamide/bis-acrylamide, to final concentration of 5%, to 125 mM Tris-HCl (pH 6.0) with 0.1% SDS, 0.1% ammonium persulphate and 0.1% TEMED. Resolving gels were prepared by combining acrylamide/bis-acrylamide, to an appropriate final concentration, in 375 mM Tris-HCl (pH 8.8), 0.1% SDS, 0.1% ammonium persulphate and 0.1% TEMED. Protein samples were mixed with 5x protein sample buffer (Table 2.6) and denatured at 95°C for 10 minutes. Electrophoresis was performed using the Bio-Rad Mini-Protean III system with SDS-PAGE running buffer (Table 2.6) at 80–120 volts. After electrophoresis, the gels were processed for immunoblot analysis as described below (Section 2.2.8.3).

2.2.8.3 Immunoblot analysis

Following SDS-PAGE, proteins in the gels were transferred to 0.45 µm PVDF membranes. PVDF membranes were first activated in methanol and then equilibrated in Transfer Buffer (Table 2.6) for at least 10 minutes with rocking. Protein transfer was carried out using western blot transfer buffer, pre-chilled to 4°C and a Mini Trans-Blot Electrophoresis transfer cell apparatus (Bio-Rad) at constant current (320 mA) for at least 1.5 hour at 4°C or in an ice-filled bucket. Following completion of the transfer the membranes

were air-dried, re-wet with methanol, and then blocked in PBS-T or TBS-T (Table 2.6) containing 5% (w/v) skim milk powder for at least 1 hour on a rocking device. PBS-T was used preferentially throughout the immunoblot procedure when blots were to be imaged using the Odyssey Infrared scanner (LiCor); however, when blots were developed using horseradish peroxidase-conjugated secondary antibodies, TBS-T was used interchangeably. Membranes were incubated with primary antibodies diluted (as described in Table 2.8) in PBS-T containing 5% (w/v) skim milk powder for 3 hours at room temperature or overnight at 4°C. After three washes with PBS-T at room temperature for a total of 1 hour, the membranes were incubated in the secondary antibody diluted (as indicated in Table 2.9) in PBS-T containing 2% (w/v) skim milk powder for 1 hour at room temperature. Lastly, membranes were washed three times with PBS-T for a total of 1 hour and then detected as described below (Section 2.2.8.4 or 2.2.8.5).

2.2.8.4 Detection of horseradish peroxidase-conjugated secondary antibodies

Membranes were incubated in Supersignal West Pico chemiluminescent substrate (Table 2.5) for 1-2 minutes, after which they were exposed to Rx film (Table 2.5).

2.2.8.5 Detection of fluorophore-conjugated secondary antibodies

Membranes were rinsed with PBS and then placed, face-down, on the scanner bed of an Odyssey Infrared Imaging system (Table 2.5). The membranes were scanned at 84 μm resolution on a quality setting of “High”. Quantification of the proteins was performed by following the protocol posted

at <http://biosupport.licor.com> using Odyssey Infrared Imaging System 1.2 Version software.

2.2.9 Biochemical analysis of protein-protein interactions

2.2.9.1 Co-immunoprecipitations

Capsid-DDX56 immunoprecipitation: HEK293T cells (3×10^5) in 60 mm culture dishes were infected with NY99 strain of WNV (MOI=2-5) or HEK293T (1.2×10^6) cells in 100 mm diameter dishes were transiently transfected with pCMV5-capsid (Section 2.2.2.1), pcDNA3.1(-)/DDX56-myc (Section 2.2.2.2), DDX56 mutants (D166N, E167Q) (Section 2.2.2.3), or DDX56 N- and C-terminal constructs (DDX56-NT, DDX56-CT) (Section 2.2.2.4) using PerFectin reagent as described in 2.2.4.2. After 48 hours, cells were washed with PBS and then lysed with NP-40 Lysis Buffer (Table 2.6) supplemented with 1 mM of dithiothreitol (DTT) and CompleteTM protease inhibitors on ice for 30 min. Cell lysates were clarified by centrifugation at $12,000 \times g$ at 4°C for 10 minutes. Small aliquots of the clarified lysates were kept for loading controls. The remaining lysates were pre-cleared with protein G-Sepharose or protein A-Sepharose beads for 1 h at 4°C before incubation with primary antibodies. Immunoprecipitations of clarified lysates were performed using rabbit anti-capsid polyclonal antibody (1:500) or mouse anti-myc monoclonal antibody (1:500) for at least 3 h at 4°C with rotation. Twenty microliters of protein A-Sepharose or protein G-Sepharose (50% suspension) beads were added and samples were then incubated for 2 hour at 4°C . After centrifugation ($500 \times g$), the beads were washed three times with lysis

buffer containing protease inhibitors and the bound proteins were eluted by heating at 95°C for 10 minutes in Protein Sample Buffer. Proteins were separated by SDS-PAGE and transferred to PVDF membranes for immunoblot analysis. Where indicated, samples were treated with RNase A (20 µg/mL) for 1 h prior to immunoprecipitation.

Capsid-claudin-1 or -JAM-1 co-immunoprecipitation: MDCK cells (3×10^5) seeded into P35 dishes, were infected with WNV the next day. After 48 hours, the cells were washed twice with cold PBS and then lysed with NP-40 lysis buffer (Table 2.6) supplemented with 1 mM of DTT and Complete™ protease inhibitors on ice for 30 min. Lysates were clarified by centrifugation for 15 min at 12,000 xg in a microcentrifuge at 4°C. Small aliquots of the clarified lysates were kept for loading controls. The remaining lysates were pre-cleared with protein G-Sepharose or protein A-Sepharose beads for 1 h at 4°C before sequential incubation with mouse anti-claudin-1 (1:500) or rabbit anti-capsid (1:500) or JAM-1 (1:500) antibodies for 3 h and then protein G-Sepharose beads or protein A-Sepharose beads for 2 h at 4°C. Immunoprecipitates were washed three times with lysis buffer before the bound proteins were eluted at 95°C in Protein Sample Buffer. Proteins were separated by SDS-PAGE and transferred to PVDF membranes for immunoblotting.

2.2.9.2 GST pull-down assay

HEK293T cells (1.2×10^6 / 100 mm dish) were transiently transfected with pEBG, pEBG-Capsid (Section 2.2.2.1), pcDNA3.1(-)/DDX56-myc (Section 2.2.2.2), or DDX56 N- and C-terminal constructs (DDX56-NT, DDX56-CT)

(Section 2.2.2.4). Forty-eight hours post-transfection, cells were lysed in NP-40 Lysis Buffer (Table 2.6) containing Complete™ Protease inhibitors (EDTA-free) on ice for 30 min. Lysates were cleared by centrifugation (12,000 x *g*) and the supernatants were incubated with glutathione-Sepharose 4B beads for 2 h at 4°C. Beads containing protein complexes were washed 3 times with lysis buffer after which the complexes were eluted at 95°C in 5x Protein Sample Buffer followed by separation by SDS-PAGE. Capsid-associated proteins were detected by Immunoblot analysis.

2.2.10 RNA techniques

2.2.10.1 RNA isolation

Total RNA from WNV-infected cells or crude virion preparations was isolated using either TRIzol reagent or TRI Reagent (Invitrogen) following the same protocol detailed below. Samples were homogenized in 1 mL TRIzol or TRI Reagent per 35 mm dish of cultured cells. Homogenized samples were incubated at room temperature for 5 minutes after which 0.2 mL chloroform was added. Tubes were mixed vigorously by hand for 15 seconds, incubated at room temperature for 3 minutes, and then centrifuged at 12,000 x *g* for 15 minutes at 4°C. The aqueous phases (400 µL) were transferred to fresh nuclease-free tubes and 100% isopropanol (500 µL) was added to precipitate total RNA. Samples were incubated at room temperature for 10 minutes, then centrifuged at 12,000 x *g* for 10 minutes at 4°C. The RNA pellets were washed once with 1 mL of 75% ethanol and centrifuged at 7,500 x *g* for 5 minutes at 4°C. The RNA pellets were air dried and then dissolved in 50 µL of RNase-free water at 55–60°C for 10

minutes. Samples were stored at -80°C until further use.

2.2.10.2 Quantitative PCR analysis for viral RNA

Before the quantitative PCR step, reverse transcriptase-PCR (RT-PCR) reaction was performed. RNA samples were treated with amplification-grade DNaseI (Invitrogen) as per the manufacturer's recommendations. The DNase-treated RNA samples were used as templates for RT-PCR reactions. SuperScriptIII Reverse Transcriptase system (Invitrogen, Table 2.4) and random primers (Invitrogen) were used for cDNA generation. Before adding reverse transcriptase, the DNase-treated templates were treated with RNase Out (Invitrogen) as per the manufacturer's recommendations.

Quantitative PCR reactions were conducted using a Stratagene MX3005P™ thermocycler (Table 2.5) using a PerfecCTa SYBR Green Supermix, UNG, low Rox real-time PCR kit (Table 2.4). Reactions (25 µL) were carried out in triplicate and contained 5 µL of cDNA and 100 nM of each gene-specific primer. To control for qPCR reaction specificity and potential genomic DNA contamination, no reverse transcriptase (NRT) and no template control (NTC) samples were included in these assays. To amplify a region of the WNV envelope gene, the primers WNV-env-F and WNV-env-R were used (Table 2.7). The amplification cycles consisted of an initial denaturing cycle at 95°C for 3 min, followed by 40 cycles of 15 s at 95°C, 30 s at 62°C, and 40 s at 72°C. Fluorescence was quantified during the 62°C annealing step, and the product formation was confirmed by melting curve analysis (57°C to 95°C). As an internal control, levels of the housekeeping gene product cyclophilin A were

determined. Amplification was performed using the primers Cyclophilin F and Cyclophilin R (Table 2.7). The amplification cycles for cyclophilin A mRNA detection consisted of an initial denaturing cycle at 95°C for 3 min, followed by 40 cycles of 15 s at 95°C, 30 s at 60°C, and 40 s at 72°C. Fluorescence was quantified during the 60°C annealing step, and the product formation was confirmed by melting curve analysis (57°C to 95°C). Quantification of the samples was performed using the two standard curves method (Wong and Medrano, 2005), and the relative amount of WNV genomic RNA were normalized to the relative levels of cyclophilin A mRNA. For analysis of viral RNA from crude virions, the relative amount of WNV genomic RNA in each sample was normalized to the amount of capsid protein which was determined by immunoblotting. Three independent PCR analyses were performed for each experiment.

2.2.10.3 Semi-quantitative PCR analysis for DDX56 mRNA

To determine how WNV infection affected levels of DDX56 mRNA, semi-quantitative PCR was employed. Total RNA (1 µg) extracted from mock- or WNV-infected cells was used for reverse transcription as described above (Section 2.2.10.1 and 2.2.10.2). Five percent of the resulting RT products were subjected to PCR (25 cycles) using primer pairs DDX56-F/DDX56-R (Table 2.7) and GAPDH-F/GAPDH-R (Table 2.7) to amplify DDX56 and GAPDH cDNAs, respectively. Products were analyzed by agarose gel electrophoresis.

2.2.10.4 Quantitative PCR analysis for tight junction protein genes

Total RNA from WNV-infected CACO-2 cells harvested at 24 h, 48 h and

72 h post-infection was isolated with TRI Reagent (Ambion) as described above (Section 2.2.10.1). RNA samples were adjusted to 100 ng/ μ L by dilution in sterile RNase/DNase free water. Relative levels of claudin-1, claudin-3, claudin-4, JAM1, ZO-1 and occluding mRNAs as well as WNV genomic RNA were determined using primers listed in Table 2.7. All genes of interest were analysed in a two-step as well as in a one-step RT-PCR approach. In the two-step reaction setup, cDNA was generated from 500 ng of RNA (5 μ L of diluted total RNA) using High Capacity RNA-to-cDNA Master Mix (Table 2.4) with random primers in a reaction volume of 20 μ L. Reaction conditions were 5 min at 25 °C, 30 min at 42°C and 5 min at 85°C. The resulting cDNA was diluted 1/10 in RNase-free water, of which 5 μ L was used for subsequent DNA amplification. The amplification was conducted with Fast SYBR Green Master Mix (Table 2.4) in a reaction volume of 25 μ L. Primer concentration was 10 pmol. Reaction conditions used were: 95°C for 30 sec, followed by 40 cycles of 95°C for 5 sec and 55–60°C for 30 sec. One-step reactions were performed in 25 μ L volumes using qScript One-Step SYBR Green qRT-PCR Kit (Table 2.4) starting with 100 ng of total RNA. Primer concentration was 10 pmol. Reaction conditions were: 50°C for 10 min, 95°C for 5 min, followed by 40 cycles of 95°C for 10 sec, 55–60°C for 20 sec and 72°C for 30 sec. Formation of primer dimers and other unspecific products was monitored by melt curve analysis (from 55°C to 95°C). Relative quantification of gene expression and successive calculation of fold-increase of gene expression of tight junction mRNAs were normalized to GAPDH mRNA levels using the comparative cT ($\Delta\Delta$ cT) method (Livak and Schmittgen, 2001).

All experiments were conducted in triplicate, resulting in a minimum of eight data points for each gene of interest. All gene expression studies were conducted on a CFX96 (Table 2.5) or an Mx3005P (Table 2.5) thermocycler. Statistical analysis on the data was conducted with SPSS Statistics 17.0 software (SPSS Inc.). Significant variance of mRNA expression at 24, 48 and 72 h post infection was evaluated using Tamhane's T2 multiple comparison.

CHAPTER 3

The capsid-binding nucleolar helicase DDX56 is important for infectivity of West Nile virus

A version of this chapter has been published in:

“Xu Z, Anderson R, and Hobman TC. (2011) The capsid-binding nucleolar helicase DDX56 is important for infectivity of West Nile virus. *J Virol.* 85(11):5571-80.”

3.1 Rationale

Similar to all other flaviviruses, WNV is “gene poor” and as such, it is completely dependent upon the host cell for most aspects of the virus life cycle. A recent study revealed that more than 300 human genes are required for replication of WNV and the closely related flavivirus, Dengue virus (Krishnan et al., 2008). Interactions between multifunctional viral proteins and host cells proteins drive replication and in some cases may result in disease. To better understand the molecular mechanisms of viral pathogenesis, it is important to study how virus proteins modulate the physiology of infected host cells. Given the medical importance of flaviviruses, it is surprising and disappointing that the study of interactions between WNV antigens and host cell proteins is so poorly understood. In spite of this, research from Hobman laboratory and others, suggests that in addition to its structural role in packaging genomic viral RNA, the WNV capsid protein is an important pathogenic determinant and plays significant non-structural functions (Bhuvanakantham et al., 2010b; Medigeshi et al., 2009; Raghavan and Ng, 2013; Urbanowski and Hobman, 2013; van Marle et al., 2007; Yang et al., 2002; Yang et al., 2008). WNV capsid functions in non-structural roles by interacting with multiple host cell encoded proteins (Bhuvanakantham et al., 2010b; Hunt et al., 2007; Ko et al., 2010; Oh et al., 2006; Oh and Song, 2006; Yang et al., 2008). Accordingly, my hypothesis is that interactions between the WNV capsid and host cell proteins are integral to virus replication and disease. Based on analogy with the HCV core protein, which reportedly binds to more than 30 host proteins (reviewed in (Urbanowski et al., 2008)), it is likely that the

list of known WNV capsid-binding proteins is incomplete. To this end, I attempted to identify novel capsid-binding proteins. By screening ~6 million potential interactions by yeast two-hybrid assay, I identified 22 putative human proteins that bind WNV capsid (Table 3.1). The first candidate that I pursued was the nucleolar RNA helicase DDX56. DDX56 is a member of the DEAD-box family of nucleolar RNA helicases that is linked to assembly of 60S ribosomal subunits (Zirwes et al., 2000). I chose DDX56 for main two reasons: First, DDX56 localizes to the nucleolus which is where a large pool of WNV capsid is targeted to in infected cells; second, other cellular helicases are known to be important for replication of flaviviruses in mammalian cells. Specifically, DDX28, DDX42 and DHX15 are involved in replication of WNV and Dengue virus (Krishnan et al., 2008). In addition, DDX3 binds to the HCV capsid protein (Mamiya and Worman, 1999; Owsianka and Patel, 1999; You et al., 1999b) and is important for replication of viral RNA (Ariumi et al., 2007). Moreover, cellular helicases are also involved in replication of other RNA viruses. For example, DDX24 is important for packaging HIV RNA into virions (Ma et al., 2008a).

In this study, I first confirmed that WNV capsid protein interacts with DDX56 in mammalian cells using independent protein-protein interaction assays. Then, I examined if /how capsid expression or WNV infection affects the cellular localization and steady-state level of DDX56. Finally, I investigated if WNV requires DDX56 for viral RNA replication, protein synthesis, or virion assembly/secretion.

Table 3.1 22 host proteins that have been identified to interact with the WNV capsid protein by yeast two-hybrid screen

Protein	Full name	Subcellular localization	Function
EBNA1BP2 (EBP2/p40/ NoBP)	EBNA1 binding protein 2	Nucleus, nucleolus	Involved in the ribosome biogenesis; related with cell growth regulation in a p53-dependent manner; important interacting partner of EBNA1 to maintain the EBV episomes
SMARCA2 (BRM)	SWI/SNF related, matrix associated, actin dependent regulator of chromatin, subfamily a, member 2	Nucleus	Component of ATP-dependent chromatin remodeling complex SNF/SWI; transcriptional co-activator cooperating with nuclear hormone receptors to potentiate transcriptional activation
DDX56 (NOH61)	DEAD (Asp-Glu-Ala-Asp) box polypeptide 56	Nucleus, nucleolus	ATP-dependent RNA helicase; involved in the assembly of 60S ribosomal subunits
DNTTIP2 (ERBP/FCF2)	Deoxynucleotidyl transferase terminal-interacting protein 2	Nucleus	Regulates the transcriptional activity of DNTT and ESR1; may function as a chromatin remodeling protein
STT3	Subunit of the oligosaccharyltransferase complex, homolog B (<i>S. cerevisiae</i>)	Endoplasmic reticulum membrane; Multi-pass membrane protein	Component of the N-oligosaccharyl transferase enzyme; involved in the N-linked protein glycosylation in the ER
DDX27	DEAD (Asp-Glu-Ala-Asp) box polypeptide 27	Nucleus (Potential)	Probable ATP-dependent RNA helicase

Table 3.1 (Continued)

SNRPD1	Small nuclear ribonucleoprotein D1 polypeptide	Nucleus	May act as a charged protein scaffold to promote snRNP assembly or strengthen snRNP-snRNP interactions through nonspecific electrostatic contacts with RNA
CCDC91	Coiled-coil domain containing 91	Membrane; Peripheral membrane protein; Golgi apparatus, trans-Golgi network	Involved in the regulation of membrane traffic through the trans-Golgi network (TGN)
CCDC146	Coiled-coil domain containing 146	Membrane	Unknown
PRDM5	Homo sapiens PR domain containing 5	Nucleus	Transcription factor; regulates hematopoiesis-associated protein-coding and microRNA genes; may cause G2/M arrest and apoptosis in cancer cells
PRDM2	Homo sapiens PR domain containing 2, with ZNF domain	Nucleus	May function as a DNA-binding transcription factor
TCEAL7	Transcription elongation factor A (SII)-like 7	Nucleus (Probable)	May be involved in transcriptional regulation
RBM34	RNA binding motif protein 34	Nucleus, nucleolus	Nucleic acid binding; nucleotide binding
PHIP	Pleckstrin homology domain interacting protein	Nucleus (Probable)	May be involved in insulin signaling

Table 3.1 (Continued)

PHF20L1	PHD finger protein 20-like 1	Nucleus; plasma membrane	Nucleic acid binding; protein binding; zinc binding; ion binding
ZNF274	Zinc finger protein 274	Nucleus, nucleolus	Function as a transcriptional repressor
ZNF189	Zinc finger protein 189	Nucleus (Probable)	May be involved in transcriptional regulation
ZNF84	Zinc finger protein 84	Nucleus (Probable)	May be involved in transcriptional regulation
F5	Coagulation factor V	Secreted	A cofactor that participates with factor Xa to activate prothrombin to thrombin
HIGD1A	HIG1 domain family member 1A	Membrane; Multi-pass membrane protein (Potential)	Unknown
RPL13	60S ribosomal protein L13	Cytoplasm	Component of the 60S subunit;
C1orf151	Chromosome 1 open reading frame 151	Membrane; Single-pass membrane protein	Unknown

3.2 Results

3.2.1 The nucleolar helicase DDX56 interacts with the WNV capsid protein

As mentioned above, I used a stringent yeast two-hybrid multitissue screen to identify novel WNV capsid-interacting host proteins. This screen was performed with the Matchmaker™ GAL4 Yeast Two-Hybrid System 3 using a pre-transformed normalized human universal cDNA library (Clontech) as described in section 2.2.3. Of 22 putative capsid protein interactors identified from the human cDNA library, the nucleolar helicase DDX56/NOH61 was the first to be examined because of previous studies documenting the roles of cellular helicases in RNA virus replication. Data in Figure 3.1 indicate that binding between WNV capsid and DDX56 is robust as evidenced by the fact that they interact under the most stringent yeast two hybrid conditions (-Ade, -His, -Leu, and -Trp with X-alpha-gal).

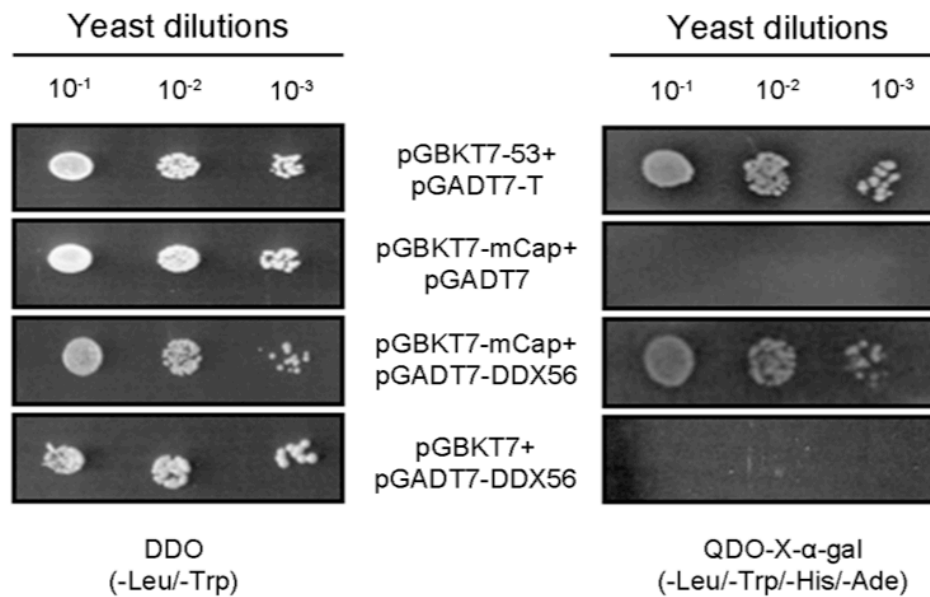
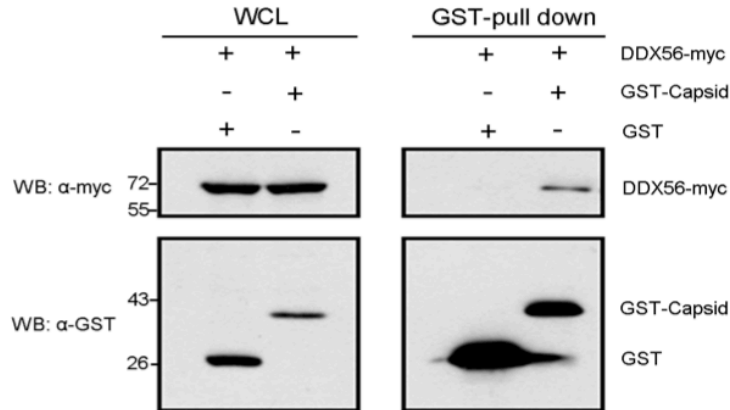


Figure 3.1 Nucleolar helicase DDX56 was identified as a binding partner of WNV capsid by yeast two-hybrid screen. The cDNA for mature capsid (mCap) was cloned into pGBKT7, which was then co-transformed with empty vector (pGADT7) or pGADT7-DDX56 into the AH109 yeast strain. Serial dilutions of the transformants were plated onto double-dropout medium lacking leucine and tryptophan (DDO) or quadruple-dropout medium lacking leucine, tryptophan, histidine, and adenine (QDO). Further evidence of the interaction was obtained by assaying for α -galactosidase activity on QDO medium. Positive controls for this system were p53 (pGBKT7-53) and simian virus 40 large T antigen (pGADT7-T).

Next, experiments were carried out to determine the authenticity of this interaction in mammalian cells. First, I confirmed this interaction by GST pull-down assays. GST-Capsid and myc-tagged DDX56 (DDX56-myc) were co-expressed in transiently transfected HEK 293T cells and 48 h later, cell lysates were extracted and incubated with glutathione-sepharose beads, and then bound proteins were subjected to SDS-PAGE and immunoblotting with mouse anti-myc or mouse anti-GST antibodies. As shown in Figure 3.2A, DDX56-myc co-purified with GST-capsid but not GST alone. Next, reciprocal co-immunoprecipitation experiments were performed to further verify the authenticity of the interaction. Specifically, immunoprecipitation of DDX56-myc followed by immunoblot analysis with anti-capsid antibodies showed that capsid co-purified with DDX56-myc in transfected HEK 293T cells (Figure 3.2B). One concern was that capsid and DDX56 are both RNA-binding proteins, which may result in a nonspecific and simply RNA-mediated interaction. To exclude this possibility, I tested whether the capsid-DDX56 interaction was sensitive to nuclease treatment. Treatment of cellular extracts with RNase A prior to immunoprecipitation did not alter the amount of capsid that co-immunoprecipitated with DDX56 (Figure 3.2B). These results indicate that intact RNA is not required for the interaction between capsid and DDX56.

A.



B.

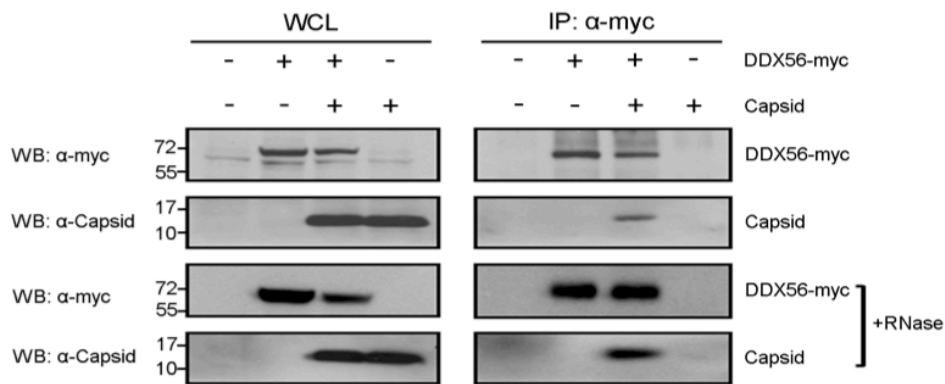


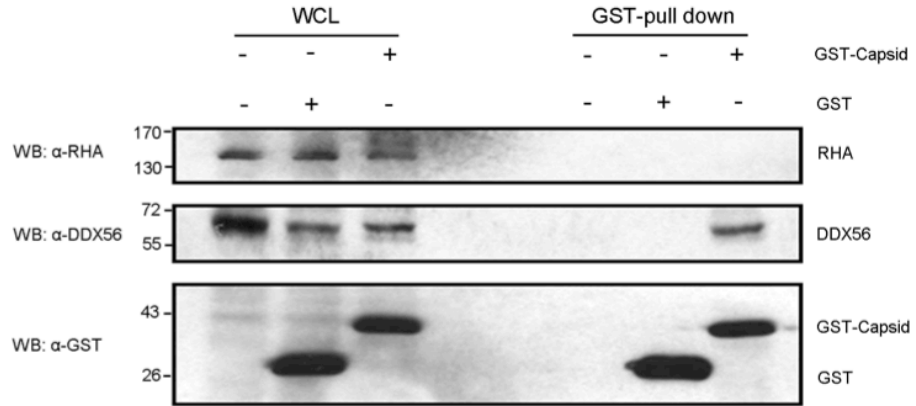
Figure 3.2 The WNV capsid protein interacts with DDX56 in mammalian cells. **A.** To show reciprocal co-purification of capsid/DDX56 complexes, HEK 293T cells were transfected with plasmids encoding GST-Capsid, GST, and/or DDX56-myc. Lysates were incubated with glutathione-Sepharose beads, and then bound proteins were subjected to SDS-PAGE and immunoblotting with anti-myc or anti-GST antibodies. Positions of molecular mass markers (in kDa) are indicated. **B.** HEK 293T cells were transfected with or without plasmids encoding WNV capsid or myc-tagged DDX56. At 48 h posttransfection whole-cell lysates (WCL) and mouse anti-myc immunoprecipitates were subjected to SDS-PAGE and Western blotting (WB) with anti-myc (α -myc) or rabbit anti-capsid antibodies. Where indicated, samples were treated with RNase A prior to immunoprecipitation. Positions of molecular mass markers (in kDa) are shown on the left.

Next, to determine if the WNV capsid interacts with nucleolar RNA helicases in a nonspecific manner, I immunoblotted GST-capsid pulldowns with antibodies to RNA helicase A (RHA). Whereas endogenous DDX56 was readily pulled down with GST-capsid, interaction between RHA and capsid was not detected (Figure 3.3A).

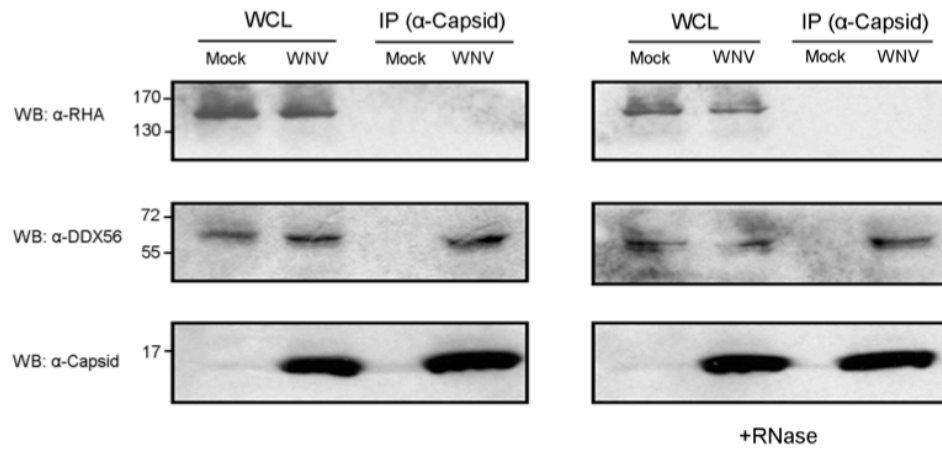
Finally, similar reciprocal co-immunoprecipitation experiments were carried out to test whether capsid could form stable complexes with endogenous DDX56 in WNV-infected cells. HEK 293T cells were infected with the NY99 strain of WNV [multiplicity of infection (MOI)=5] and 48 hours later lysates were processed for co-immunoprecipitation with rabbit anti-capsid antibody or mouse anti-DDX56 antibody followed by SDS-PAGE and immunoblotting with antibodies to DDX56, RHA, or capsid. Indeed, immunoblot analysis showed the reciprocal immunoprecipitation of capsid and DDX56 in virus infected HEK 293T cells in the absence of RNA (Figure 3.3B and C). Together these data suggest that capsid specifically associates with endogenous DDX56 in an RNA-independent manner.

Figure 3.3 WNV capsid protein forms a stable complex with endogenous DDX56. **A.** HEK 293T cells were transfected with plasmids encoding GST or GST-WNV capsid. At 48 h posttransfection whole-cell lysates (WCL) and GST-pull-down products were subjected to SDS-PAGE and immunoblotting with rabbit anti-capsid, mouse anti-DDX56, or mouse anti-RNA helicase A (α -RHA). **B and C.** HEK 293T cells were infected with the NY99 strain of WNV (MOI, 5) and 48 h later lysates were subjected to co-immunoprecipitation (co-IP) with rabbit anti-capsid antibody (B) or mouse anti-DDX56 (C) followed by SDS-PAGE and immunoblotting with antibodies to DDX56, RHA, or capsid. The position of the IgG heavy chain is indicated by the asterisk. Nonimmune mouse serum was used for the negative-control IP. WCL, whole-cell lysate. Where indicated, samples were treated with RNase A prior to immunoprecipitation. Positions of molecular mass markers (in kDa) are indicated.

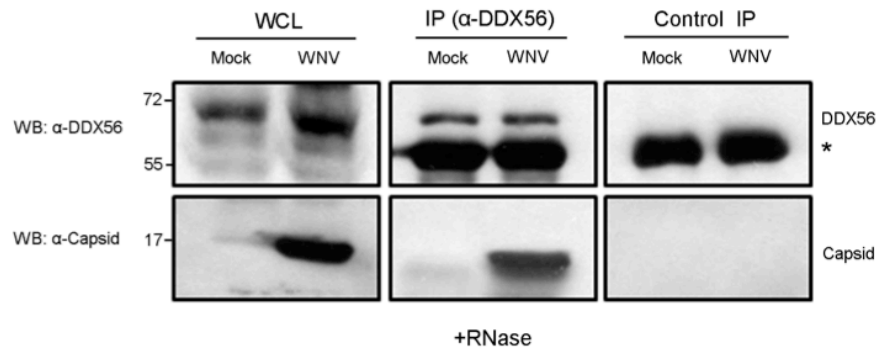
A.



B.



C.



3.2.2 WNV infection results in depletion of the nucleolar pool of DDX56

A number of effects, including relocalization, function-modulation, and degradation have been described to occur to some capsid-interacting host proteins upon WNV infection or capsid expression (Bhuvanakantham et al., 2010b; Hunt et al., 2007; Ko et al., 2010; Medigeshi et al., 2009; Oh et al., 2006; Yang et al., 2008). With respect to DDX56, comparatively little is known about this helicase except for its nucleolar localization and its role in 60S ribosomal subunit formation (Zirwes et al., 2000). Based on the fact that a large pool of WNV capsid protein localizes to nucleoli of transfected and infected cells (Hunt et al., 2007; Westaway et al., 1997a) and towards understanding the functional role of capsid-DDX56 interaction, it is important to investigate the cellular distribution of DDX56 in capsid-expression or WNV-infected cells. First, A549 cells were transfected with capsid and then processed for indirect immunofluorescence microscopy. Consistent with previous report (Zirwes et al., 2000), DDX56 was exclusively associated with nucleolus of mock- and capsid-transfected cells. As expected, extensive colocalization between DDX56 and WNV capsid protein was apparent in the nucleoli (Figure 3.4, arrowheads).

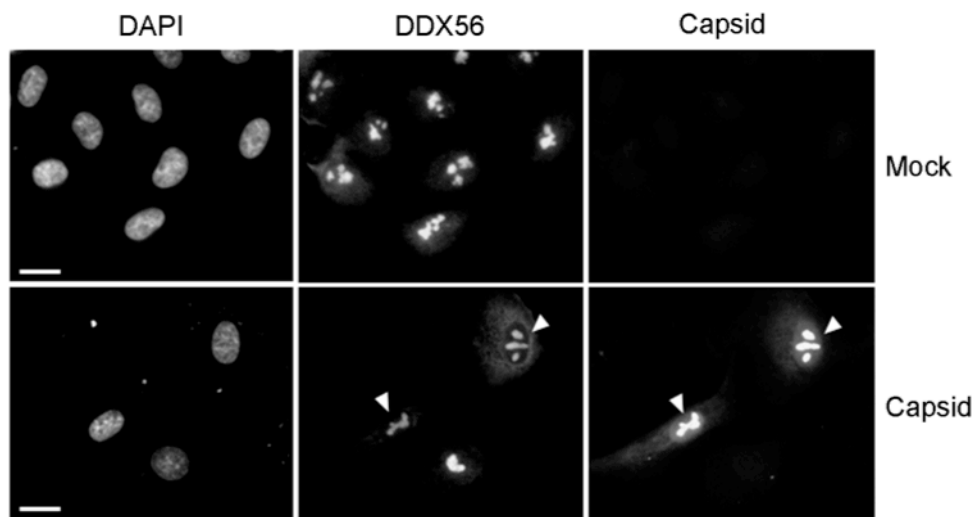


Figure 3.4 The WNV capsid colocalizes with DDX56 in the nucleoli. Forty hours posttransfection with a plasmid encoding WNV capsid, A549 cells were processed for indirect immunofluorescence using mouse anti-DDX56 and rabbit anti-capsid antibodies. Primary antibodies were detected with donkey anti-rabbit Alexa 488 and chicken anti-mouse Alexa 594. Nuclear DNA was stained with DAPI. Images were captured with a Zeiss Axioskop 2 microscope. Bar=10 μ m.

Next, I set out to investigate whether the nucleolar localization of DDX56 was affected in infected cells. A549 cells were infected with WNV (MOI=2) and at various time points postinfection, cells were processed for indirect immunofluorescence. At 24 h postinfection, the localizations of DDX56 in mock- and WNV-infected cells were very similar. Distinct nucleolar pools of capsid proteins that overlapped with DDX56 were also evident at this time point (Figure 3.5, arrowheads). However, starting at 48 h postinfection, a diminished signal intensity of nucleolar DDX56 was clearly evident, and by 72 h, many infected cells exhibited little or no detectable DDX56 in nucleoli (Figure 3.5, arrows). Interestingly, at 72 h postinfection, many more cells with cytoplasmically localized capsid protein were evident.

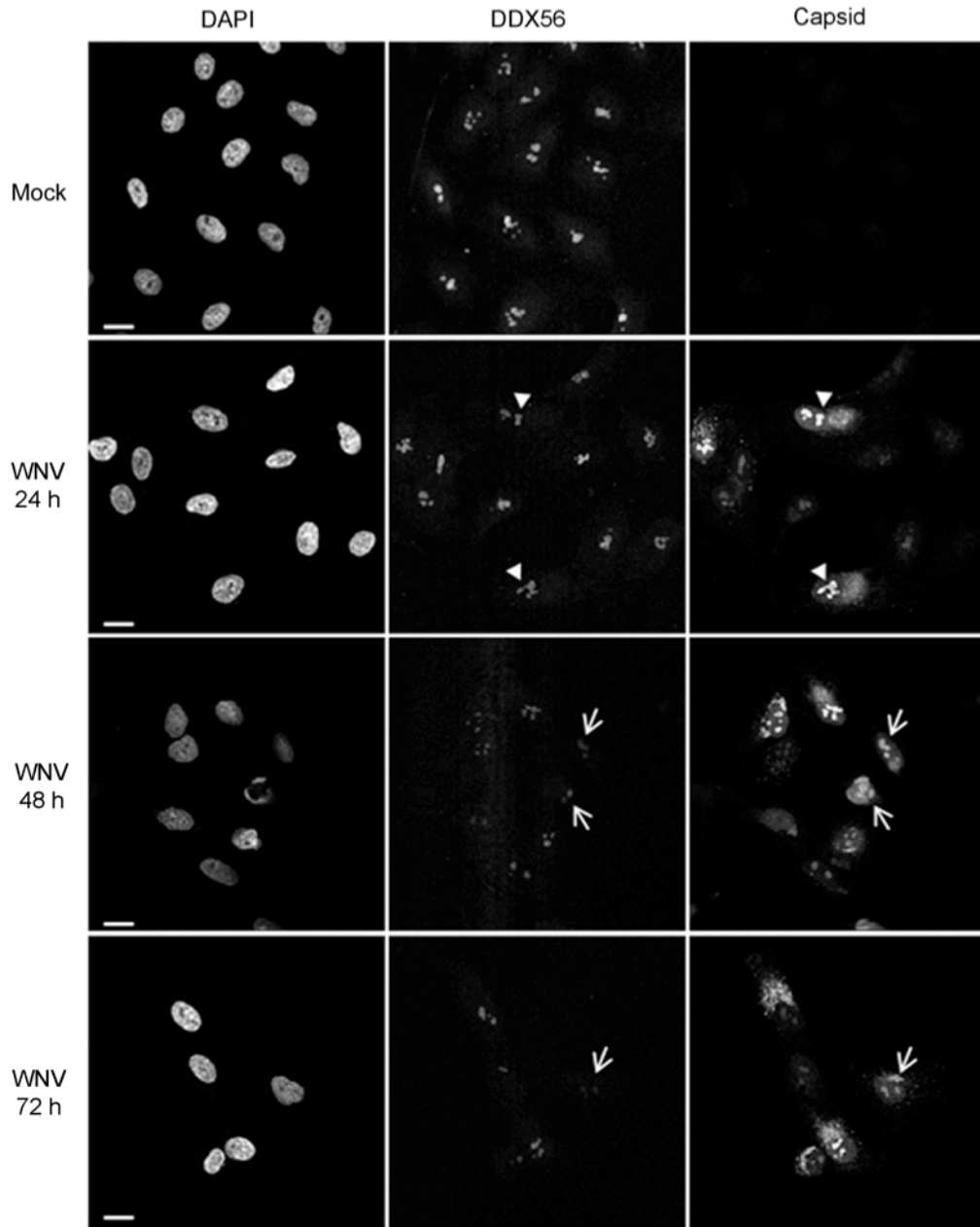


Figure 3.5 WNV infection results in depletion of the nucleolar pool of DDX56. A549 cells were infected with WNV (MOI, 2), and at 24, 48, and 72 h postinfection cells were processed for indirect immunofluorescence by using rabbit and mouse antibodies to capsid and DDX56, respectively. Primary antibodies were detected using goat anti-mouse Alexa 647 and donkey anti-rabbit Alexa 488. Images were captured using a Leica TCS SP5 confocal scanning microscope. Arrowheads indicate colocalization between DDX56 and WNV capsid in nucleoli. Arrows point to infected cells that have decreased levels of DDX56 in the nucleoli. Bar=10 μ m.

To determine if WNV infection led to a general loss of nucleolar components, I monitored the localization of another nucleolar resident protein, nucleolin. The immunofluorescence data in Figure 3.6A indicate that WNV infection did not cause a general loss of nucleolar components. Next, I questioned whether infection with other positive-strand RNA viruses led to loss of DDX56 from nucleoli. A549 cells that were infected with Rubella virus (Figure 3.6B) or Dengue virus 2 (Figure 3.6C) were subjected to analyses by indirect immunofluorescence. In contrast to WNV-infected cells, infection with these two viruses did not result in detectable loss of DDX56 from the nucleoli. Similarly, infection of Huh7.5 cells with HCV did not appear to affect the nucleolar pool of DDX56 (data not shown).

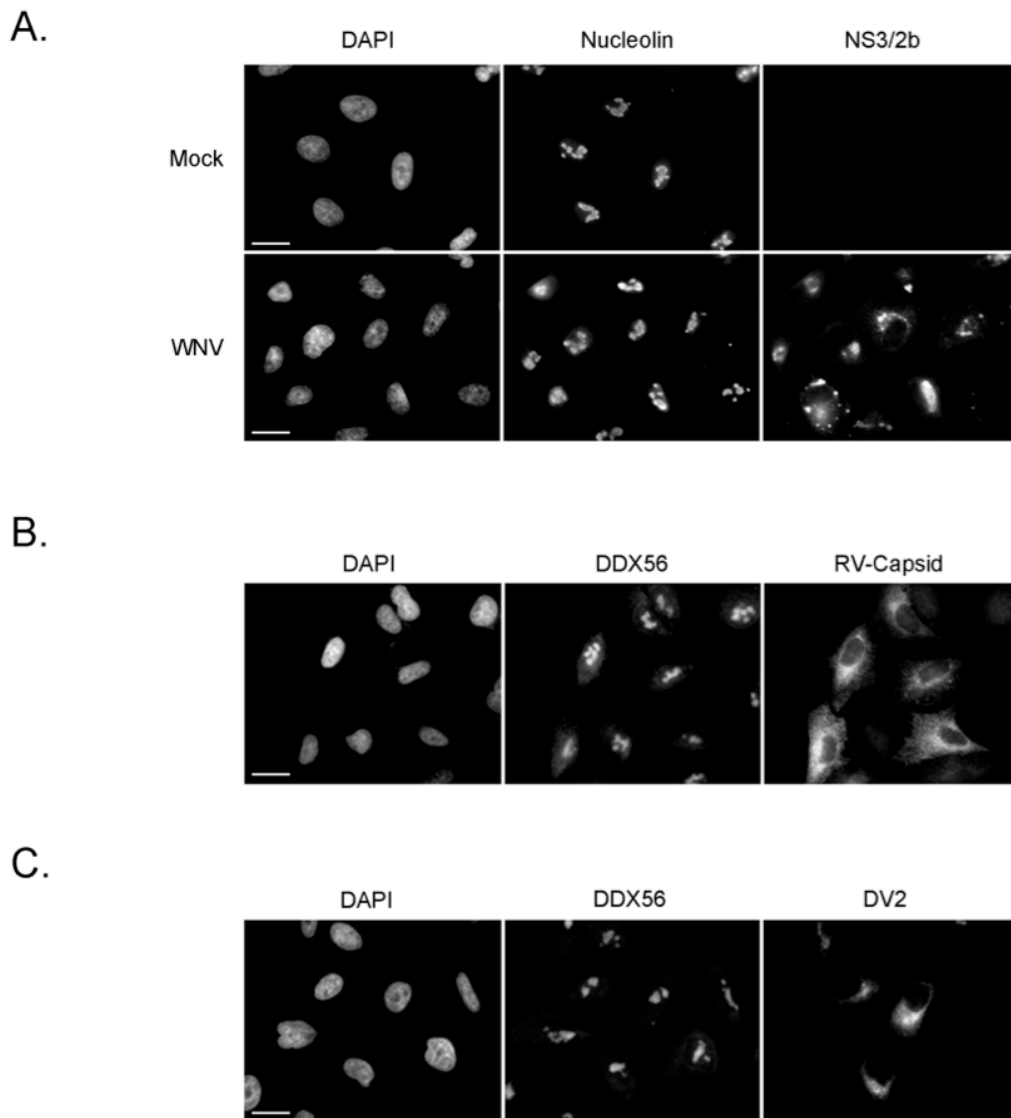


Figure 3.6 Rubella and Dengue viruses do not induce loss of nucleolar DDX56. **A.** WNV-infected cells were detected by using a mouse monoclonal antibody to NS3/2b, and nucleolin was detected with a rabbit antibody. **B and C.** A549 cells were infected with RV (B) or Dengue virus 2 (DV2) (C), and 48 h postinfection cells were processed for indirect immunofluorescence by using mouse antibodies to DDX56 and rabbit anti-RV capsid or human anti-DV2, respectively. Nuclei were counterstained with DAPI. Images were captured using a Zeiss Axioskop 2 microscope. Bar=10 μ m.

3.2.3 WNV infection induces proteasome-dependent degradation of DDX56

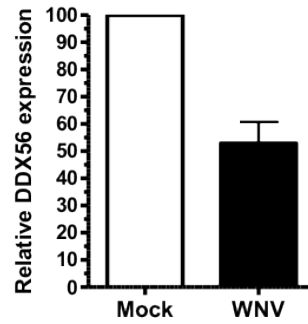
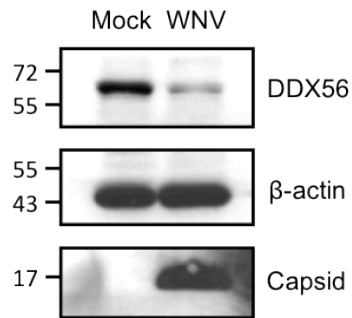
The loss of DDX56-specific immunofluorescence from the nucleolar compartment in response to WNV infection could be due to dispersion of DDX56 over a larger volume in the cytoplasm after transport of this protein from the nucleus. Alternatively, DDX56 could be degraded following transport to the cytoplasm. To test these possibilities, I performed western blot experiments to compare the steady-state levels of DDX56 in mock- and WNV-infected cells. At 48 h postinfection, WNV-infected A549 cells were lysed and then processed for immunoblot analyses with antibodies to DDX56 and the housekeeping protein β -actin (loading control). The normalized level of DDX56 (relative to β -actin) was calculated from three independent experiments. The data in Figure 3.7A show that at 48 h, mock-treated cells contained approximately twice as much DDX56 protein as WNV-infected cells. In contrast, infection of A549 cells with another RNA virus, rubella virus, had no apparent effect on DDX56 protein levels (Figure 3.7B).

Less protein level of DDX56 in WNV-infected cells could be due to decreased RNA transcription or protein degradation. To further distinguish between these two possibilities, I first tested the DDX56 mRNA levels in mock- and WNV-infected cells. Semi-quantitative PCR analyses revealed that DDX56 mRNA levels were not decreased upon infection (Figure 3.7C), suggesting that WNV-induced downregulation of DDX56 occurred at the posttranscriptional step. Then, I treated WNV infected cells with protein degradation inhibitors to confirm loss of DDX56 is truly due to protein degradation. Briefly, A549 cells were

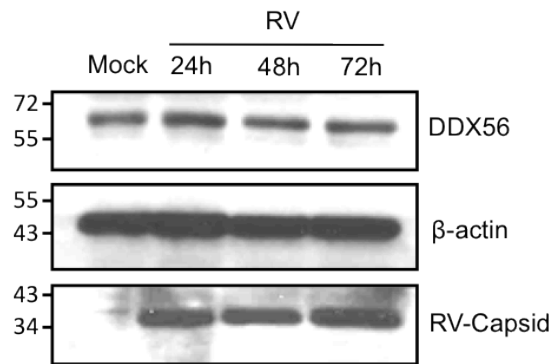
infected with WNV (MOI=2) and 24 h later were treated with proteasome inhibitor MG132 (50 μ M), or lysosomal degradation inhibitor bafilomycin A (BAF, 200 nM) for a further 24 h, respectively. The immunoblot data showed that treatment of infected cells with the proteasome inhibitor MG132 prevented WNV-induced loss of DDX56, whereas blocking lysosomal degradation (BAF) had no effect (Figure 3.7D and E). In addition, treatment with the nuclear export inhibitor leptomycin B (Figure 3.7E) did not block WNV-induced degradation of DDX56. However, because this inhibitor blocks CRM1-dependent export (Fukuda et al., 1997; Ossareh-Nazari et al., 1997), it is possible that WNV infection induces nucleus to cytoplasm export of DDX56 via another pathway.

Figure 3.7 WNV infection induces proteasome-dependent degradation of DDX56. **A.** A549 cells were infected with WNV (MOI, 2), and 48 h later cell lysates were subjected to immunoblot analyses for DDX56 and β -actin. Data from three independent experiments were used to determine the normalized level of DDX56 (relative to β -actin). Positions of molecular mass markers (in kDa) are indicated. **B.** A549 cells were infected with rubella virus (MOI, 2) for 24 to 72 h, after which cell lysates were subjected to SDS-PAGE before immunoblotting for DDX56, rubella virus capsid protein, and β -actin. **C.** Total RNA was extracted from mock- or WNV-infected cells at 24 and 48 h postinfection. After DNase treatment, RNA was subjected to reverse transcription or mock treatment before semi-quantitative PCR. Agarose gel electrophoresis and ethidium bromide staining were used to detect PCR products. GAPDH mRNA served as the internal control. **D and E.** A549 cells were infected with WNV and 24 h later were treated with 50 μ M MG132, 200 nM bafilomycin A (BAF), 50 ng/ml leptomycin B (LMB), or the solvent dimethyl sulfoxide (DMSO) for a further 24 h. Lysates were subjected to SDS-PAGE and immunoblotting with anti-capsid, GAPDH, or DDX56.

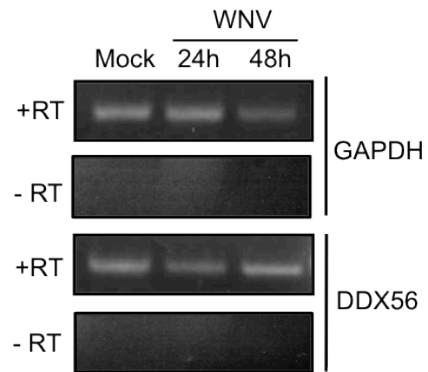
A.



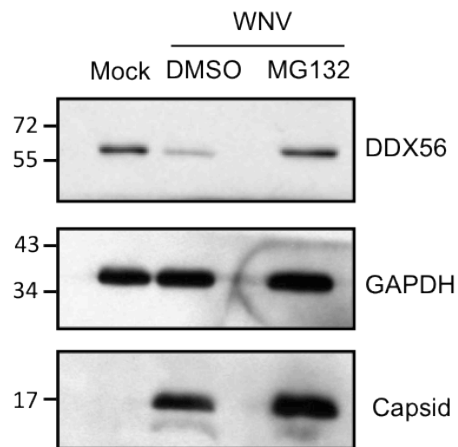
B.



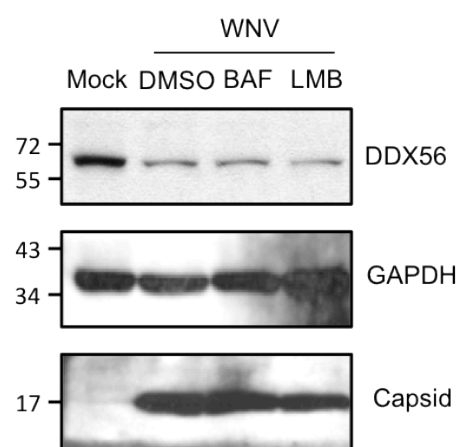
C.



D.

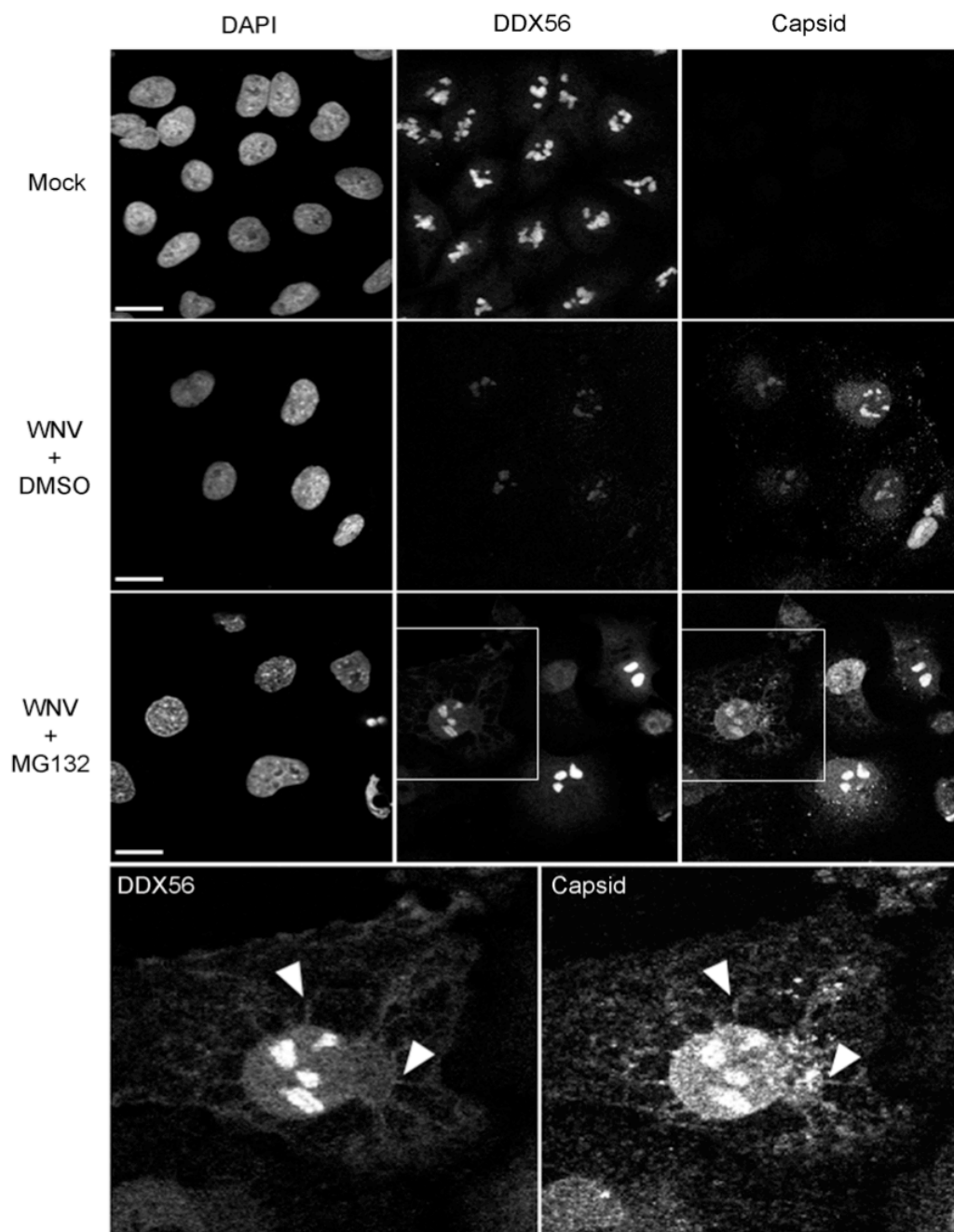


E.



Given that proteins can be degraded in proteasomes in the cytoplasm, I asked whether DDX56 could be detected in the cytoplasm of WNV-infected cells that were treated with MG132. As the data in Figure 3.8 (arrowheads) show, in some cells, colocalization of capsid and DDX56 on cytoplasmic reticular structures occurred when the proteasomal degradation system was inhibited. Together, these data suggest that WNV infection causes transport of DDX56 from the nucleus to cytoplasm, followed by degradation in the proteasome.

Figure 3.8 WNV infection causes relocalization of DDX56 from the nucleus to cytoplasm. A549 cells were mock infected or infected with WNV for 24 hours after which infected cells were treated with the proteasomal inhibitor MG132 or DMSO for 24 hours. Cells were then processed for indirect immunofluorescence using rabbit anti-capsid and mouse anti-DDX56. Brightened enlarged versions of the boxed regions are shown at the bottom of the figure. Arrows indicate co-staining of DDX56 and capsid in cytoplasmic reticular elements. Nuclei were counter stained with DAPI. Bar = 10 μ m.

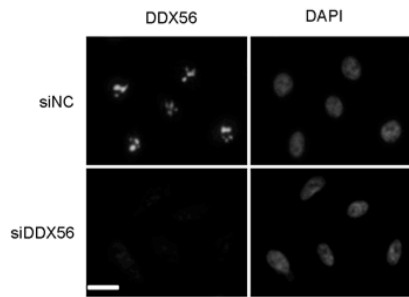


3.2.4 DDX56 is important for infectivity of WNV virions

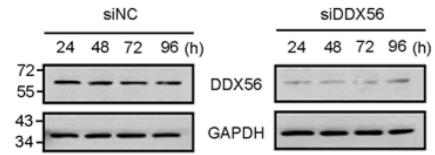
As a first step toward understanding the potential role of DDX56 in WNV replication, RNA interference was used to reduce cellular levels of DDX56 in HEK 293T and A549 cells. In cells transiently transfected with pooled DDX56-specific siRNAs, levels of DDX56 remained low for up to 96 h without any significant effect on cell viability indicating that this helicase is not required for cell growth *in vitro* (Figure 3.9A-C).

Figure 3.9 siRNA-mediated depletion of DDX56 affects infectivity of WNV virions. A549 cells were transfected with non-silencing control (siNC) or DDX56-siRNAs and at 48 hours post-transfection, were processed for indirect immunofluorescence using a monoclonal antibody specific for DDX56. **A.** Nuclei were counter stained with DAPI. Bar = 10 μ m. **B.** Levels of DDX56 protein in siNC or DDX56-siRNA transfected cells, were monitored by immunoblot analyses at indicated time points. The housekeeping protein GAPDH serves as a loading control. Positions of molecular mass markers (kDa) are indicated. **C.** The numbers of viable cells among siRNA-treated cells were determined at the indicated times post-transfection. The data points were derived from three independent experiments. A549 (**D**) and HEK 293T (**E**) cells were transfected with siNC or DDX56-siRNAs and then 24 hours later were infected with WNV. Culture supernatants were harvested for up to 72 hours post-infection and levels of infectious WNV were determined by plaque assay. * $p = < 0.05$. N = 3.

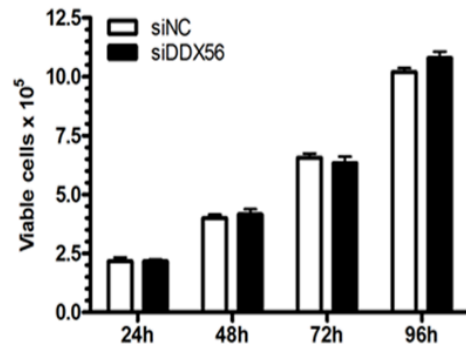
A.



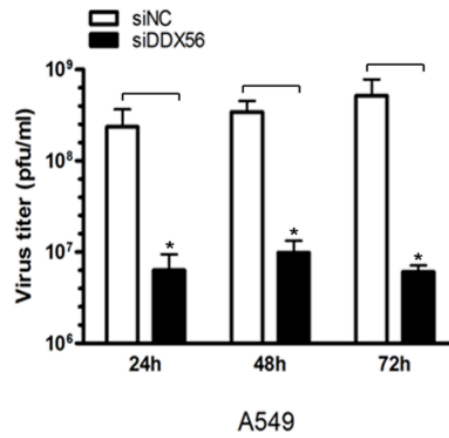
B.



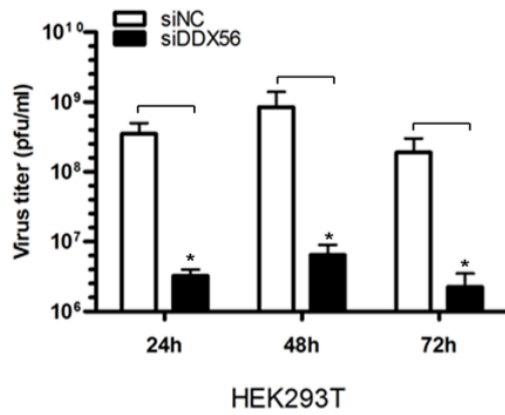
C.



D.



E.



To exclude the possibility that off-target effects by pooled siRNAs could lead to effects on WNV replication, I prepared stable cell lines which DDX56 levels were reduced using a single miRNA. Specifically, an shRNAmir-encoding lentivirus was used to construct stable polyclonal cell lines with reduced DDX56 as described in section 2.2.5. As shown in Figure 3.10A, relative to a lentivirus encoding a non-silencing control miRNA, transduction of cells with the DDX56-specific miRNA resulted in 5-fold reduction of DDX56 protein levels. Next, I infected the DDX56 knockdown (KD-DDX56) and a matched nonsilencing control cell line (NS) with WNV (MOI=2), and at 24 and 48 hours cell supernatants were harvested for viral titer plaque assays. Data in Figure 3.10B show that downregulation of DDX56 in HEK 293T cells results in >100-fold decrease in viral titers. Similar results were obtained using HEK 293T and A549 cells transiently depleted of DDX56 by using pooled siRNAs (Figure 3.9D-E) indicating that the importance of this helicase for production of infectious WNV is not limited to one cell type.

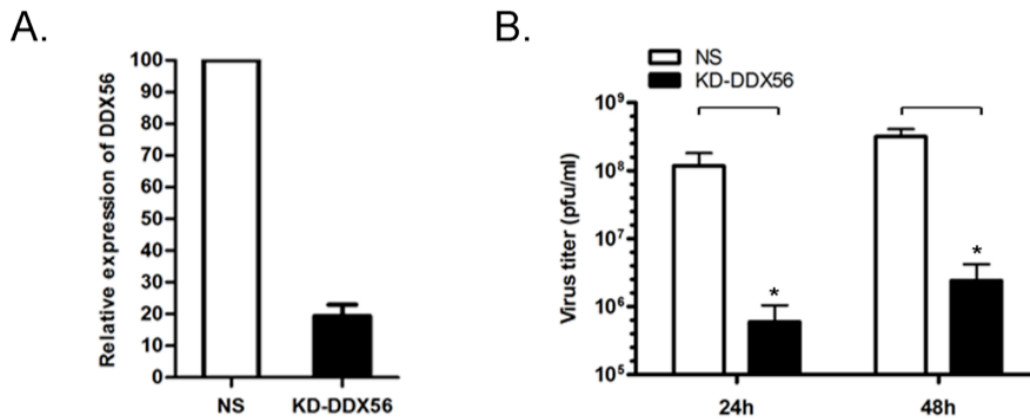
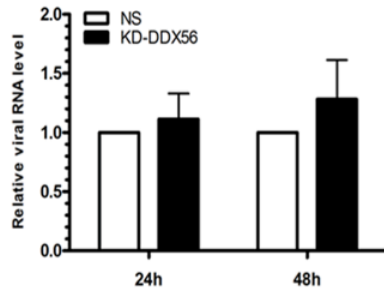


Figure 3.10 shRNA-mediated depletion of DDX56 decreases WNV titers. Stable polyclonal HEK 293T cells with reduced DDX56 (KD-DDX56) were obtained after transduction with a lentivirus encoding a DDX56-specific shRNAmir. A matched nonsilencing control cell line (NS) was produced using a lentivirus encoding a control shRNAmir that has no homology to any mammalian genes. **A.** Relative levels of DDX56 protein were determined by immunoblotting, and the results from three independent experiments were quantitated. **B.** Cell lines were infected with WNV (MOI, 2) for up to 48 h, after which cell supernatants were collected and used for plaque assays. *, $P < 0.05$.

3.2.5 Depletion of DDX56 does not affect replication of WNV RNA or protein synthesis

It is possible that decreased WNV titers in DDX56-depleted cells result from decreased synthesis of viral RNA or proteins. To examine these possibilities, WNV-infected cell lysates from nonsilencing and DDX56 knockdown HEK 293T cells were first subjected to quantitative RT-PCR to determine relative levels of genomic RNA. Surprisingly, loss of DDX56 did not significantly affect the production of viral genomic RNA (Figure 3.11A). Similarly, immunoblot analyses of the same cell lysates revealed that the steady-state levels of WNV structural proteins (capsid) and nonstructural proteins (NS3) were not affected by loss of DDX56 (Figure 3.11B). Together, these data indicate that DDX56 is not required for replication of viral RNA or protein synthesis.

A.



B.

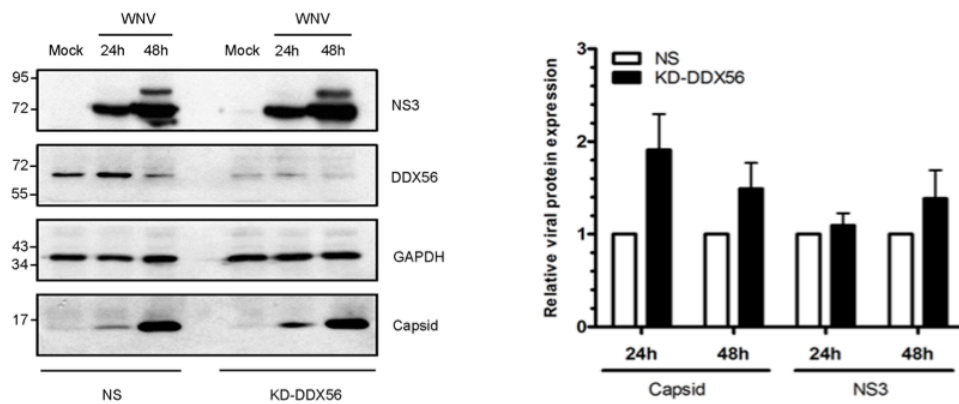


Figure 3.11 Depletion of DDX56 does not affect WNV viral RNA and protein production. Stable polyclonal HEK 293T cells with reduced DDX56 (KD-DDX56) and a matched non-silencing control cell line (NS) were infected with WNV and at 24 and 48 h post-infection, cell lysates were harvested and subjected to qRT-PCR (A) and immunoblot analyses (B) to determine relative levels of genomic RNA and viral proteins, respectively. Positions of molecular mass markers (in kDa) are indicated. Error bars represent standard errors from three independent experiments. $p < 0.05$, $N = 3$.

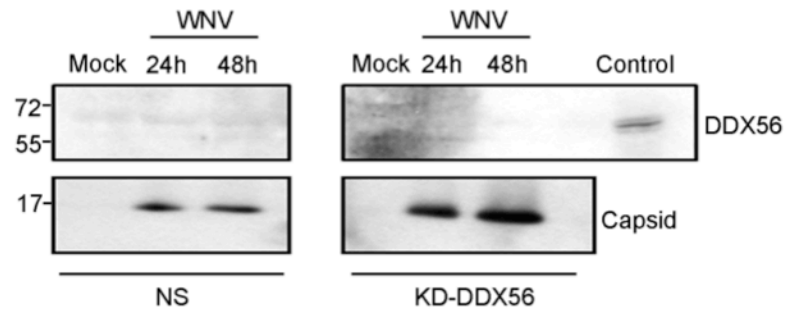
3.2.6 DDX56 is important for assembly of infectious WNV particles

Since DDX56 is not required for replication of WNV RNA or protein expression, it is possible that this helicase is needed for assembly and/or secretion of infectious virus particles. Alternatively, virions that are secreted from DDX56-depleted cells may be less infectious. To distinguish between these possibilities, virus particles secreted from the infected cells were recovered and the crude virions were subjected to immunoblot analyses with anti-capsid and anti-DDX56 antibodies. The data in Figure 3.12A show that DDX56 is not incorporated into WNV virions and that knockdown of DDX56 protein did not inhibit assembly or secretion of WNV particles.

Next, I used quantitative RT-PCR to determine the relative amount of viral RNA in WNV virions secreted from DDX56-depleted cells. Interestingly, when normalized to the amount of capsid protein found in virions, the genomic RNA content of virions secreted from DDX56 knockdown cells was 3 to 4 times lower than in virions isolated from non-silencing control cells (Figure 3.12B). These data suggest that DDX56 is important for assembly of infectious WNV virions.

Finally, I determined whether DDX56 expression is required for replication and/or infectivity of another positive-strand RNA virus, Rubella virus. The data in Figure 3.13 show that siRNA-mediated knockdown of DDX56 did not affect replication of viral RNA, expression of viral proteins or infectivity of this virus.

A.



B.

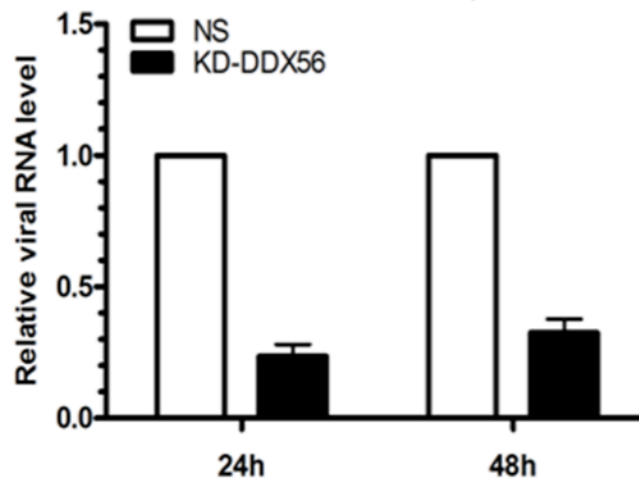


Figure 3.12 DDX56 is important for assembly of infectious WNV particles. A. WNV virions were recovered from precleared conditioned medium from infected stable DDX56 knockdown (KD-DDX56) and nonsilencing control (NS) HEK 293T cells by ultracentrifugation. **A.** The crude virion preparations were subjected to SDS-PAGE and immunoblot analyses with rabbit anti-capsid antibody and mouse anti-DDX56. Positions of molecular mass markers (in kDa) are indicated. **B.** Levels of viral genomic RNA in the virions were determined by qRT-PCR. The average relative levels of viral RNA (normalized to capsid level) from three independent experiments (each conducted in triplicate) were quantitated. Bars indicate standard error values. $p < 0.05$, $N = 3$.

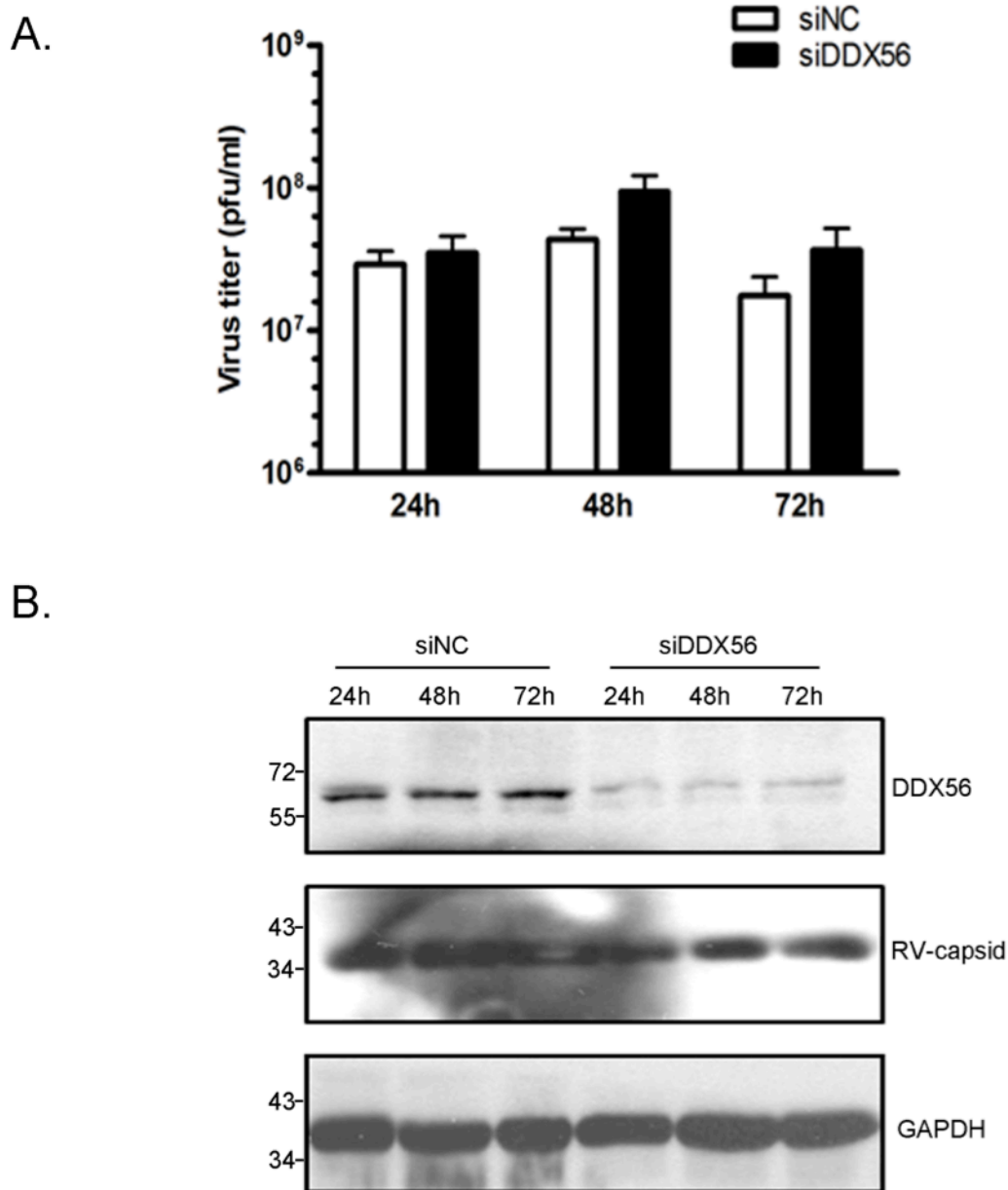


Figure 3.13 DDX56 is not required for replication of Rubella virus or assembly of infectious virions. A549 cells were transfected with non-silencing control (siNC) or DDX56 siRNAs and then 24 h later were infected with Rubella virus (MOI, 2). **A.** Cell lysates and conditioned media were harvested for up to 72 h postinfection, and levels of infectious virus were determined by plaque assay. **B.** Immunoblot analysis was used to determine relative levels of viral (RV-capsid) and cellular proteins (DDX56 and GAPDH [loading control]) in cell lysates. Positions of molecular mass markers (in kDa) are indicated. $p < 0.05$, $N = 3$.

3.3 Summary

In this chapter, I described the identification of a host cell-encoded capsid-binding nucleolar RNA helicase, DDX56. Extensive colocalization between DDX56 and capsid in the nucleolus was evident in infected cells and co-immunoprecipitation was used to confirm that these two proteins stably interact. Interestingly, infection of cells with WNV but not a related flavivirus, DENV, led to degradation of DDX56 in a proteasome-dependent manner. Blocking the proteasome resulted in accumulation of DDX56 on capsid-positive structures in the cytoplasm of WNV-infected cells suggesting that infection induces loss of nucleolar DDX56 and/or blocks import into the nucleus. My data showed that DDX56 is not required for WNV replication, virus assembly or secretion but, infectivity of the virus particles produced in DDX56-depleted cells is >100-fold lower than for virions secreted from control cells. Subsequent analyses revealed that DDX56 is not incorporated into virions but may have a role in packaging viral RNA into nascent virions. Together, all these data suggest that WNV infection induces the translocation of DDX56 from the nucleolus to the cytoplasm where it interacts with a pool of capsid protein at the site of virus assembly. I further postulate that interaction between capsid protein and DDX56 stimulates incorporation of genomic RNA into nucleocapsids; however, the precise mechanism by which DDX56 facilitates production of infectious WNV virions remains to be determined.

CHAPTER 4

The helicase activity of DDX56 is required for its role in assembly of infectious West Nile virus particles

A version of this chapter has been published in:

“Xu, Z and Hobman, T.C. (2012) The helicase activity of DDX56 is required for its role in assembly of infectious West Nile virus particles. *Virology*. 433(1): 226-35.”

4.1 Rationale

Genome-wide screens indicate that more than 300 human genes are required for replication of WNV and Dengue virus (Krishnan et al., 2008). In addition to replication, we anticipate that many other human genes are needed for assembly and secretion of nascent WNV virions. Here, we focused on cellular factors that interact with the capsid protein. Recently, we showed that expression of the capsid-binding nucleolar helicase DDX56 is important for infectivity of WNV virions (Xu et al., 2011). Accumulating evidence suggests that both cellular and viral RNA helicases play critical roles in the biology of flaviviruses (Ariumi et al., 2007; Krishnan et al., 2008; Mamiya and Worman, 1999; Owsianka and Patel, 1999; You et al., 1999a). However, by and large, the mechanisms of action for viral and cellular helicases are not known. With regard to the former, some flavivirus helicases are required in *cis* for virus assembly whereas others function in *trans* via a mechanism that does not require helicase activity (Patkar and Kuhn, 2008). Accordingly, considerable efforts have been directed toward determining the feasibility of targeting cellular and viral helicases as a means to block viral infections (Geiss et al., 2009; Kwong et al., 2005; Maga et al., 2011; Stankiewicz-Drogon et al., 2010).

To aid in development of antiviral therapies that rely on inhibition of RNA helicases, it is critical to understand how these enzymes function in virus biology. Indeed, evidence suggests that some RNA helicases are required for replication of viral RNA whereas others are needed for assembly of infectious virus particles. In addition to serving as co-factors in different aspects of virus biology, the

mechanism in which a given helicase functions in the virus infection cycle can vary tremendously (Patkar and Kuhn, 2008). In this section, I describe experiments designed to further dissect the mechanism by which the nucleolar helicase DDX56 functions in morphogenesis of infectious WNV virions.

4.2 Results

4.2.1 Construction of RNAi-resistant forms of DDX56 mutants

DDX56 belongs to the DEAD-box family of nucleolar RNA helicases. Previous studies report that the DEAD box motif is highly conserved in a subgroup of RNA helicases (Schmid and Linder, 1992) and mutagenic analyses revealed that substitution of asparagine (N) for aspartate (D) or glutamine (Q) for glutamate (E) results in complete loss of helicase activity (Pause and Sonenberg, 1992). In order to determine whether the enzymatic activity of DDX56 is required for infectivity of WNV particles, first, I constructed two DEAD box mutants (D166N and E167Q) of DDX56 that lack helicase function. In addition to creating these mutations in DDX56, I also introduced silent mutations downstream of the DEAD box motif in an shRNA target site (Figure 4.1). The latter mutations allow the expression of the DEAD box mutants in stable cell lines in which endogenous levels of DDX56 have been reduced by RNA interference (Figure 4.2 A).

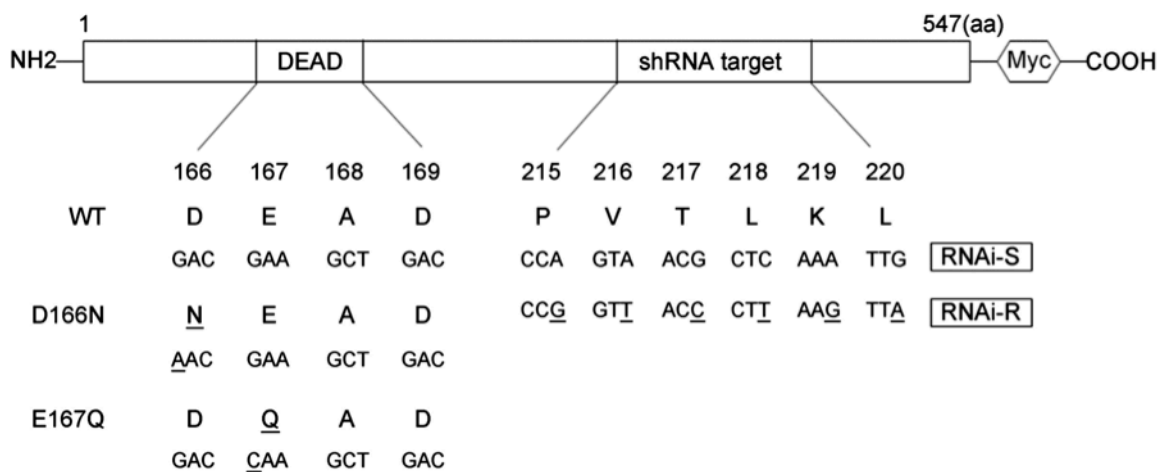
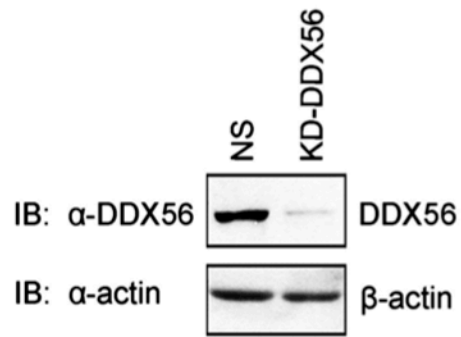


Figure 4.1 Construction of RNAi-resistant forms of DDX56 with mutations in the DEAD box motif. Aspartate (D) and glutamate (E) residues in the DEAD box motif of DDX56 were changed to asparagine (N) and glutamine (Q) to produce D166N and E167Q mutants, respectively. In addition, silent mutations were introduced into siRNA-binding sites to make the resulting constructs resistant to RNAi. All constructs contain a myc tag at the C-terminus of the helicase which is comprised of 547 amino acid residues (aa).

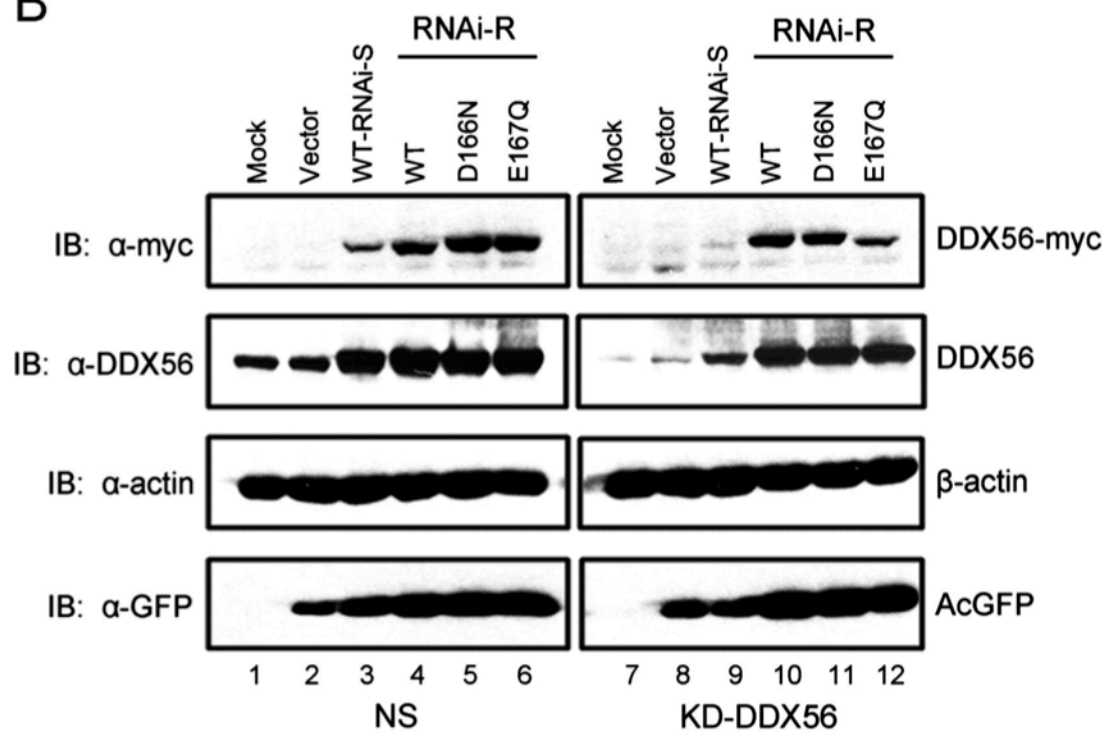
Next, expression of RNAi-resistant forms of DDX56 mutants was tested in stable cell lines depleted of endogenous DDX56. Briefly, HEK 293T cells stably expressing DDX56-specific or non-silencing shRNAs (described in Chapter 3) were transiently transduced with lentiviruses encoding AcGFP and myc-tagged wild type DDX56 or DEAD box mutants. Expression of the myc-tagged DDX56 proteins was monitored by immunoblot analyses at 48 hour post-transduction. Immunoblot analyses show that compared to expression in non-silencing (NS) cells, the level of wild type myc-tagged DDX56 (WT-RNAi-S) in DDX56 knockdown cells was just on the threshold of detection with the anti-myc monoclonal antibody (Figure 4.2 B, lanes 3 and 9). In contrast, the myc-tagged RNAi-resistant forms of wild type DDX56 as well as the D166N and E167Q mutants were robustly expressed in the DDX56 knockdown cells (Figure 4.2 B, lanes 10-12). Furthermore, probing for the total amount of DDX56 with anti-DDX56 antibody in KD-DDX56 cells confirmed these results. Together, these experiments demonstrate that catalytically inactive versions of DDX56 are stable in a cellular background in which the majority of endogenous DDX56 is depleted by RNAi.

Figure 4.2 Expression of RNAi-resistant DDX56 mutants in stable cell lines depleted of endogenous DDX56. **A.** Immunoblot analyses of DDX56 in stable HEK293T cell lines expressing DDX56-specific (KD-DDX56) or non-silencing (NS) shRNAs. **B.** The stable HEK293T cell lines were transduced with lentiviruses encoding normal (RNAi-sensitive) or RNAi-resistant versions of myc-tagged WT and D166N and E167Q mutants. The lentiviruses also encode AcGFP, which is used to monitor transduction of cells. Forty-eight hours post-transduction, levels of endogenous and myc-tagged DDX56 proteins were determined by immunoblotting.

A



B



4.2.2 DEAD box mutants are correctly targeted to the nucleolus

Next, I set out to determine whether DEAD box mutants were targeted to the nucleolus similar to wild type DDX56 (Zirwes et al., 2000). A549 cells were transfected with plasmids encoding myc-tagged wild type or DEAD box mutants of DDX56. At 24 h post-transfection, cells were infected with WNV (MOI=5) and 24 h later were fixed and processed for indirect immunofluorescence microscopy. As data in Figure 4.3 show, both RNAi-sensitive and -resistant forms of myc-tagged DDX56 are targeted to the nucleoli as evidenced by colocalization with the nucleolar marker protein nucleolin. Similarly, the DEAD box mutants D166N and E167Q localized to nuclei of A549 cells. These data confirm that mutations in the DEAD box motif or shRNA targeting sites within the DDX56 open reading frame do not alter targeting of the helicase.

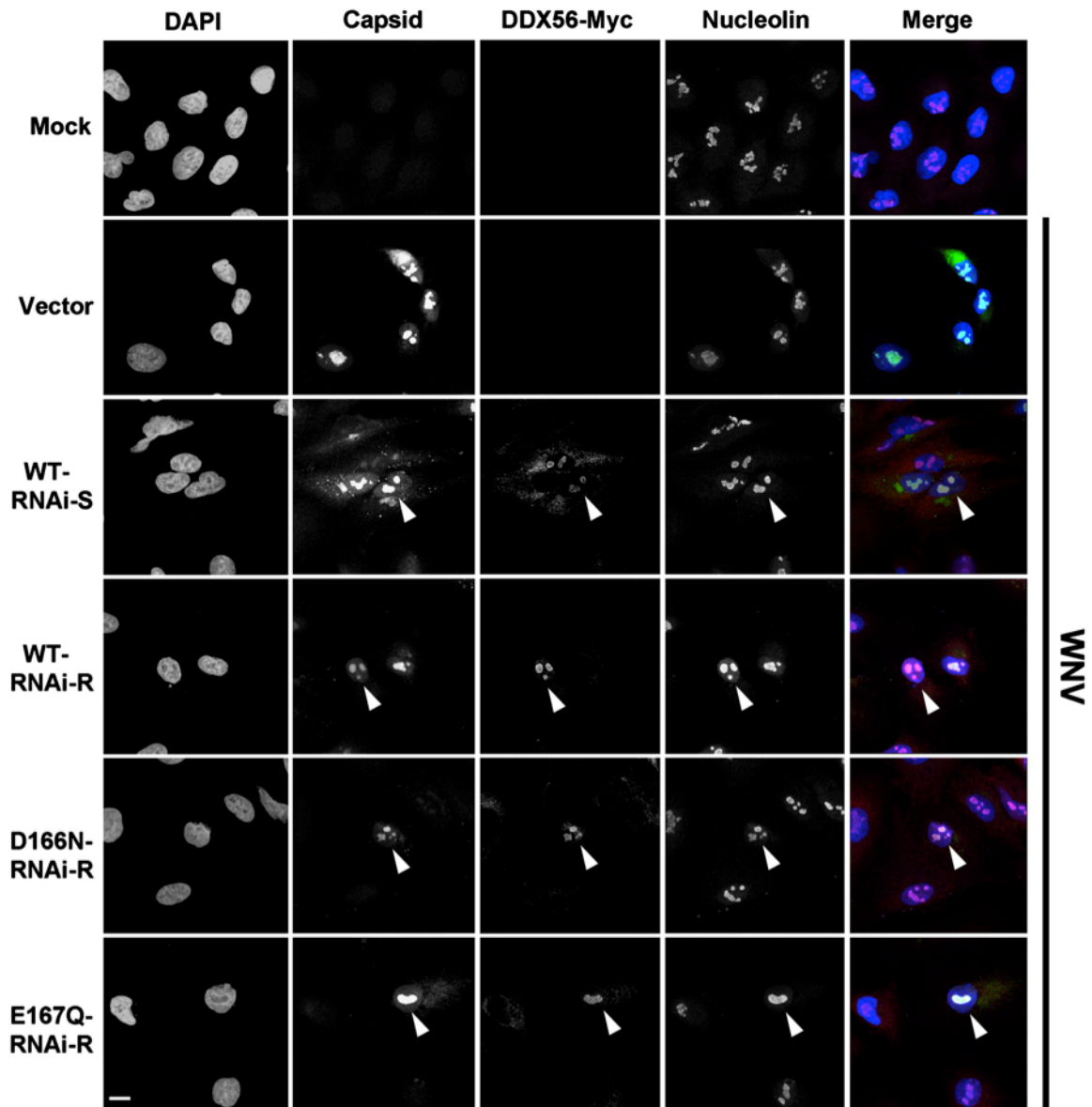
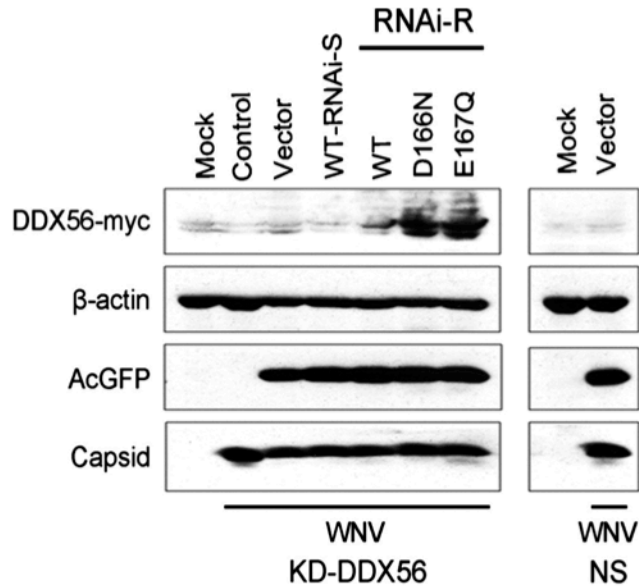


Figure 4.3 Mutations in the DEAD box site of DDX56 do not affect targeting to the nucleolus. A549 cells were transfected with plasmids encoding myc-tagged wild type (WT), DEAD box mutant (D166N and E167Q) DDX56 proteins or vector alone. Twenty-four hours post-transfection, cells were infected with WNV (MOI=5) for 24 h and then fixed and processed for indirect immunofluorescence using mouse anti-myc, rabbit anti-nucleolin, and guinea pig anti-WNV capsid antibodies. Primary antibodies were detected using donkey anti-mouse Alexa546, donkey anti-rabbit Alexa647 and goat anti-guinea pig Alexa488 secondary antibodies. Arrowheads indicate colocalization between capsid, DDX56 proteins and the nucleolar resident protein nucleolin. Nuclei were stained with DAPI. RNAi-sensitive (RNAi-S) and RNAi-resistant (RNAi-R) forms of WT and DDX56 mutants are indicated. Images were captured using a Leica TCS SP5 confocal scanning microscope. Size bar =10 μ m.

4.2.3 Helicase activity of DDX56 is important for infectivity of WNV

To determine whether enzymatic activity of DDX56 was important for replication and/or infectivity of WNV, DDX56 knockdown cells expressing RNAi-sensitive or resistant forms of myc-tagged DDX56 proteins were infected with WNV. At 48 hours post-infection, cell lysates and supernatants were subjected to immunoblot analyses and plaque assays, respectively. The immunoblot data in Figure 4.4A show that based on AcGFP expression, similar levels of transduction efficiencies were achieved for all of the DDX56 constructs. As expected, only RNAi-resistant forms of DDX56 were detected when anti-myc was used to probe lysates of transduced KD-DDX56. Regardless of whether wild type or helicase dead mutants of DDX56 were expressed in DDX56 depleted cells, similar levels of capsid protein were detected in infected cells (Figure 4.4B) indicating that enzymatic activity of DDX56 is not critical for WNV replication.

A



B

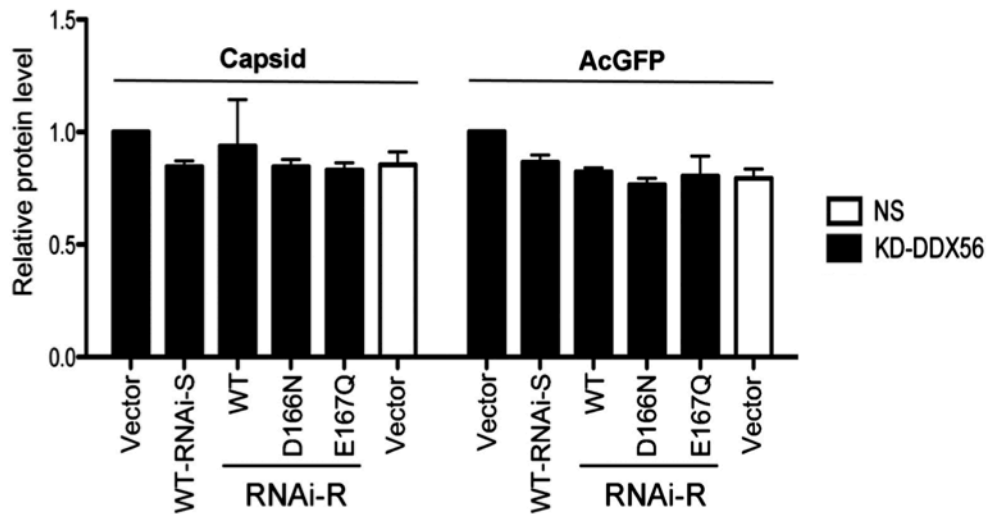


Figure 4.4 Absence of DDX56 helicase activity does not affect WNV replication. DDX56 knockdown (KD-DDX56) and non-silencing (NS) stable HEK293T cells were transduced with lentiviruses encoding myc-tagged DDX56 RNAi resistant (RNAi-R) or sensitive (RNAi-S) constructs. Cells were then infected with WNV (MOI=5) and at 48 h cell lysates were analyzed by immunoblotting (A). Relative levels of capsid and AcGFP (normalized to actin) from three independent experiments are shown in panel B. Bars indicate standard error values. $p < 0.05$, $N = 3$.

Consistent with my recently published studies (Xu et al., 2011), titers of WNV from DDX56 depleted cells were more than 100 fold lower than those from non-silencing controls (Figure 4.5A). However, infection of cells expressing RNAi-resistant wild type DDX56 resulted in normal viral titers, which were well over 1×10^8 pfu/ml. In contrast, infection of cells expressing RNAi-sensitive DDX56 or DEAD box mutants produced viral titers that were similar to DDX56 knockdown cells that had been transduced with a lentivirus encoding AcGFP only. To exclude the possibility that the failure of these DEAD box mutants to complement the production of infectious WNV virions was due to an inability to bind to capsid, co-immunoprecipitation experiments between capsid and DDX56 mutants were performed in WNV-infected HEK 293T cells. As the data in Figure 4.5B show, capsid protein was efficiently co-immunoprecipitated with D166N and E167Q mutants. All together, these data suggest that expression of DEAD box mutants did not interfere with replication of WNV but significantly reduce the infectivity of WNV virions.

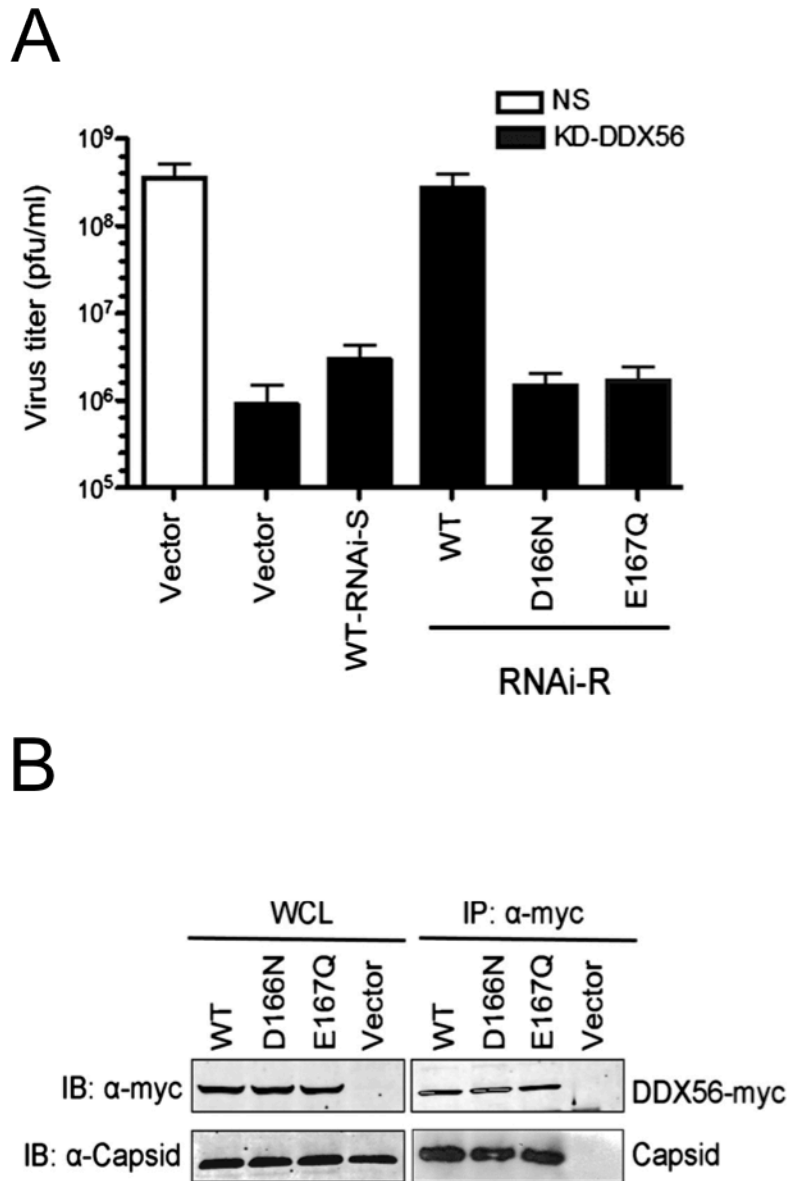


Figure 4.5 Helicase activity of DDX56 is important for WNV infectivity. A. Levels of infectious virus in the conditioned media of the transduced and infected cells were determined by plaque assays. Bars indicate standard error values. $p < 0.05$, $N = 3$. **B.** HEK293T cells were transfected with myc-tagged wt and DEAD box mutants of DDX56. At 24 h post-transfection, cells were infected with WNV (MOI=5) for 24 h and then whole-cell lysates (WCL) and mouse anti-myc immunoprecipitates were subjected to SDS-PAGE and immunoblotting with mouse anti-myc or rabbit anti-WNV capsid antibodies.

4.2.4 Helicase activity of DDX56 is important for packaging viral RNA into virions

My recent study suggests that DDX56 may function in packaging viral genomic RNA into nascent virions (Xu et al., 2011). To establish whether the helicase activity of DDX56 is important for this process, I assayed the relative amounts of genomic RNA in WNV particles secreted from cells expressing D166N and E167Q mutants. First, immunoblot results showed that loss of DDX56 helicase activity did not affect expression of WNV capsid protein (Figure 4.4) nor its secretion from infected cells in the form of virus particles (Figure 4.6A). Next, to determine if packaging of viral RNA was affected, total RNA was extracted from WNV particles and the relative amounts of genomic RNA (normalized to capsid protein) were determined by qRT-PCR. Data in Figure 4.6B show that virus particles isolated from infected cells expressing helicase dead mutants D166N and E167Q contained 3-4 times less genomic RNA than those isolated from non-silencing cells or cells expressing RNAi-resistant wild type DDX56. These data indicate that the enzymatic activity of DDX56 is important for packaging genomic RNA into WNV virions.

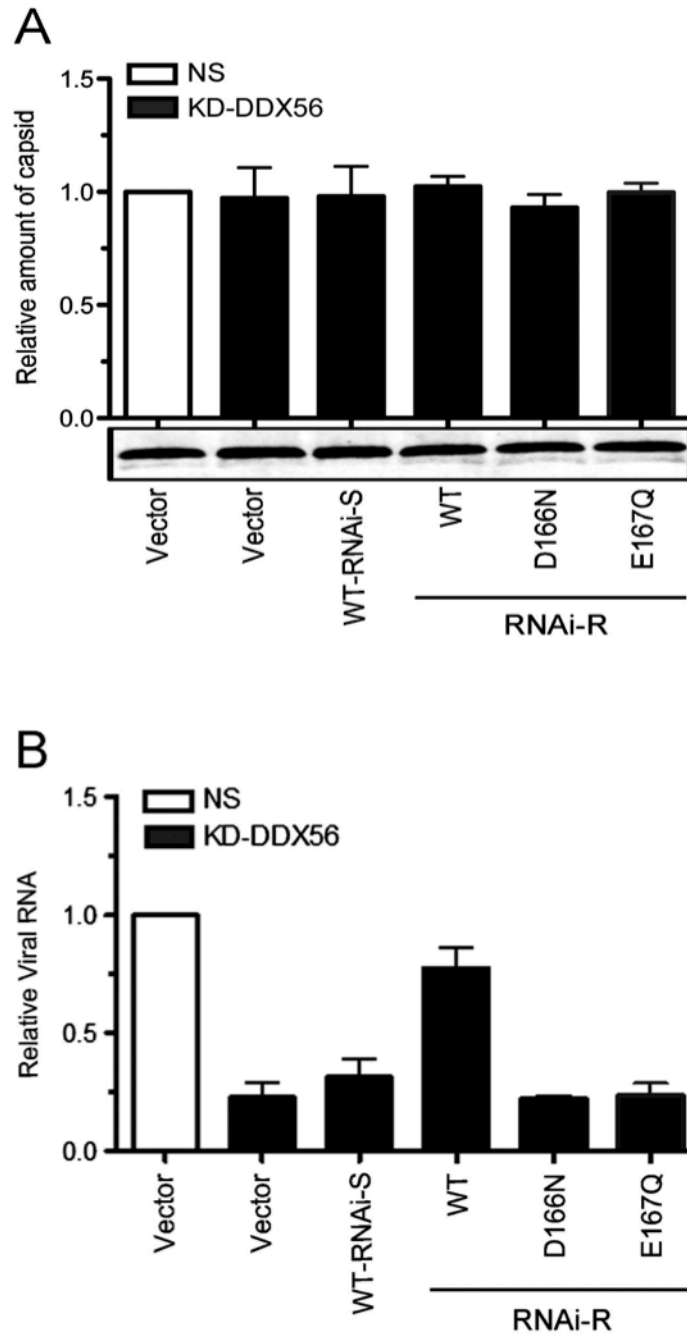


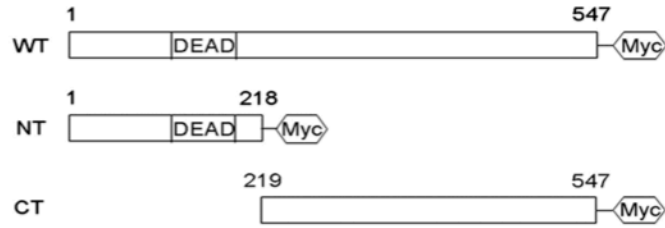
Figure 4.6 Helicase activity of DDX56 is important for packaging genomic RNA into WNV particles. **A.** WNV virions were recovered from the conditioned media of infected stable DDX56 knockdown (KD-DDX56) and non-silencing control (NS) HEK 293T cells by ultracentrifugation. The crude virion preparations were subjected to SDS-PAGE and immunoblot analyses with rabbit anti-capsid antibody. The relative amounts of capsid from three independent experiments were quantitated. **B.** Levels of viral genomic RNA in the virions were determined by RT-PCR. The average relative levels of viral RNA (normalized to capsid protein) from three independent experiments (each conducted in triplicate) were quantitated. Bars indicate standard error values.

4.2.5 Over-expression of the capsid-binding region of DDX56 reduces infectivity of WNV

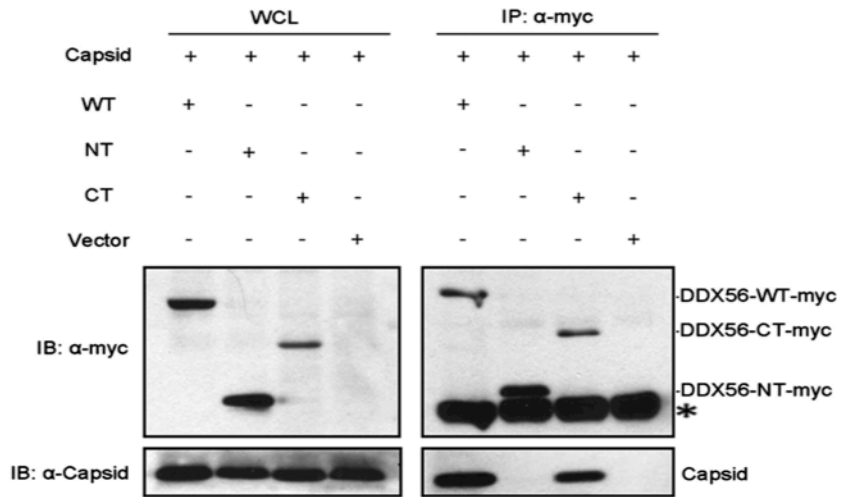
The data shown above together with results from my previous study (Xu et al., 2011) are consistent with a scenario in which interaction between WNV and catalytically active DDX56 plays an important role in assembly of infectious virions. If this is indeed the case, blocking interaction between capsid and DDX56 should also reduce the yield of infectious WNV. To test that hypothesis, I planned to overexpress the capsid-binding region of DDX56 in order to prevent interaction of endogenous DDX56 with capsid. To identify the region of DDX56 that binds to capsid, myc-tagged constructs encoding the N- and C-terminal segments of DDX56 (Figure 4.7A) were co-expressed with WNV capsid in transfected HEK293T cells followed by co-immunoprecipitation and immunoblotting. Data in Figure 4.7B show that the WNV capsid protein does not bind to the DEAD box helicase-containing region of DDX56 (DDX56-NT-myc), but rather, the C-terminal part of the protein, which was produced in cells expressing DDX56-CT-myc. I also confirmed this interaction by GST pull-down assays. GST-capsid and myc-tagged wild type DDX56 (WT), NT- and CT-domains were co-expressed in transiently transfected HEK293T cells. Lysates prepared from the transfected cells were incubated with glutathione-sepharose beads, and then bound proteins were subjected to SDS-PAGE and immunoblotting with anti-myc or anti-GST antibodies. As shown in Figure 4.7C, WT and DDX56-CT but not DDX56-NT co-purified with GST-capsid.

Figure 4.7 The C-terminus of DDX56 binds to the WNV capsid protein in transfected cells. **A.** Structure and size (amino acid residues) of myc-tagged wild type (WT), N-terminal (NT) and C-terminal (CT) DDX56 constructs. **B.** HEK293T cells were co-transfected with plasmids encoding DDX56 constructs with WNV capsid protein. In the left panel, relative levels of myc-tagged DDX56 proteins and capsid were determined in whole cell lysates (WCL) by immunoblotting with antibodies to the myc epitope and WNV capsid protein. In the right panel, cell lysates were subjected to immunoprecipitation followed by immunoblotting with antibodies to myc and capsid. The protein marked by * is IgG light chain. **C.** HEK293T cells were co-transfected with plasmids encoding GST-capsid together with WT, NT and CT DDX56 constructs or vector alone. In the left panel, relative levels of myc-tagged DDX56 proteins and capsid were determined in whole cell lysates (WCL) by immunoblotting with antibodies to the myc epitope and GST. In the right panel, cell lysates were subjected to GST-pulldown followed by immunoblotting with antibodies to myc and GST.

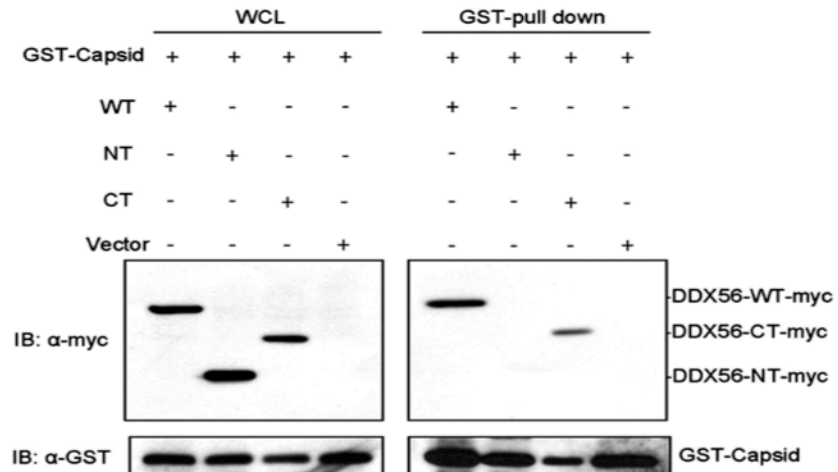
A



B



C



To further verify the authenticity of the capsid/DDX56-CT interaction under physiologically relevant conditions, co-immunoprecipitation was performed on lysates from WNV-infected cells. HEK293T cells were co-transfected with plasmids encoding DDX56 constructs (WT, NT, and CT) and then infected with WNV followed by co-immunoprecipitation and immunoblotting. Data in Figure 4.8 show that the WNV capsid protein binds to the C-terminus of DDX56 in infected cells. Meanwhile, indirect immunofluorescence analysis showed that the C-terminal region of DDX56 contains the targeting information that is required for localization to the nucleolus (Figure 4.9).

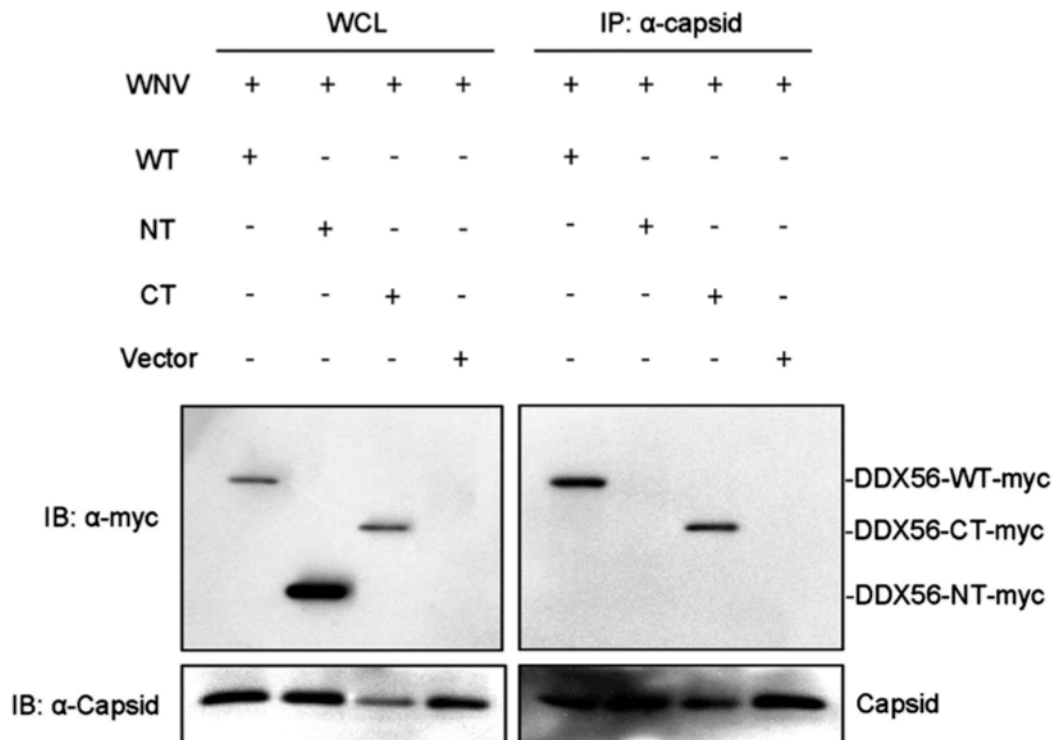


Figure 4.8 The C-terminus of DDX56 binds to the WNV capsid protein in infected cells. HEK293T cells were co-transfected with plasmids encoding DDX56 constructs and then infected with WNV. Levels of myc-tagged DDX56 proteins and capsid were detected in whole cell lysates (WCL) by immunoblotting with antibodies to the myc epitope and WNV capsid protein. In the right panel, cell lysates were subjected to immunoprecipitation by anti-capsid antibody followed by SDS-PAGE and immunoblotting with antibodies to myc and capsid.

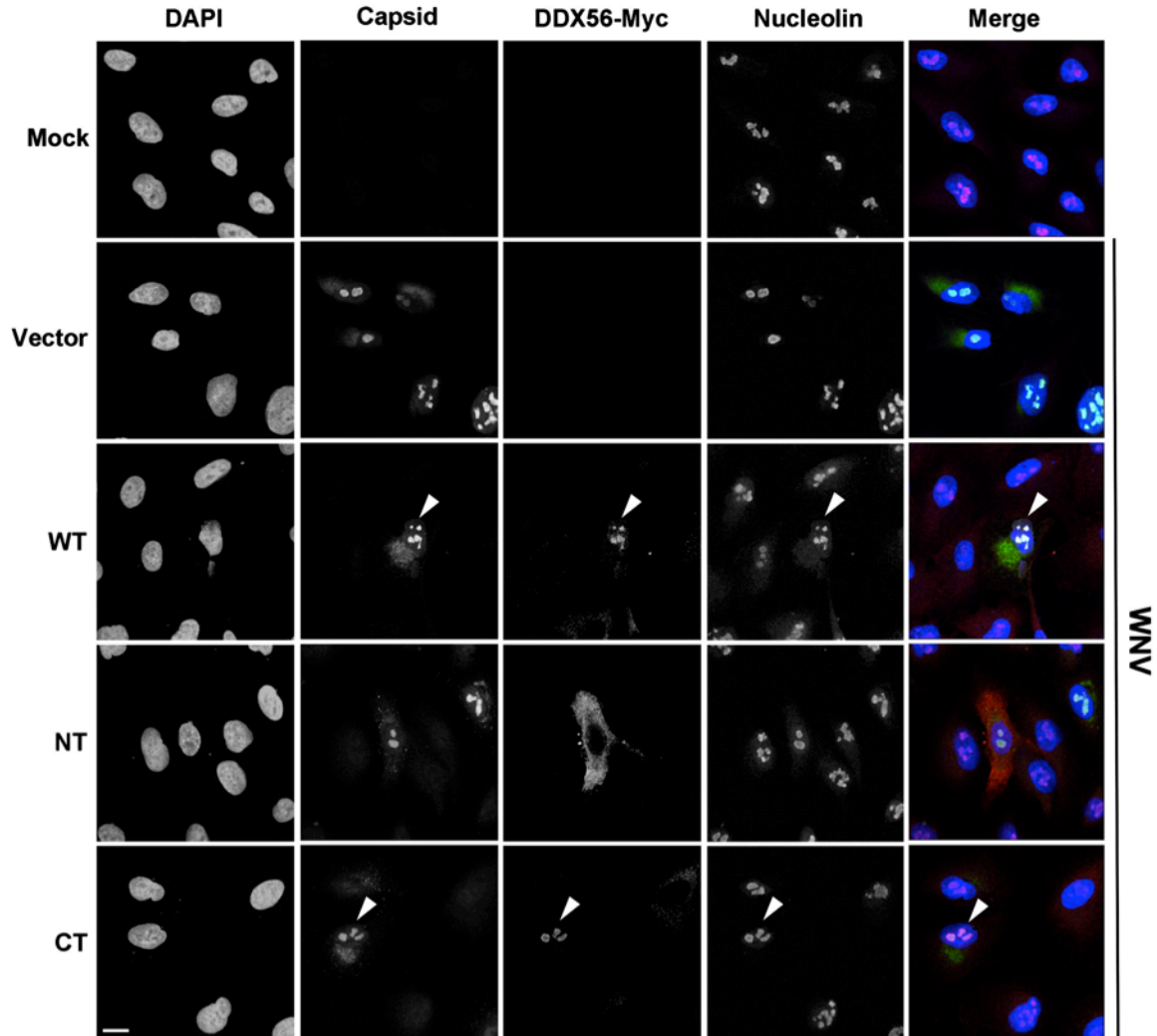
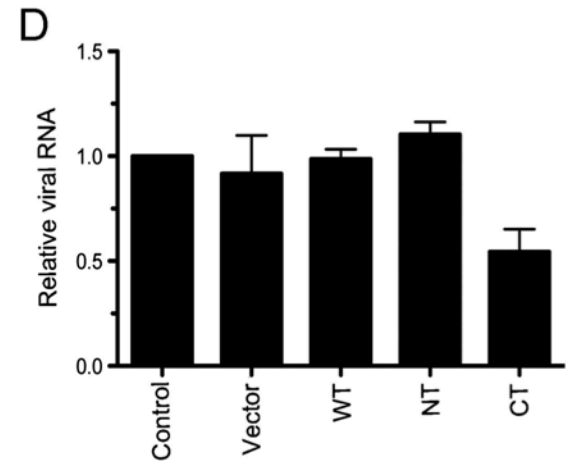
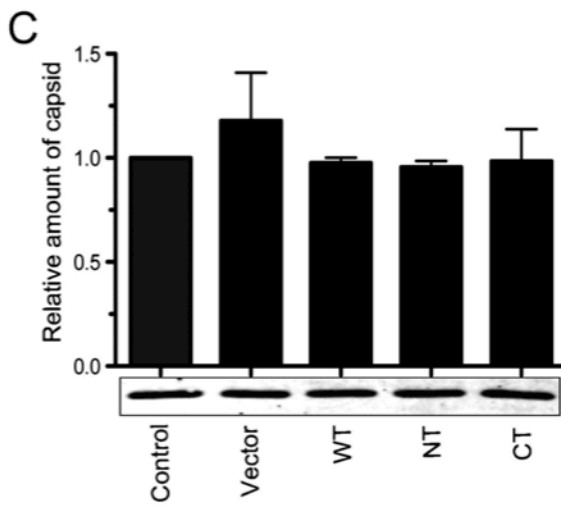
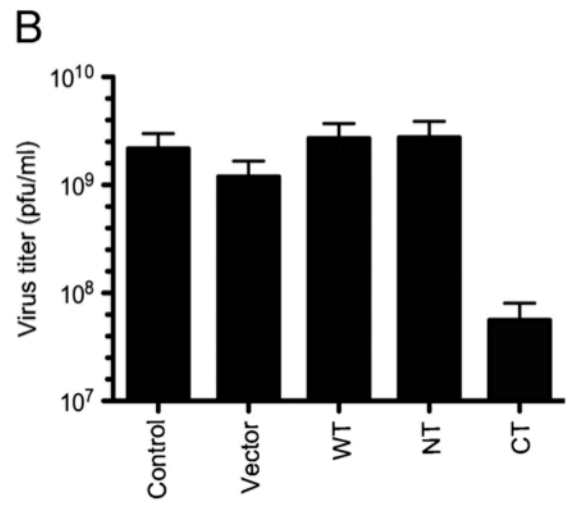
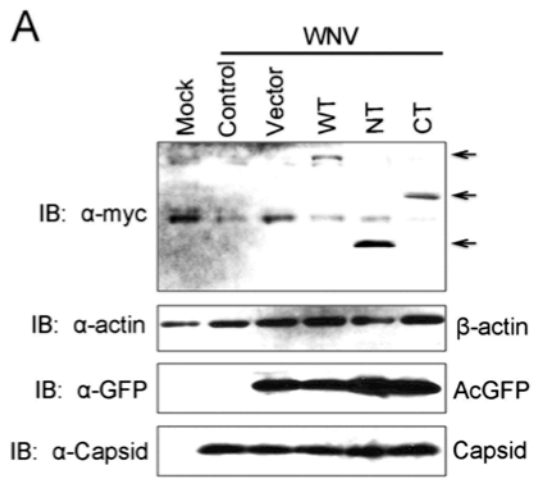


Figure 4.9 Nucleolar targeting information of DDX56 is contained in the C-terminal 329 amino acid residues. A549 cells were transfected with plasmids encoding myc-tagged wild type (WT) DDX56, DDX56-NT or DDX56-CT. Twenty-four hours post-transfection, cells were infected with WNV (MOI=5) for 24 h and then fixed and processed for indirect immunofluorescence using mouse anti-myc, rabbit anti-nucleolin, and guinea pig anti-WNV capsid antibodies. Primary antibodies were detected using donkey anti-mouse Alexa546, donkey anti-rabbit Alexa647 and goat anti-guinea pig Alexa488 secondary antibodies. Arrowheads indicate colocalization between capsid, DDX56 constructs and the nucleolar resident protein nucleolin. Nuclei are stained with DAPI. Images were captured using a leica TCS SP5 confocal scanning microscope. Size bar=10 μ m.

Finally, lentiviruses encoding myc-tagged DDX56 N- and C-terminal constructs were used to transduce HEK293T cells, which were then infected with WNV. At 48 hours post-infection, cell lysates and culture supernatants were subjected to immunoblot and plaque assays, respectively. The immunoblot data in Figure 4.10A show that expression of full length, N- or C-terminal regions of DDX56 did not affect virus gene expression based on the observation that similar levels of capsid protein were detected in all of the infected cell lysates. However, expression of DDX56-CT-myc reduced viral titers approximately 50 fold compared to full length DDX56-myc or NT-DDX56-myc (Figure 4.10B). While these results suggest that interaction between WNV capsid and DDX56 is important for a post-replication step in the WNV infection cycle, assembly and secretion of WNV particles was not affected by expression of DDX56-CT-myc (Figure 4.10C). However, significantly less viral RNA was detected in the virus particles secreted from DDX56-CT-myc-expressing cells (Figure 4.10D), an observation which is consistent with our hypothesis that capsid-DDX56 interactions are important for packaging viral genomes into nascent virions.

Figure 4.10 Expression of the capsid-binding region of DDX56 reduces infectivity of WNV. HEK293T cells were transduced with lentiviruses encoding AcGFP and myc-tagged wild type (WT), N-terminal (NT) and C-terminal (CT) regions of DDX56. The next day, cells were infected with WNV and at 48 h post-infection, cell lysates and culture supernatants were harvested. **A.** Immunoblot analyses showing expression of myc-tagged DDX56 constructs (arrows), actin (loading control), AcGFP (transduction efficiency indicator) and WNV capsid protein. Arrowheads indicate the positions of WT, NT and CT DDX56 constructs. **B.** Plaque assay was used to determine the titers of WNV secreted from cells transduced with lentiviruses encoding AcGFP alone (vector), WT DDX56, NT or CT constructs. **C.** WNV virions secreted from HEK293T cells transduced with lentiviruses encoding AcGFP alone (vector), DDX56 WT, NT or CT constructs were recovered by ultracentrifugation. The crude virion preparations were subjected to SDS-PAGE and immunoblot analyses with rabbit anti-capsid antibody. The relative amounts of capsid from three independent experiments were quantitated (A). **D.** Levels of viral genomic RNA in the virions were determined by RT-PCR. The average relative levels of viral RNA (normalized to capsid protein) from three independent experiments (each conducted in triplicate) were quantitated. Bars indicate standard error values. $p < 0.05$, $N = 3$.



4.3 Summary

In this chapter, I examined whether the catalytic helicase activity of DDX56 is required for its role in assembly of infectious WNV particles. Indeed, it was determined that less infectious virus is secreted from cells expressing DEAD box mutants of DDX56. This was not due to decreased virus replication, virus assembly defects nor the inability of the DEAD box mutants to bind to capsid protein. Moreover, loss of helicase activity does not affect targeting of the DDX56 to the nucleolus. Mapping and over-expression studies suggest that interaction of the capsid with the C-terminal region of DDX56 is important for infectivity of WNV. Together, my data are consistent with a scenario in which capsid protein recruits DDX56 to specific sites in the cytoplasm, possibly where nucleocapsid and/or virion assembly occurs. Binding to the C-terminal region of DDX56 may leave the helicase domain-containing N-terminus to function in remodeling of genomic RNA in a manner that benefits incorporation into virus particles. Planned future studies include determining if the helicase activity of DDX56 is also required for infectivity of other flaviviruses such as DENV, HCV, and JEV.

CHAPTER 5

West Nile virus infection causes endocytosis of a specific subset of tight junction membrane proteins

A version of this chapter has been published in:

“Xu Z, Waeckerlin R, Urbanowski MD, van Marle G, and Hobman TC. (2012). West Nile virus infection causes endocytosis of a specific subset of tight junction membrane proteins. *PLoS One*. 7(5):e37886.”

5.1 Rationale

WNV is a mosquito-borne flavivirus that can cause serious and even fatal neurological disease in humans. Before this occurs, the virus must breach multiple polarized epithelial and endothelial cell layers to gain access to the central nervous system following mosquito bite. Resistance to trans-cellular movement of macromolecules and pathogens across epithelia and endothelia is mediated in large part by tight junctions. The latter are apically located protein complexes, which are composed of integral membrane proteins including claudins, occludins and junctional adhesion molecules (JAM). Tight junction membrane proteins form intracellular interactions with cytoplasmic components such as ZO-1, ZO-2, ZO-3 and the actin cytoskeleton (Shen et al., 2011). Homotypic interactions between claudins, occludins and JAMs on apposing cells constitute the main barrier to intercellular passage of macromolecules and pathogens. Tight junctions are highly dynamic structures whose permeability can be altered in response to physiological and pathological conditions. With respect to the latter, it is evident that the pathogenic effects of notable human viruses such as severe acute respiratory coronavirus, influenza and ebola viruses are due to loss of tight junction barrier function (Golebiewski et al., 2011; Teoh et al., 2010; Wahl-Jensen et al., 2005).

A number of studies have reported that WNV infection compromises the integrity of the blood brain barrier (Verma et al., 2010; Verma et al., 2009; Wang et al., 2008a; Wang et al., 2004), however, the collective findings do not agree with respect to the underlying mechanism. For example, one group reported that

expression of capsid protein inhibits the barrier function of tight junctions by inducing degradation of claudin proteins in lysosomes (Medigeshi et al., 2009). In contrast, Verma *et al.* report that infection of endothelial cells by WNV *per se* does not reduce levels of tight junction components, but rather, matrix metalloproteases that are secreted from infected astrocytes cause breakdown of these structures (Verma et al., 2010; Verma et al., 2009). Moreover, they indicate that WNV infection actually results in a small but significant increase in claudin-1 levels. Finally, pathogenesis studies in mice from another laboratory support a role for matrix metalloproteinase 9 in WNV-induced disruption of the blood brain barrier through degradation of basement membranes (Wang et al., 2008a). However, the effects of viral infection on tight junction components were not investigated in this study.

While it is clear that WNV infection can negatively impact tight junctions, there is controversy as to whether or not they directly affect the expression and/or degradation of tight junction proteins. To address this question, I employed a coordinated study to understand the effects of WNV infection on tight junction proteins in both epithelial and endothelial cells.

5.2 Results

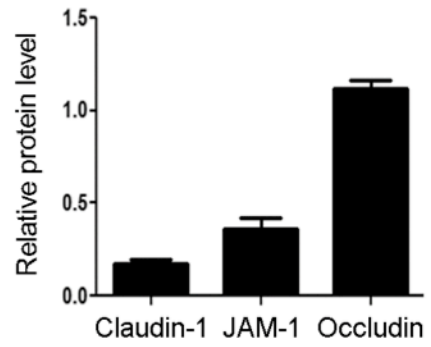
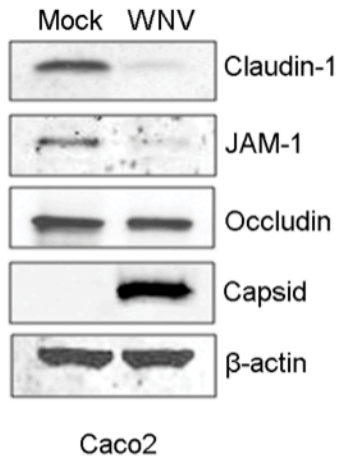
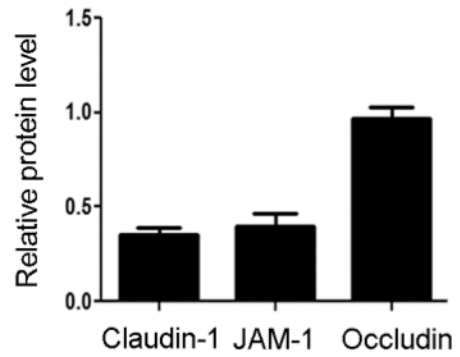
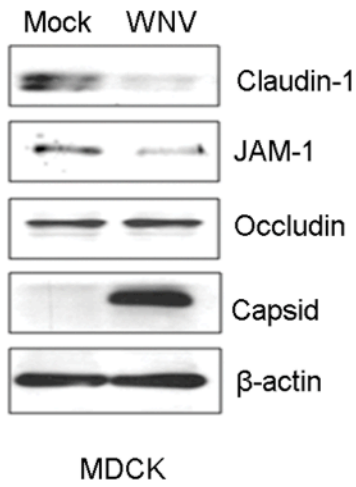
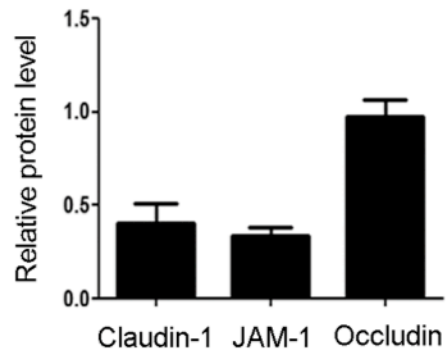
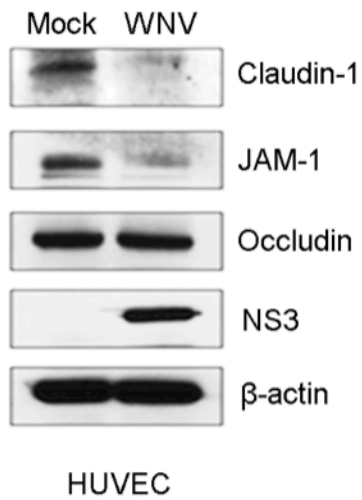
5.2.1 WNV infection results in degradation of the tight junction membrane proteins claudin-1 and JAM-1

Previous studies reporting the effects of WNV infection on tight junctions are not in agreement. Some of the discrepancies may be due to the fact that one study employed epithelial cells (Medigeshi et al., 2009) whereas others used

endothelial cells (Verma et al., 2010; Verma et al., 2009). To determine if those data vary due to cell type specific differences, I first analyzed the effects of WNV infection on tight junctions in a number of well characterized epithelial and endothelial cell lines. Mock- or WNV-infected cell lysates from epithelial (CACO2 and MDCK) and endothelial (HUVEC) cells were processed respectively and subjected to immunoblot analysis. Data in Figure 5.1 show that in all cases, the tight junction membrane proteins claudin-1 and JAM-1 are decreased in WNV infected cells. In contrast, levels of occludin protein were not affected. Since lysosomal degradation (Medigeschi et al., 2009) has been implicated in WNV-induced turnover of tight junction proteins, I set out to confirm if WNV-induced loss of claudin-1 and JAM-1 was due to protein degradation. Because a large pool of the WNV capsid protein is targeted to the nuclei of infected cells (Hunt et al., 2007; Xu et al., 2011), transcription of claudin-1 and JAM-1 genes could be affected by WNV replication. Therefore, our collaborator Dr. Regula Waeckerlin (University of Calgary) employed qRT-PCR to assess the relative levels of tight junction-specific mRNAs in WNV-infected cells. Data in Figure 5.2 show that WNV infection does not decrease the levels of claudin-1- or JAM-1-specific or other mRNAs that encode tight junction proteins such as claudin-3, claudin-4, ZO-1 and occludin. Instead, levels of tight junction specific mRNAs were significantly increased as a result of WNV infection. For example, at 24 h post-infection, claudin-1 mRNA levels were >1.8 fold higher than in mock-treated cells and at 72 h post-infection, they were 3.9 times higher ($p = 0.039$). Claudin-3 and claudin-4 mRNA levels steadily increased during

WNV infection and between 48 and 72 h were as much as 2.2 ($p = 0.005$) and 4.6 ($p = 0.043$) fold higher, respectively, than in mock samples. Levels of JAM-1 and ZO-1 mRNAs also increased significantly with peak expression levels observed at 48 h post-infection. Accordingly, we conclude that WNV-induced loss of specific tight junction membrane proteins results exclusively from protein degradation. Moreover, it is likely that this process occurs in all polarized cells regardless of whether they of epithelial or endothelial origin.

Figure 5.1 WNV infection results in loss of claudin-1 and JAM-1 proteins in epithelial and endothelial cells. CACO-2 (A), MDCK (B), and HUVEC (C) cells were infected with WNV for 48 hours after which cell lysates were subjected to immunoblot analyses with antibodies to WNV capsid or NS3, claudin-1, JAM-1, occludin and β -actin. The ratios of the relative levels of tight junction proteins (compared to β -actin) from 3 independent experiments were averaged and plotted. Error bars represent standard error of the mean. $p < 0.05$, $N = 3$.

A**B****C**

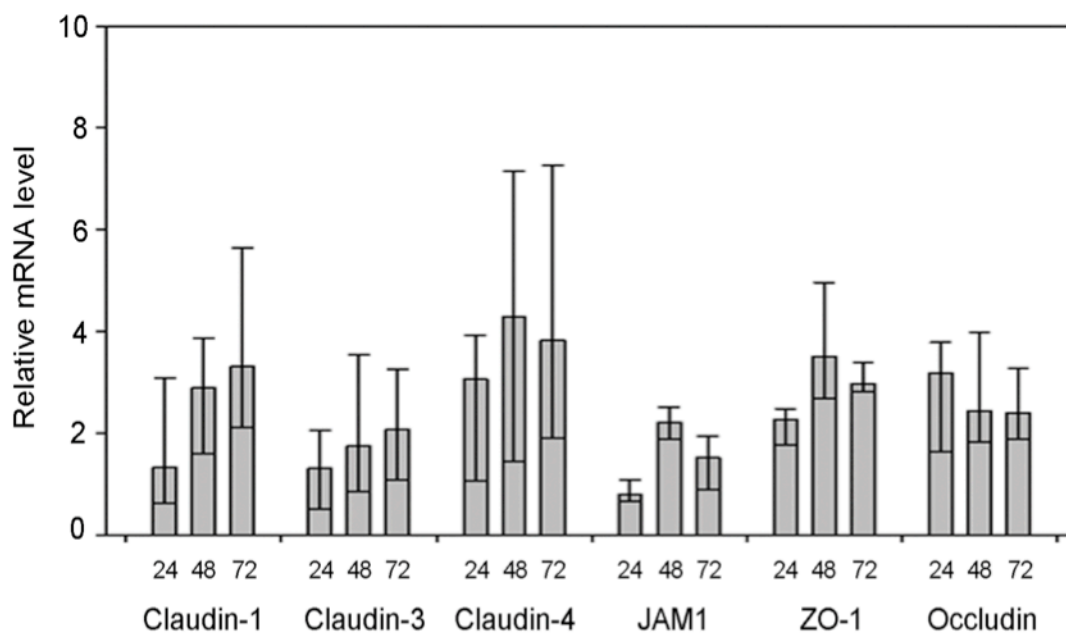


Figure 5.2 WNV infection leads to increased transcription of multiple tight junction genes. Total RNA extracted from mock and WNV-infected CACO-2 cells at 24, 48 and 72 h post-infection was subjected to quantitative RT-PCR. The levels of tight junction protein encoding mRNAs relative to GAPDH were determined using a comparative cT method. In the mock-infected samples, values were normalized to 1.0 but are not shown on the graph. The bars and associated values denominate the mean values, with one-fold standard deviations depicted in the high and low bars. Data provided by Dr. Regula Waeckerlin (University of Calgary).

5.2.2 Dynamin and microtubules are required for WNV-induced degradation of claudin-1 and JAM-1

Having ruled out the possibility that WNV infection affects the transcription and/or degradation of tight junction protein-encoding mRNAs, I next focused on determining how virus infection induces degradation of claudin-1 and JAM-1 proteins. There are a number of ways in which integral membrane proteins of the plasma membrane can be targeted for degradation, the most common of which involves clathrin- or caveolae-dependent endocytosis followed by lysosomal degradation. Moreover, because it has been reported that in response to various physiological and pathological stimuli, tight junction barrier function can be modulated by selective endocytosis of components such as claudins (Daugherty et al., 2004; Ivanov et al., 2004; Takahashi et al., 2009), I decided to investigate this pathway first. Internalization of plasma membrane proteins via clathrin-coated vesicles or caveolae requires the action of the GTPase dynamin (Hinshaw and Schmid, 1995). As such, if WNV-induced degradation of tight junction membrane proteins involves their removal from the cell surface by canonical endocytic pathways, blocking dynamin function should inhibit the turnover of claudin-1 and JAM-1 in infected cells. Indeed, treatment of cells with the dynamin-specific inhibitor Dynasore (Macia et al., 2006) completely protected these proteins from degradation during viral infection (Figure 5.3).

Next, I investigated whether drugs that affect polymerization of actin filaments and microtubules impact the stability of claudin-1 and JAM-1 in WNV-infected cells. Many membrane trafficking events in mammalian cells are

dependent upon microtubules and their associated motor proteins (Caviston and Holzbaaur, 2006), including transport from endosomes to lysosomes (Jin and Snider, 1993). Accordingly, drugs such as nocodazole that inhibit formation of microtubules, should protect claudin-1 and JAM-1 from WNV-induced degradation if the pathway involves transport from endosomes to lysosomes. In contrast to drugs that stabilize microtubules (paclitaxel) or inhibit formation of actin filaments (latrunculin B), treatment of WNV-infected cells with nocodazole completely blocked the degradation of claudin-1 and JAM-1 (Figure 5.3).

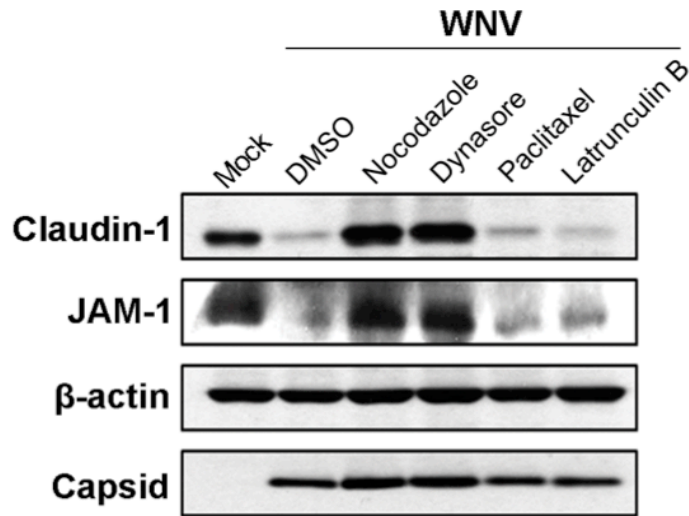
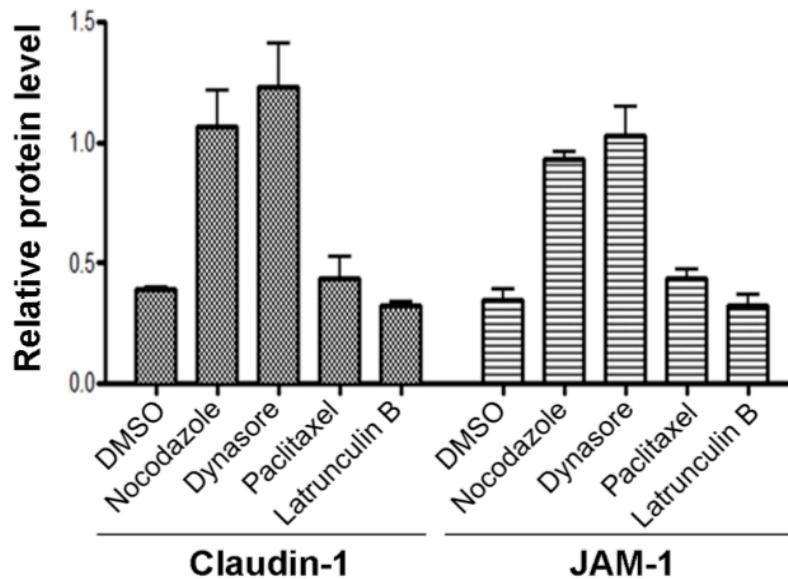
A**B**

Figure 5.3 WNV-induced degradation of claudin-1 and JAM-1 requires dynamin and microtubules. **A.** CACO-2 cells were infected with WNV and 24 hours later were treated with nocodazole (10 μ M), Dynasore (10 μ M), paclitaxel (1 μ M), latrunculin B (10 μ M) or DMSO for a further 8 hours. The corresponding cell lysates then subjected to immunoblot analyses. **B.** Data from three independent experiments were used to determine the normalized levels of claudin-1 and JAM-1 (relative to β -actin). Bars indicate standard error of the mean. $p < 0.05$, $N = 3$.

Together, these data are consistent with a scenario in which WNV infection causes dynamin-dependent endocytosis of claudin-1 and JAM-1 followed by transport along microtubules *en route* to endosomes/lysosomes. However, it still cannot be ruled out that viral infection causes misrouting of nascent claudin-1 and/or JAM-1 to lysosomes. For example, the nef protein of HIV-1 downregulates cell surface expression of MHC 1 complexes by stimulating their endocytosis as well as diversion of nascent MHC 1 complexes from the trans-Golgi network to the lysosomes (Roeth et al., 2004). Similar to endocytosis, trafficking of proteins along this route is sensitive to nocodazole (Scheel et al., 1990) and requires dynamin for vesicle scission from the *trans*-Golgi network (Jones et al., 1998). Therefore, to differentiate whether WNV infection induces endocytosis of tight junction membrane proteins from the plasma membrane or re-routing of nascent claudin-1 and JAM-1 from the trans-Golgi network to the lysosomes, I monitored the localization of these proteins in WNV infected cells that had been treated with Dynasore or nocodazole. If WNV infection causes re-routing of nascent claudin-1 and JAM-1 from the *trans*-Golgi network to lysosomes using a mechanism that requires dynamin activity and microtubule-dependent transport, then treatment of infected cells with Dynasore or nocodazole should result in their accumulation in the *trans*-Golgi network and/or associated vesicles in the juxtannuclear region. Based on the data shown in Figures 5.4 and 5.5, this does not appear to be the case. When infected cells were treated with these inhibitors, there was no significant build up of claudin-1 or JAM-1 in the juxtannuclear region but rather, I observed that the plasma membrane localization of these proteins was preserved.

Therefore, I conclude that the primary mechanism by which WNV induces turnover of tight junction membrane proteins is through dynamin-dependent endocytosis followed by microtubule-dependent transport to lysosomes.

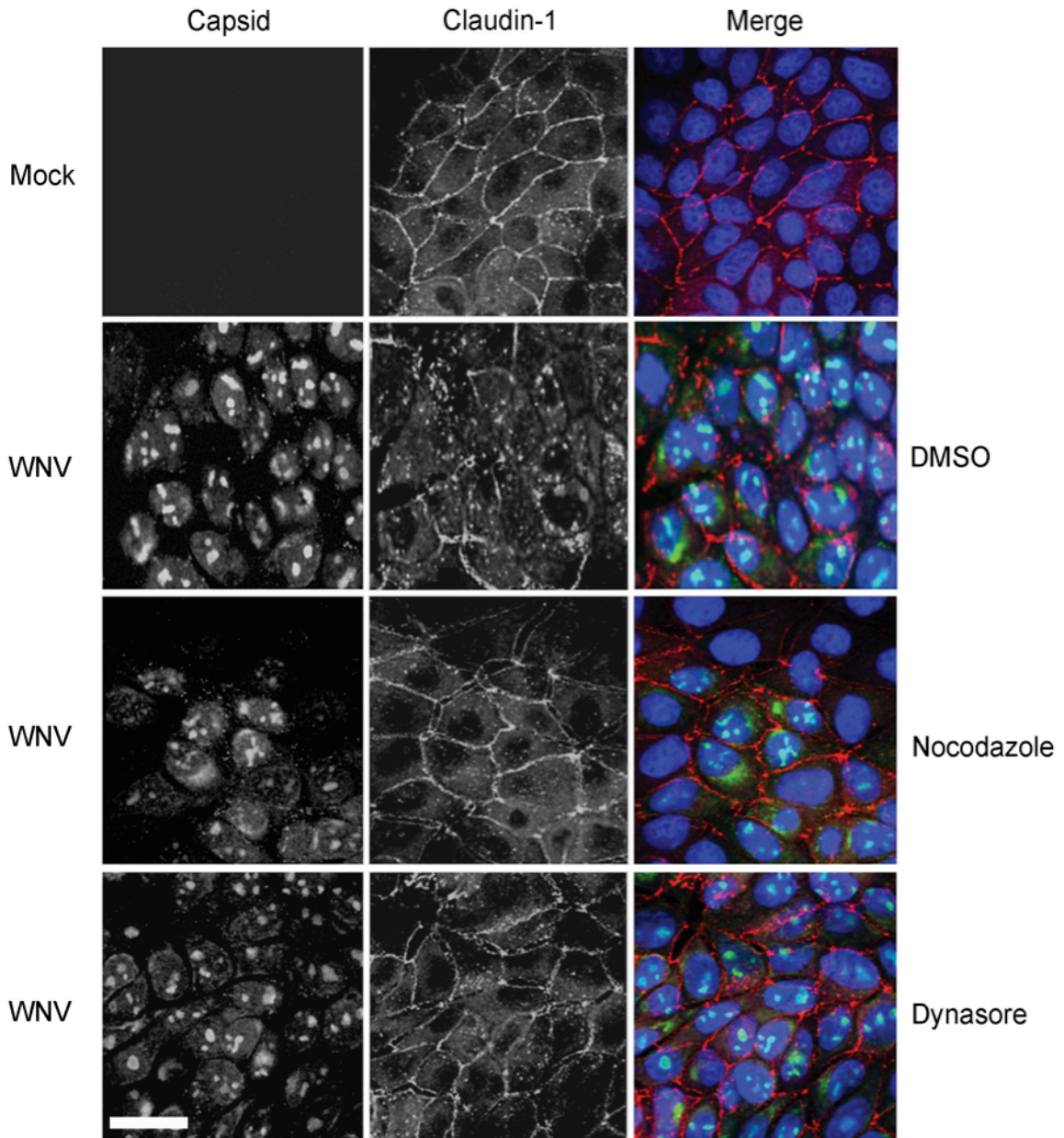


Figure 5.4 Internalization of claudin-1 is blocked by disrupting microtubules or inhibiting dynamin function. MDCK cells were infected with WNV and 24 hours later were treated with 10 μ M nocodazole, 10 μ M Dynasore or DMSO for a further 8 hours. Samples were then processed for indirect immunofluorescence using mouse anti-claudin-1 and rabbit anti-WNV capsid. Primary antibodies were detected using donkey anti-mouse Alexa546 and donkey anti-rabbit Alexa488 secondary antibodies. Nuclei were counter stained with DAPI. Images were captured using a Leica TCS SP5 confocal scanning microscope. Size bar =10 μ m.

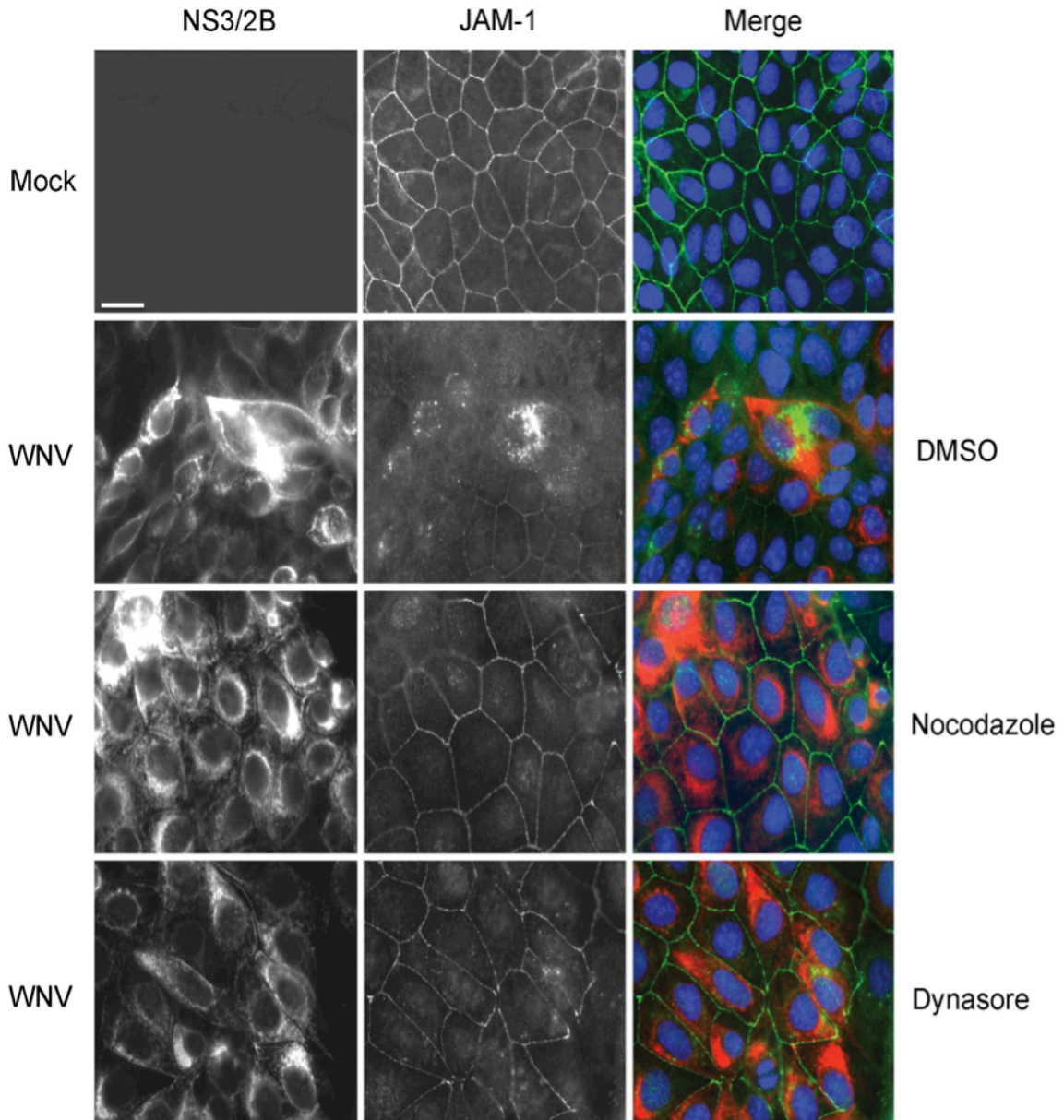


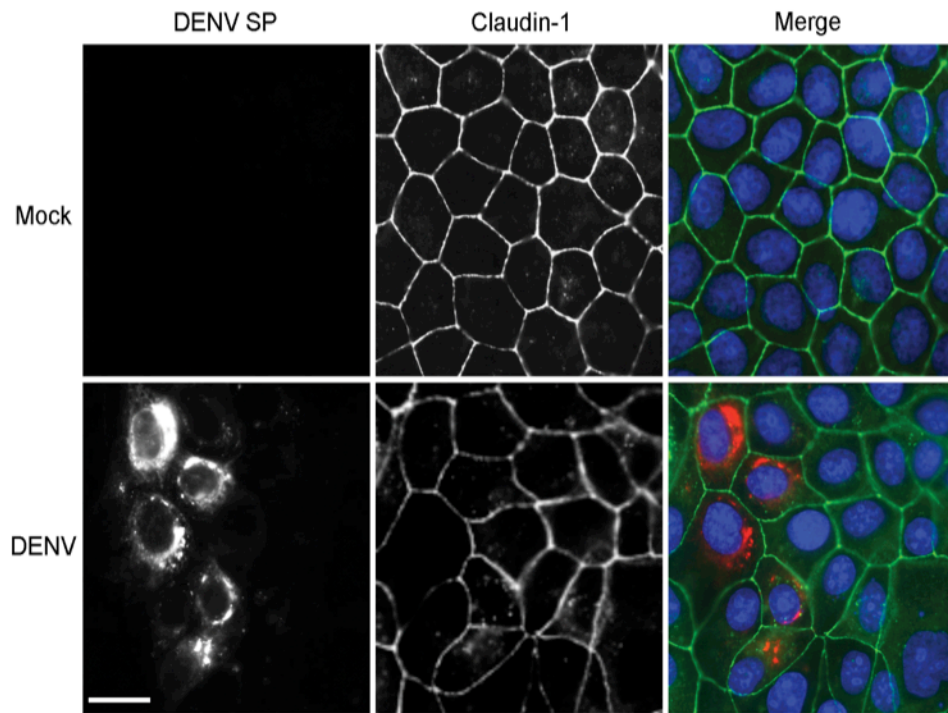
Figure 5.5 Internalization of JAM-1 is blocked by disrupting microtubules or inhibiting dynamin function. MDCK cells were infected with WNV and 24 hours later were treated with 10 μ M nocodazole, 10 μ M Dynasore or DMSO for a further 8 hours. Samples were then processed for indirect immunofluorescence using rabbit anti-JAM-1 and mouse anti-WNV NS3/2B. Primary antibodies were detected using donkey anti-mouse Alexa546 and donkey anti-rabbit Alexa488 secondary antibodies. Nuclei were counter stained with DAPI. Images were captured using a Leica TCS SP5 confocal scanning microscope. Size bar = 10 μ m.

5.2.3 Dengue virus infection does not affect tight junction membrane proteins

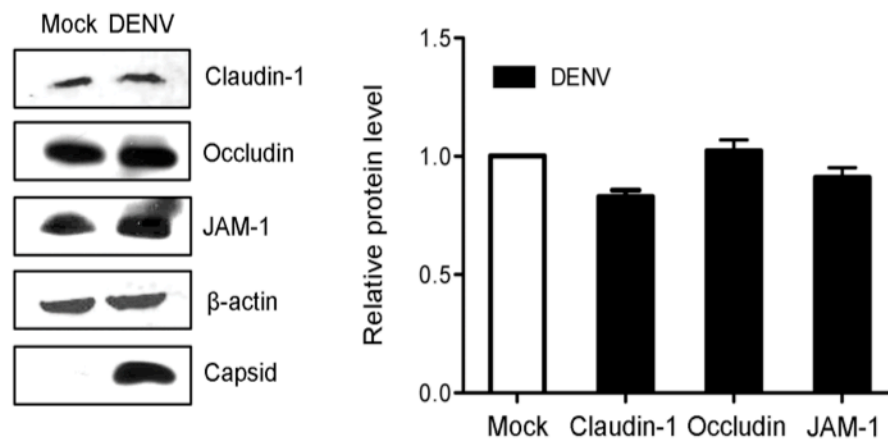
I next investigated whether infection of polarized cells by the related flavivirus, DENV, has a similar effect on tight junction membrane proteins. DENV is best known for the serious hemorrhagic disease that it causes following mosquito-borne transmission. Infection by DENV can result in vascular leakage by affecting tight junction permeability through a process involving cytokines (Chuang et al., 2011). For example, macrophage migration inhibitory factor, which is secreted by virus-infected cells, can directly affect tight junction permeability by activating MAP kinase pathways or indirectly by inducing monocytes to secrete tumor necrosis factor α (TNF- α) and other cytokines that influence the barrier function of endothelial cells. DENV has also been shown to cause neuroinvasive disease which requires the virus to breach the blood brain barrier (Sips et al., 2012). In contrast to WNV, my data showed that DENV infection did not significantly alter the localization tight junction membrane proteins such as claudin-1 (Figure 5.6A). A discernable reduction in claudin-1 protein levels (Figure 5.6B) was observed but this decrease was very small compared to the loss of claudin-1 in WNV-infected cells. Similarly, JAM-1 and occludin protein levels were not significantly affected by DENV infection.

Figure 5.6 DENV infection does not affect tight junctions. **A.** MDCK cells were infected with DENV-2 and after 48 hours, samples were processed for indirect immunofluorescence using human anti-DENV serum and mouse anti-claudin-1. The human serum recognizes DENV structural proteins (DENV SP). Primary antibodies were detected using donkey anti-human Texas Red and donkey anti-mouse Alexa488 secondary antibodies. Nuclei were counter stained with DAPI. Images were captured using a Leica TCS SP5 confocal scanning microscope. Size bar is 10 μm . **B.** CACO2 cells were infected with DENV-2 and after 48 hours, relative levels of claudin-1, JAM-1, and occudin were determined by immunoblotting. DENV capsid protein was detected using a guinea pig polyclonal antibody and β -actin was detected using a mouse monoclonal antibody. Data from 3 independent experiments were averaged and plotted. Bars indicate standard error of the mean. $p < 0.05$, $N = 3$.

A



B

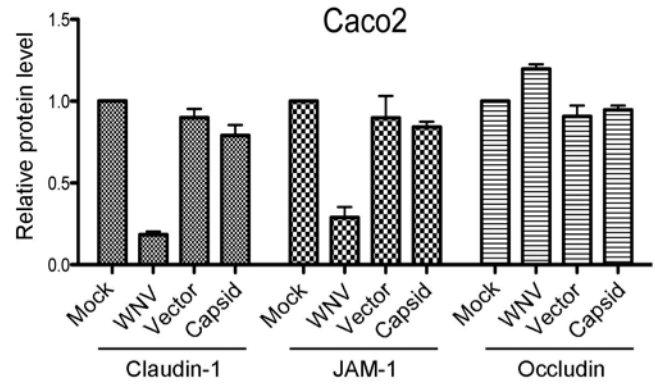
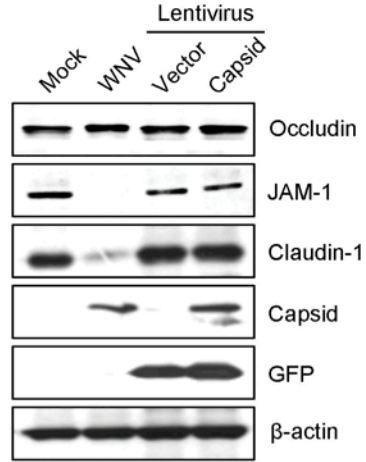


5.2.4 Expression of WNV capsid protein does not cause degradation of tight junction membrane proteins

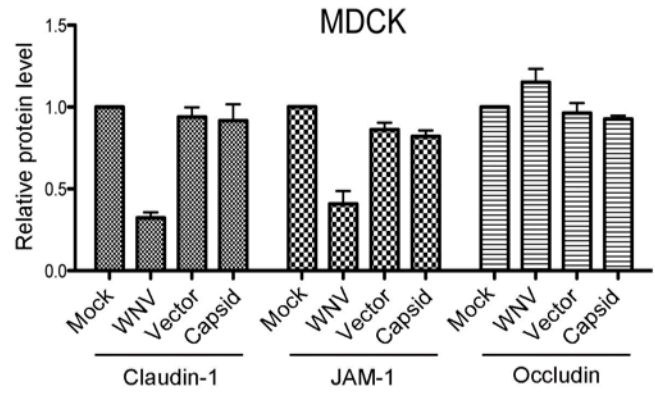
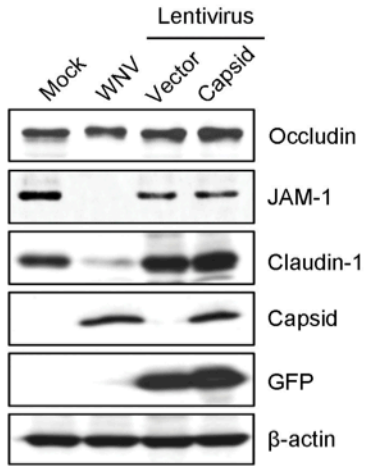
Finally, I endeavoured to understand how the WNV capsid protein, which was recently reported as the virus antigen that disrupts tight junction barrier function (Medigeshi et al., 2009), interacts with the dynamin-dependent endocytosis machinery. As the first step in this process, it was necessary to confirm that expression of capsid protein in the absence of other WNV proteins results in degradation of claudin-1. For these experiments, I used lentiviral pseudoparticles to transduce CACO-2 and MDCK cells with a cassette encoding the mature form of WNV capsid protein. In contrast to Medigeshi et al (Medigeshi et al., 2009), I did not observe significant degradation of claudin-1 or JAM-1 in capsid-expressing cells (Figure 5.7A, B), nor was there any appreciable loss of tight junction membrane proteins from the cell surface (Figure 5.8). I also examined if capsid interacts with claudin-1 and/or JAM-1 in WNV-infected cells. Data from reciprocal co-immunoprecipitation experiments indicate that capsid does not form a stable complex with either of these proteins (Figure 5.7C). Moreover, consistent with what was observed in WNV-infected cells, significant co-localization between capsid and claudin-1 or JAM-1 in the transduced cells was not evident (Figure 5.8).

Figure 5.7 Expression of capsid in the absence of other WNV proteins does not cause degradation of tight junction proteins. CACO-2 (A) and MDCK (B) cells were infected with WNV or transduced with lentiviruses encoding GFP alone (Vector) or GFP and WNV capsid (Capsid). Forty-eight hours post-infection/transduction, lysates were subjected to immunoblot analyses. Data from three independent experiments were used to determine the normalized level (to β -actin) of claudin-1, JAM-1, occludin in each sample. C. MDCK cells were infected with WNV and 48 hours later, lysates were subjected to immunoprecipitation (IP) with rabbit anti-capsid, anti-JAM-1 or mouse anti-claudin-1 antibodies followed by immunoblotting with antibodies to claudin-1, JAM-1 or capsid. WCL=whole cell lysate.

A



B



C

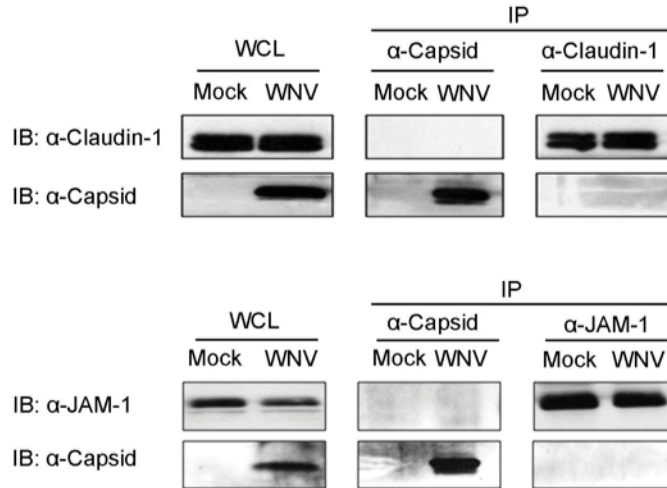
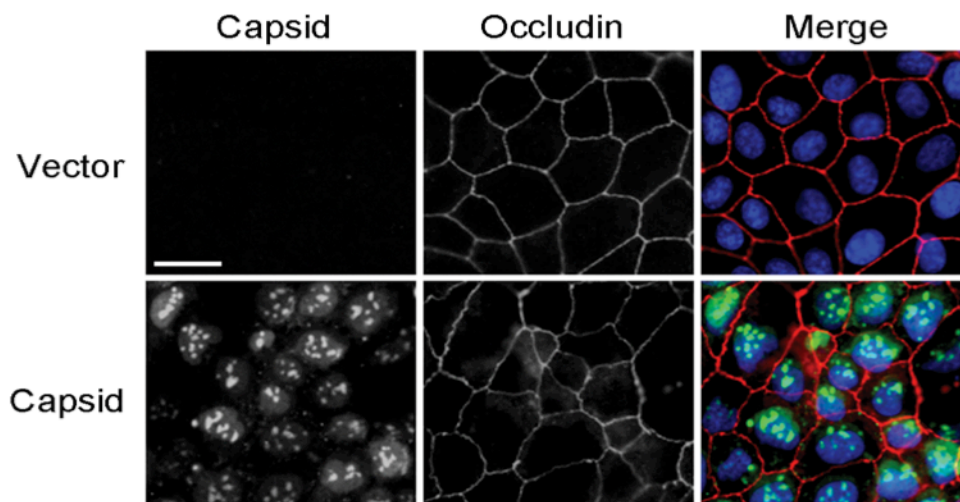
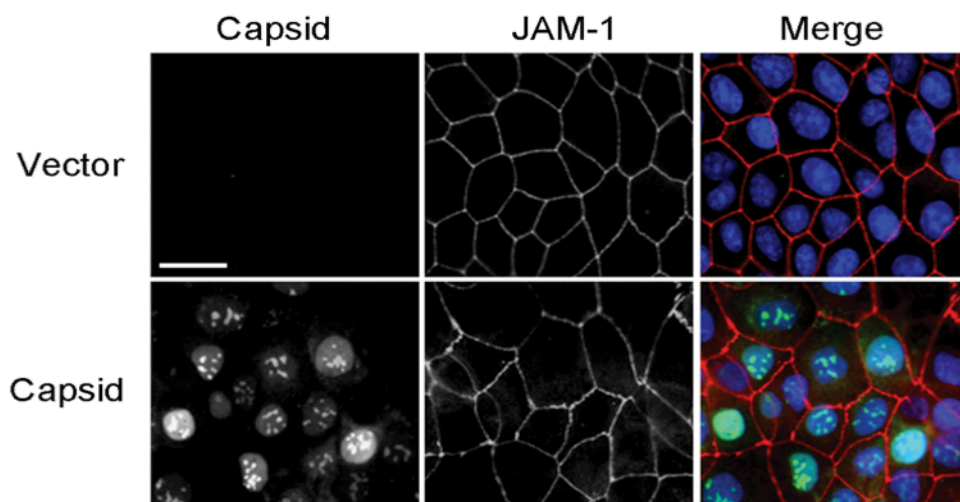
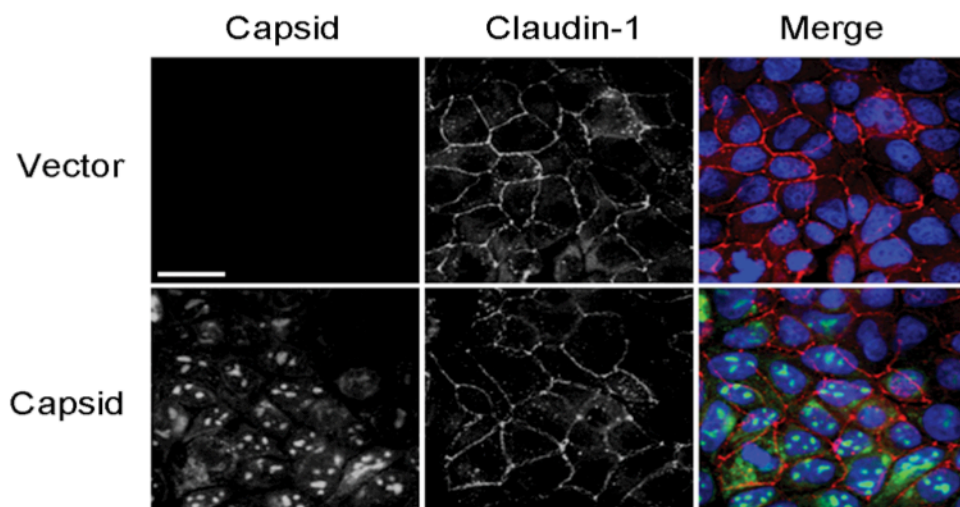


Figure 5.8 WNV capsid expression does not affect localization of claudin-1 or JAM-1. MDCK cells were transduced with vector or capsid-expressing lentiviruses and at 48 hour post transduction, were processed for indirect immunofluorescence using mouse anti-claudin-1, mouse anti-occludin, rabbit anti-JAM-1, and rabbit or guinea pig anti-WNV capsid. Primary antibodies were detected using donkey anti-mouse Alexa546, donkey anti-rabbit Alexa647, and goat anti-guinea pig Alexa546 secondary antibodies. Nuclei were counter stained with DAPI. Images were captured using a Leica TCS SP5 confocal scanning microscope. Size bar=10 μ m.



5.3 Summary

In this chapter, I examined the effects of WNV infection on tight junction proteins. For the first time, I reported that WNV infection specifically induces loss of tight junction membrane proteins claudin-1 and JAM-1 but not occludin in both epithelial and endothelial cells. Loss of claudin-1 and JAM-1 was not due to decreased mRNA transcription level but exclusively from protein degradation in lysosomes; a process that requires the endocytic regulatory GTPase dynamin and microtubules. WNV infection disrupts the typical tight junction localization of claudin-1/JAM-1 and large pools of claudin-1/JAM-1 were visible in intracellular vesicles of infected cells. However, blocking the activity of dynamin or preventing polymerization of tubulin effectively blocked the relocalization of claudin-1 and JAM-1 from the plasma to vesicles in WNV-infected cells. Together, my data suggest that WNV infection leads to selective endocytosis of a subset of tight junction membrane proteins (claudins, JAM but not occludin) followed by lysosomal degradation. In contrast to a previous study, I did not find any evidence that expression of WNV capsid alone induces claudin-1 or JAM-1 degradation or relocalization. Accordingly, future studies should be focused on determining which WNV protein causes tight junction breakdown.

CHAPTER 6

Discussion

6.1 Overview

As with all viruses, WNV is an obligate intracellular parasite that is completely reliant on host cell proteins for multiple aspects of its replication cycle. Given the genetic simplicity of WNV, it is also beneficial that some viral proteins play multiple roles in the battle with host cells for survival. The outcome of these interactions ultimately determines the fate of the virus and the cell. Although comparatively little is known about WNV virus-host interactions at the cellular level, recent evidence suggests that in addition to its structural role in nucleocapsid formation, the WNV capsid protein also plays important nonstructural functions by interacting with a multitude of host cell proteins (Bhuvanakantham et al., 2010a; Bhuvanakantham et al., 2009; Bhuvanakantham et al., 2010b; Hunt et al., 2007; Ko et al., 2010; Raghavan and Ng, 2013; Xu et al., 2011; Xu and Hobman, 2012). Undoubtedly, elucidating the interactions between this virus protein and host cell proteins will contribute to our understanding of WNV disease and may reveal potential targets for antiviral therapy. In the first two sections of this thesis, I focused on identifying novel antiviral targets for WNV and found that the capsid-binding nucleolar helicase DDX56 has a critical role in assembly of infectious virions.

Another focus of this thesis was to study how WNV breaks through the blood-brain-barrier to gain access to the central nervous system. Although a series of recent *in vitro* and *in vivo* studies have documented that WNV infection negatively impacts the barrier function of tight junctions (Medigeschi et al., 2009; Verma et al., 2010; Verma et al., 2009; Wang et al., 2008a), the collective

findings are not consistent with a unifying mechanism. For the first time, I employed a coordinated study to understand the direct effects of WNV infection on tight junction proteins in both epithelial and endothelial cells. My findings indicate that WNV infection results in targeted endocytosis of a specific subset of tight junction membrane proteins including claudin-1 and JAM-1 followed by microtubule-based transport to and degradation in lysosomes.

6.2 Cellular helicases as antiviral targets

6.2.1 A role for DDX56 in assembly of infectious WNV virions

Recently, a large-scale siRNA screen revealed that hundreds of human genes are required for WNV replication (Krishnan et al., 2008). Although these types of screens provide invaluable information for understanding the virus-host interactions on a global level, the specific mechanisms by which individual host proteins contribute to virus replication cannot usually be discerned. In the course of my PhD research, I focused on functional interactions between the WNV capsid protein and host cell proteins. Through interactions with host cell proteins, WNV has been implicated in viral pathogenesis through inhibition of antiviral activities, modulation of immune response signaling pathways, induction of apoptosis and breakdown of cellular tight junctions (Bhuvanakantham et al., 2010b; Hunt et al., 2007; Medigeshi et al., 2009; Raghavan and Ng, 2013; Yang et al., 2002). Compared to the number of nonstructural functions attributed to the WNV capsid, the number of known host cell-encoded binding partners is limited. Therefore, I conducted a large-scale yeast two-hybrid screen to identify interacting host cell proteins. One of the candidates identified in this screen, a

nucleolar RNA helicase called DDX56, was shown to play an important role in assembly of infectious virions.

DNA and RNA helicases are nucleic acid-dependent ATPases. They are divided into six super-families (SF1-6) based on sequence similarities within conserved motifs (Singleton et al., 2007). Most of RNA helicases fall into the SF2 superfamily that includes the DExH/D (x represents variable residues) box proteins (Jankowsky and Jankowsky, 2000). DDX56 is a member of the DEAD-box RNA helicases, named after a highly conserved Asp-Glu-Ala-Asp (D-E-A-D) amino acid motif which is found in all members. DEAD-box helicases contain nine conserved motifs that together are responsible for the RNA-dependent ATPase and helicase activity. They are found in all organisms from bacteria to humans and are involved in RNA splicing, RNA transport, transcription, translation, RNA degradation and ribosome biogenesis (reviewed in (Cordin et al., 2006)). RNA helicases mediate conformational changes of their substrates through ATP hydrolysis, and can unwind double-stranded RNA duplexes via the helicase activity. DDX56 was first identified as a constituent of nucleoplasmic 65S preribosomal particles. It is highly conserved within eukaryotes and localizes primarily to nucleoli (Zirwes et al., 2000). Recently, this helicase has been also reported to modulate the function of HIV-1 Rev (Yasuda-Inoue et al., 2013).

DEAD-box helicases have been shown to play important roles during virus infection. For example, the RIG-I-like receptors RIG-I/DDX58 (retinoic acid-inducible gene 1) and MDA-5 (melanoma differentiation-associated gene 5) act to sense intracellular viral dsRNA and trigger the host innate immune response

in order to limit viral replication (reviewed in (Ranji and Boris-Lawrie, 2010)). DDX3 is incorporated into hepatitis B virus (HBV) nucleocapsids, binds to HBV pol and inhibits its reverse transcription activity (Wang et al., 2009). In contrast, other viruses utilize DExH/D helicases to promote virus replication. For instance, DDX3, DDX5/p68, and DDX6 are required for HCV RNA replication (Ariumi et al., 2007; Goh et al., 2004; Jangra et al., 2010; Scheller et al., 2009). DDX3 is also important for replication of DENV replicons (Khadka et al., 2011) and DDX6 has a role in assembly or release of infectious DENV particles (Ward et al., 2011). The poxvirus protein K7 targets DDX3 to inhibit IFN-mediated antiviral response (Mulhern and Bowie, 2010; Oda et al., 2009). Moreover, DDX1 interacts with coronavirus nsp14 protein and enhances viral replication (Xu et al., 2010).

Unlike the RNA viruses described above (HCV, DENV, and coronavirus) which encode their own RNA helicases, HIV-1 does not encode an RNA helicase but instead relies on host RNA helicases for replication. For example, RNA helicase A (RHA/DHX9) associates with HIV-1 Gag and participates in virion assembly (Roy et al., 2006). RHA also promotes HIV-1 reverse transcription (Roy et al., 2006) and enhances Rev/RRE (Rev response element)-mediated gene expression (Li et al., 1999). Several other DEAD box helicases including DDX1, DDX3, DDX5, DDX17, DDX21 and DDX56 have been implicated in the replication of HIV-1 (Edgcomb et al., 2012; Fang et al., 2005; Fang et al., 2004; Ishaq et al., 2008; Robertson-Anderson et al., 2011; Yasuda-Inoue et al., 2013; Yedavalli et al., 2004). All these helicases can enhance nuclear export of unspliced viral RNA by interacting with HIV-1 Rev.

During the course of my PhD studies, I found that the capsid-binding nucleolar helicase DDX56 is important for assembly of infectious WNV virions (Xu et al., 2011). Due to their role in packaging genomic viral RNA into nucleocapsids, capsid proteins are completely necessary for virus assembly. As well as direct binding to viral RNA, capsid proteins of RNA viruses may also facilitate the production of infectious virions through interactions with host cell-encoded proteins. For example, a previous study from our laboratory suggests that interactions between the host protein p32 and the Rubella virus capsid protein promote virus replication (Beatch et al., 2005). Similarly, interactions between flavivirus capsids and host cellular DEAD helicases are important for virus replication. Multiple groups reported that the DEAD box helicase DDX3 binds to the HCV core protein (Ariumi et al., 2007; Mamiya and Worman, 1999; Owsianka and Patel, 1999; You et al., 1999b) and, more recently, this helicase was shown to be critical for replication of viral RNA (Ariumi et al., 2007). However, the functional relevance of DDX3-core protein interaction is questionable because the core mutant that is unable to interact with DDX3 still allows efficient HCV replication (Angus et al., 2010). DDX6, another DEAD helicase required for efficient HCV replication, reportedly interacts with the core protein of HCV as well as RNA (Jangra et al., 2010). However, the biological relevance of these interactions in viral replication is uncertain. Additionally, DDX5/p68 associates with HCV NS5B RNA-dependent RNA polymerase and depletion of endogenous DDX5 correlates with a reduction in the transcription of negative-strand HCV RNA (Goh et al., 2004).

Recently, a genome-wide screen revealed that DDX28, DDX42, and DHX15 are important for replication of WNV and DENV in mammalian cells (Krishnan et al., 2008). This screen did not measure the production of infectious virus but rather, only assayed expression of viral proteins. Since DDX56 is not required for replication of WNV genomic RNA or viral protein synthesis *per se* (Figure 3.11), it could not have been identified in this type of RNAi screen. Instead, DDX56 seems to play an essential post-replication role in assembly of infectious WNV virions.

Current studies suggest that flavivirus morphogenesis does not simply involve the stochastic interaction between genomic RNA, viral capsid and membrane proteins. In fact, virus assembly is closely correlated with replication of viral RNA such that only genomic RNA that is derived from active replication complexes is selectively packaged into virions (Khromykh et al., 2001b). This process is dependent in part on the viral-encoded helicase NS3, but interestingly, the mode of action varies significantly among flaviviruses. For example, assembly of infectious Kunjin virus, a subtype of WNV, requires expression of NS3 protein in *cis* (Liu et al., 2002). On the other hand, production of infectious yellow fever virus particles does not rely on *cis* activity of NS3, and surprisingly, the helicase activity of this protein is dispensable for *trans*-complementation (Patkar and Kuhn, 2008). The NS3 helicase of HCV may function in virus assembly possibly by acting as a scaffold for interaction with viral or cellular cofactors. Mutagenesis of the helicase domain of HCV NS3 revealed a role in virus assembly that is independent of its role in RNA replication (Ma et al., 2008b). These findings

agree with my own studies which indicate that cellular helicases such as DDX56 can act at post-replication steps.

In DDX56 knockdown cells, assembly and secretion of WNV particles was not dramatically affected, however, the infectivity of the resulting virus particles was >100-fold lower compared to virions secreted from control cells (Figure 3.9 and 3.10). Assembly and/or release of infectious DENV virions is compromised when expression of the 3'UTR-binding helicase DDX6 is decreased (Ward et al., 2011). DDX6 localizes to and is required for the formation of processing (P) bodies, which are sites of translational silencing and mRNA storage (Weston and Sommerville, 2006). However, in DENV-infected cells, a fraction of DDX6 colocalizes with dsRNA at DENV replication sites. Knockdown of DDX6 reduces DENV RNA in secreted virions as well as viral titers (2- to 3-fold). In so far as we are aware, other than DDX56, DDX6 is the only cellular helicase that functions in assembly of flavivirus particles.

DDX6 also appears to be important for packaging of certain foamy virus genomes (Yu et al., 2011). Similar to DENV-infected cells, relocation of DDX6 from P-bodies and stress granules to virus assembly sites at the perinuclear region occurs in foamy virus-infected cells. Knockdown of DDX6 results in decreased levels of viral RNA in extracellular virions but intracellular viral protein synthesis, replication of viral RNA, and capsid assembly and release are not affected (Yu et al., 2011). Moreover, as with DDX56, DDX6 is not incorporated into virions, however, it is important to point out that DDX6 does not form stable complexes with Gag proteins.

Other retroviruses appear to coopt DDX6 for assembly of virions. For example, DDX6 together with the RNAi effector protein Ago2, binds to HIV-1 Gag to facilitate capsid assembly independent of RNA packaging (Reed et al., 2012). Conversely, the cellular RNA helicase DDX24 plays a role in packaging HIV RNA into virions (Ma et al., 2008a). My data suggest that DDX56 has a similar role in packaging viral RNA in WNV virions. Specifically, depletion of DDX24 does not reduce production of HIV-1 proteins or secretion of virus particles, but the infectivity of virions released from DDX24-knockdown cells was significantly lower. Because loss of DDX24 only decreases HIV-1 titers 3-fold (Ma et al., 2008a), this suggests that DDX56 is more important for morphogenesis of infectious WNV virions than DDX24 is for HIV-1 infectivity.

DDX56 is thought to function in assembly of pre-ribosomal particles, but it is not incorporated into mature ribosomes (Zirwes et al., 2000). By analogy, it is tempting to speculate that DDX56 functions similarly in assembly of other large ribonucleoprotein particles such as viral nucleocapsids. The fact that DDX56 is not detected in mature WNV virions (Figure 3.12) is consistent with this postulation. So far, the precise mechanism by which DDX56 facilitates assembly of infectious WNV particles is not defined. However, given the observation that when proteasomal degradation is inhibited, DDX56 accumulates on capsid-positive structures in the cytoplasm (Figure 3.8), it is tempting to consider the following scenario: WNV infection results in translocation of DDX56 from the nucleolus to the cytoplasm, where it interacts with the pool of capsid protein at the site of virus assembly, the ER. Since helicases are motor enzymes that use energy

derived from nucleoside triphosphate hydrolysis to unwind double-stranded nucleic acids, the interaction between capsid protein and DDX56 could facilitate packaging genomic RNA into nucleocapsids by separating it from the dsRNA, a replication intermediate. DDX56 itself is not incorporated in WNV virions (Figure 3.12), suggesting that its association with capsid is transient. Accordingly, dissociation of DDX56 from capsid proteins that are incorporated into nascent virions may trigger proteasome-dependent turnover of DDX56 as a result of its inadvertent exposure to the cytoplasmic degradation machinery. Although expression of capsid alone does not induce translocation of DDX56 from the nucleolus to the cytoplasm, it is possible that this viral protein is required for this process. Indeed, the accumulation of capsid in the cytoplasm coincided with the loss of DDX56 from the nucleolus at later times during infection. Together, studying capsid-DDX56 interactions in more detail will provide us with novel insights into the biology of DDX56 and potentially lead to the development of antiviral drugs and the therapeutic targeting of DDX56.

6.2.2 DDX56 as an antiviral target for WNV or other flaviviruses

Targeting host factors that are essential for virus replication rather than viral proteins is an attractive prospect since traditional antiviral therapies that inhibit virus-encoded enzymes suffer from a number of limitations. First, viral genes are more prone to mutate than the human genes and therefore it is easy for the viruses to develop drug resistance. This is particularly true of RNA viruses whose polymerases do not possess proof reading activity and are therefore error prone and mutable. Second, the choice of virus-encoded targets is often very

limited due to the small number of enzymes encoded by most RNA viruses. In contrast, exploiting host factors as means to control viral replication is a viable option that has shown promise, particularly for flaviviruses. Since more than hundreds of host genes have been reported to be required for replication and assembly of infectious flavivirus particles (Krishnan et al., 2008), it may be possible to target a variety of host proteins, particularly enzymes, as a means to control viral infection. Although this approach may also have its own drawbacks such as causing cytotoxicity and side effects to the host, viral resistance to small molecules that block host enzymes should be minimal. Excitingly, exploitation of non-anti-infective drug therapies that target cellular enzymes, such as angiotensin-converting enzyme (ACE) to treat hypertension, congestive heart failure, breast cancer, and Alzheimer disease is successful and reveals the feasibility of such an approach (Menard and Patchett, 2001).

Approximately 80% of all viruses are RNA viruses. Most RNA viruses that replicate in the cytoplasm mostly encode a helicase protein, whereas those that replicate in the nucleus utilize cellular helicases. Recently, RNA helicases have received a great deal of interest as potential antiviral targets (Geiss et al., 2009; Kwong et al., 2005; Maga et al., 2011; Stankiewicz-Drogon et al., 2010). Among the helicase superfamily, DExD/H box proteins form the largest group of these enzymes. In most cases, the physiological substrates of DExD/H box helicases have not been defined but it is clear that a number of pathogenic RNA viruses require these enzymes for replication and/or assembly. For example, DDX1, DDX3, DDX6, DDX24, and RHA have been linked to HIV-1 replication. RHA

was the first cellular helicase shown to be involved in HIV replication (Reddy et al., 2000) and is encapsulated into the HIV particles (Roy et al., 2006). DDX1 and DDX3 promote replication of HIV by facilitating export of HIV RNA from the nucleus to the cytoplasm through interaction with Rev (Fang et al., 2004; Yedavalli et al., 2004). DDX6 facilitates HIV capsid assembly independent of RNA packaging (Reed et al., 2012) and DDX24 facilitates packaging of viral RNA (Ma et al., 2008a). Other human pathogenic viruses such as influenza A virus, coronavirus and poxviruses rely cellular helicases for their replication (Lin et al., 2012; Oda et al., 2009; Xu et al., 2010). As discussed earlier, DEAD box helicases play significant roles in the biology of flavivirus infections too (Ariumi et al., 2007; Goh et al., 2004; Jangra et al., 2010; Khadka et al., 2011; Krishnan et al., 2008; Mamiya and Worman, 1999; Scheller et al., 2009; Ward et al., 2011; Xu et al., 2011).

6.2.2.1 Examples of host RNA helicases that have been considered for antiviral therapy

In order to serve as viable targets for antiviral therapy, one should focus on host cell proteins that are essential for one or more steps in the virus life cycle, but dispensable for the cell survival. Recently, the human DEAD-box RNA helicase DDX3 was considered a prime target for antiviral therapy. First, DDX3 knockdown in several cell lines, did not reveal any deleterious effects on cell proliferation or vitality (Ishaq et al., 2008; Yedavalli et al., 2004); Second and perhaps most excitingly, genetically unrelated viruses such as HCV, HBV, HIV-1 and poxviruses encode proteins that interact with DDX3 (Ariumi et al., 2007;

Mulhern and Bowie, 2010; Oda et al., 2009; Wang et al., 2009; Yedavalli et al., 2004).

Small molecules that suppress HIV-1 replication by targeting DDX3 have been reported. Through a random-screening approach, a series of synthesized new ring-expanded nucleoside (REN) analogs (the most potent being REN, CID 44586781) were shown to suppress HIV-1 replication in T cells and macrophages by inhibiting the RNA helicase activity of DDX3 (Yedavalli et al., 2008). Moreover, the availability of crystallographic structures for DDX3 helicase (PDB entries code 2JGN and 2I4I) has facilitated the use of classical structure-based approaches for identification of small molecule inhibitors. Using docking, virtual screening, and tests of the ability of compounds to inhibit DDX3-catalyzed ATP hydrolysis or DNA unwinding, Maga *et al.* showed that rhodanine-based inhibitors targeting the ATP binding site of DDX3 inhibit HIV-1 replication by disrupting HIV mRNA export (Maga et al., 2008). This was the first successful example of rational-based drug design approach applied to a DEAD box protein to inhibit virus replication. Biphenyls (N,N'-diaryurea (CID 29766776)) that target the RNA binding site of DDX3 also inhibit HIV-1 replication at micromolar concentrations ($IC_{50} = 15 \mu\text{M}$) (Radi et al., 2012). Importantly, the small molecule DDX3 inhibitors did not show significant toxicity in mouse models (Maga et al., 2008; Radi et al., 2012; Yedavalli et al., 2008). Together, these data provide proof-of-principle for the feasibility of blocking HIV-1 infection using small molecule that target cellular enzymes.

Since DDX3 is also required for HCV replication, targeting this enzyme

could also lead to novel HCV drugs. However, comparatively little is known regarding the interaction between HCV components and DDX3. Furthermore, it has been reported that inactivation of DDX3 during HCV infection leads the development of liver carcinoma (Chang et al., 2006). Therefore, development of antiviral drugs that specifically target the interaction of virus components with DDX3 is essential.

Another potential antiviral target is the helicase RHA. Human RHA also known as DHX9, is a DEIH RNA helicase that predominantly localizes to nucleus where it interacts with RNA polymerase II and transcription factors to modulate gene transcription (Nakajima et al., 1997; Tetsuka et al., 2004). In the cytoplasm, RHA selectively facilitates efficient cap-dependent mRNA translation (Hartman et al., 2006). At least three different types of viruses including HIV-1, HCV and FMDV (foot and mouth disease virus) are known to utilize RHA in their replication cycles. Interaction between RHA and the terminal regions of viral RNA appears to be important for replication. For example, RHA promotes translation of HIV-1 RNA by interacting with structures in the 5' UTR (Bolinger et al., 2010). Knockdown of RHA does not affect the cell growth, but infectivity of HIV-1 virions was significantly reduced. RHA is actually incorporated into progeny virions where it increases the activity of reverse transcriptase, a process that appears to be important for infectivity (Bolinger et al., 2010; Roy et al., 2006).

Using a replicon model, it was shown that downregulation of RHA in cells results in decreased HCV RNA and protein levels (He et al., 2008). Similarly,

knockdown of RHA inhibits replication of FMDV (He et al., 2008).

Future studies should focus on identifying the domain(s) or amino acid residues of RHA that are required for interaction with viral RNA. It will also be of interest to test whether a common domain or motif is required by multiple viruses. These fundamental investigations will provide invaluable information that is needed to develop antiviral therapies that selectively discriminate between the cellular and viral RNA targets of RHA.

6.2.2.2 DDX56, a potential antiviral target for WNV and/or other flaviviruses?

Since DDX56 is not required for viability of cells *in vitro* (Figure 3.9), targeting this enzyme is in theory at least, a potential target for controlling WNV and potentially other flavivirus infections. Rather than using RNA interference to down-regulate expression of DDX56 in cells, it would be advantageous to use small molecule inhibitors that target the enzymatic activity of this protein. This is because, although DDX56 is not essential for cell survival, we cannot exclude the possibility that this helicase plays other essential roles in cell physiology. Indeed, very little is known about the cellular functions of DDX56. Furthermore, it is also possible that not all of the cellular functions of DDX56 require its ATPase and helicase activity. Hence inhibiting this enzymatic activity of DDX56 should leave the ATPase-independent cellular functions of DDX56 intact. If this is to be a feasible approach, it was important to demonstrate that the helicase activity of DDX56 is in fact required for its role in WNV infectivity.

I constructed two inactivating mutations (D166N and E167Q) in the DEAD box motif and analyses of these mutants indicated that the helicase activity

of DDX56 is not required for replication or assembly of WNV virions, but it is critical for infectivity of virus particles (Figure 4.4 and 4.5). Moreover, overexpression of the capsid-binding region of DDX56 had a similar effect as reducing expression of DDX56 or knocking out its helicase activity (Figure 4.10). Together, these findings indicate that the interaction between catalytically active DDX56 and the WNV capsid protein is important for packaging genomic RNA into nascent virions and is essential for assembly of infectious WNV particles.

Based on the data from the study of DDX56 in WNV biology, I hypothesize that interaction between capsid and helicase DDX56 facilitates loading and/or organization of viral RNA during virus assembly. Through an unknown mechanism, WNV infection causes relocalization of DDX56 from the nucleolus to cytoplasmic structures that are enriched in capsid protein (Figure 3.8). It is likely that these capsid-positive cytoplasmic elements are virus assembly sites on the ER. Next, it will be of interest to study whether DDX56 is also required for infectivity of other flaviviruses such as DENV, HCV, JEV, SLEV (St Louis Encephalitis virus) and TBEV (Tick-borne Encephalitis virus). These studies will provide novel insights into the biology of DDX56 and could also aid in development of antiviral therapies that rely on blocking the activities of cellular RNA helicases. Ideally, development of small molecule inhibitors that specifically and selectively target the ATPase/helicase activity of DDX56 has two key requirements: 1) Knowledge of the crystal structure of DDX56; 2) Knowledge regarding the mechanism of action of the enzyme.

To my knowledge, the structure of DDX56 has not yet been solved,

however, it is likely that small molecules that disrupt this enzyme could act via one or more of the following mechanisms: 1) Inhibition of the ATPase activity; 2) Interference with RNA binding; 3) Uncoupling between ATP hydrolysis and RNA unwinding; 4) Inhibition of the RNA translocation activity. Based on what we know about DDX56 and WNV from my studies, I anticipate that these inhibitors would not block replication of WNV *per se*, but exert their effects by decreasing the infectivity of nascent virions. This would be expected to reduce viral spread by allowing the immune system to contain the infection. Interestingly, DDX56 has recently been shown to modulate the HIV-1 Rev function (Yasuda-Inoue et al., 2013), and as such, it is a potentially viable target for novel HIV-1 drugs.

6.3 Mechanism by which WNV causes failure of tight junctions

WNV is a neurotropic, arthropod-borne flavivirus that can infect the CNS and cause severe neurological diseases. Although the neuropathogenesis of WNV in humans is poorly understood, studies from animal models have provided insights into the mechanisms that cause WNV disease. In the mouse model, WNV-caused neuropathology is associated with the breakdown of the BBB, enhanced infiltration of activated immune cells into the CNS, microglia activation, production of inflammatory cytokines, and loss of neurons (Glass et al., 2005; Klein et al., 2005; Samuel and Diamond, 2006; Sitati et al., 2007).

While feeding on humans, WNV-carrying mosquitos deposit viruses that infect and replicate in keratinocytes (Lim et al., 2011) as well as skin-resident dendritic cells (DCs), primarily Langerhans cells (Johnston et al., 2000). The

latter transports the virus to the regional draining lymph nodes and after initial replication at these sites, a primary viremia occurs after which the virus spreads systemically to peripheral organs, including the spleen and kidney, where a second round of replication takes place. The target cells for WNV infection in peripheral tissues are not well defined, but are presumed to be epithelial cells, subsets of DCs, and macrophages (Rios et al., 2006; Samuel et al., 2006). Following replication in the peripheral organs, WNV reaches the BBB via the blood system. The virus is able to breach the BBB thereby gaining access to the CNS where it infects neurons and glial cells. Neuronal damage is thought to occur through a number of mechanisms. First, direct infection of neurons has been reported to cause apoptosis via a caspase-3 dependent pathway (Samuel et al., 2007a). WNV-infected neurons may also up-regulate pro-inflammatory cytokines that induce cell death in these cells (Kumar et al., 2010). Finally, collateral damage from the immune response against infected lymphocytes and glial cells has been implicated in development of CNS disease (Bai et al., 2010; van Marle et al., 2007).

The mechanism by which WNV enters into the CNS is still not well defined, although a number of pathways have been implicated. These pathways include: i) direct infection of brain microvascular endothelial cells (Verma et al., 2009); ii) direct axonal retrograde transport from infected peripheral neurons (Samuel et al., 2007b); iii) infection of olfactory neurons and spread to brain through the olfactory bulb (Getts et al., 2008); and iv) infection of immune cells (leukocytes) that traffic to the brain via a “Trojan horse” mechanism (Bai et al.,

2010). Given the fact that high viremia in the blood correlates with early virus entry into the CNS (King et al., 2007), it is tempting to speculate that a blood-borne route through the BBB is one of the major ways by which WNV gains access to the CNS.

The BBB is the interface between circulating blood and the CNS. It is comprised of several cell layers including microvascular endothelial cells and perivascular astrocytes, separated by the basement membrane. While endothelial cells comprise the first selective barrier, astrocytes form a network of foot processes called the glia limitans which regulate the passage of molecules and cells (e.g. lymphocytes) across the BBB. The tight junctions of endothelial cells form the main structural basis of BBB integrity and limit paracellular permeability.

Increased permeability of the BBB is a pathological hallmark in several neurotropic virus infections including HIV (Dallasta et al., 1999), measles virus (Cosby and Brankin, 1995), and flaviviruses such as JEV (Mishra et al., 2009) and WNV (Morrey et al., 2008; Wang et al., 2004). BBB breakdown is correlated with the degradation of specific tight junction proteins, which contributes to virus entry (Afonso et al., 2007; Luabeya et al., 2000) and increased infiltration of immune cells into the CNS (Boven et al., 2000). These events also correlate with simultaneous production of matrix metalloproteinases (MMPs), a large family of peptidase, which play a major role in promoting disruption of the BBB via tight junction protein degradation in the CNS (Rosenberg, 2002).

There are a number of reports indicating that WNV infection compromises

the integrity of the blood brain barrier (Arjona et al., 2007; Dai et al., 2008; Verma et al., 2010; Verma et al., 2009; Wang et al., 2008a; Wang et al., 2008b; Wang et al., 2004) and collectively, these data suggest that both viral and host factors are involved. With respect to the latter, WNV infection induces expression of matrix metalloproteinases such as MMP9, a host factor that is necessary for viral infection of the central nervous system (Wang et al., 2008a). One theory is that MMP9 compromises the blood brain barrier by degrading the extracellular matrix. This scenario does not rule out virus-mediated effects on tight junctions nor transcytosis as being important for crossing this barrier because once the virus breaches the endothelium, it must still traverse the extracellular matrix before it can access the CNS. Proinflammatory cytokines are also thought to play a role in WNV neuroinvasion. For example, WNV infection of immune cells results in secretion of TLR-3 dependent TNF- α which dampens viral replication in peripheral tissues (Diamond and Klein, 2004). However, high levels of peripheral viremia in TLR3-deficient mice did not result in increased viral entry into the brain. In contrast, TLR3-deficient mice were resistant to lethal WNV infection, suggesting that this antiviral cytokine negatively affects BBB integrity and inadvertently facilitates WNV entry into the CNS (Wang et al., 2004). Moreover, TNF- α also induces endocytosis of the tight junction membrane protein occludin (Marchiando et al., 2010), which may inadvertently facilitate transmission of the virus across the blood brain barrier. Other host factors such as MIF, Drak-2, and ICAM-1 have also been implicated in facilitating WNV entry into the CNS by increasing the BBB permeability (Arjona et al., 2007; Dai et al., 2008; Wang et

al., 2008b). Similarly, cytokines released from DENV-infected cells can directly or indirectly influence the permeability of endothelial tight junction complexes (Chuang et al., 2011; Sips et al., 2011).

Although these studies collectively suggest that flavivirus infection can negatively alter tight junction integrity, there is controversy as to whether or not they directly affect the expression and/or degradation of tight junction proteins. Therefore, I examined the direct effects of WNV infection on tight junction membrane proteins in both epithelial and endothelial cells. My results are in partial agreement with Medigeshi *et al.* in that WNV infection results in time-dependent degradation of claudin-1 protein but not occludin or ZO-1 (Figure 5.1). Moreover, I observed that infection of human endothelial cells (HUVECs) results in loss of claudin-1 and JAM-1 proteins (Figure 5.1). While I cannot reconcile the result of Verma *et al.* who did not observe loss of tight junction proteins in WNV-infected human brain microvascular endothelial cells, my findings and those of Medigeshi *et al.* indicate that viral infection induces loss of tight junction membrane proteins in both epithelial and endothelial cells. However, unlike what was observed from the work of Medigeshi *et al.*, I saw no evidence that expression of capsid protein alone affected levels of claudin-1 (or JAM-1) (Figure 5.7); despite the fact that in both studies, capsid protein from the NY99 strain of WNV was employed. The apparent discrepancy in these results may be related to the fact that different expression systems were employed. Whereas Medigeshi *et al.* used stably transfected cells expressing capsid protein for their experiments, I used lentiviral transduction to induce robust transient expression of capsid in cells

which arguably, more closely parallels the expression kinetics of capsid protein in WNV-infected cells. My co-immunoprecipitation experiments failed to detect interaction between capsid and tight junction membrane proteins (Figure 5.7) nor did I observe significant localization between these proteins and capsid in infected cells (Figure 5.4). Thus it seems unlikely that capsid protein is directly involved in targeting claudin-1 or JAM-1 to lysosomes.

Upon closer examination of the data from Medigeshi *et al.*, I noticed that some claudin protein degradation occurred when epithelial cells were infected with subviral particles that lack the capsid gene, an observation which was attributed to the possibility that there was sufficient residual capsid protein in the virus particles to induce claudin degradation or that a redundant, capsid-independent claudin turnover mechanism is also involved (Medigeshi *et al.*, 2009). These scenarios seem unlikely, however, it cannot be ruled out that capsid protein is required, but not sufficient for degradation of tight junction membrane proteins in WNV-infected cells.

Together, my data suggest that the primary mechanism for loss of claudin-1 and JAM-1 in WNV-infected cells involves endocytosis from the cell surface. Because capsid protein does not appear to be physically involved in this process, I hypothesize that WNV replication and/or assembly triggers a signaling event that leads to endocytosis of a subset of tight junction membrane proteins. Endocytosis of these proteins is in fact a normal process that is used to regulate the permeability of tight junctions in response to physiological stimuli (Shen *et al.*, 2011). For example, inflammatory cytokines such as TNF- α induce caveolae-

dependent endocytosis of occludin (Marchiando et al., 2010). Even though cytokine expression and secretion is a common cellular response to virus infection, it is unlikely that this is the primary mechanism by which WNV induces lysosomal degradation of selected tight junction membrane proteins in epithelial cells at least. First, I am unaware of any data showing that WNV infection of MDCK and CACO-2 cells results in production of proinflammatory cytokines. Moreover, infection of these cells with other RNA viruses does not significantly affect production of cytokines such as TNF- α and interleukins (Cuadras et al., 2002; Grone et al., 2002). Second, while treatment of CACO-2 cells with TNF- α or IL-1 β can lead to tight junction failure through degradation of occludin and possibly other mechanisms (Al-Sadi et al., 2009), exposure to IL-1 β actually increases levels of claudin-1 (Al-Sadi and Ma, 2007). In contrast, I observed that in WNV-infected epithelial cells, occludin levels remain stable while claudin-1 and JAM-1 protein levels are significantly lower (Figure 5.1).

In summary, it is likely that WNV employs multiple strategies to cross polarized cell layers. These include; stimulating endocytosis and degradation of key transmembrane proteins of the tight junction; inducing production of matrix metalloproteases that degrade basement membranes; stimulating immune cells and possibly endothelial cells to secrete proinflammatory cytokines that disrupt tight junctions. A clearer understanding how WNV causes these events may lead to therapeutic treatments that block viral spread or design of attenuated vaccine strains.

6.4 Future Directions

Both viral and cellular helicases have been considered as targets for antiviral therapy. In the course of my PhD studies, I demonstrated that DDX56, a novel WNV capsid-interacting nucleolar RNA helicase, is critical for assembly of infectious WNV virions. While it appears that this helicase has a role in packaging viral RNA, further investigation is needed. To this end, it will be of interest to use super resolution microscopy to compare the structures of WNV replication complexes and virus assembly sites in wild type and DDX56-deficient cells. Moreover, plans are underway to study whether DDX56 is required for infectivity of other pathogenic flaviviruses including DENV, HCV, JEV, SLEV and TBEV. If so, it is possible that DDX56 could be exploited as a wide-spectrum antiviral target.

I also discovered that WNV infection induces endocytosis and degradation of specific tight junction membrane proteins including claudin-1 and JAM-1 in both epithelial and endothelial cells. Future studies are focused on determining which WNV protein(s) causes tight junction breakdown and the mechanism by which this occurs. My preliminary studies confirm that indeed, capsid protein is not required for this process and a host factor that is needed for virus-induced tight junction breakdown has been tentatively identified. Next, I will determine which viral protein(s) triggers endocytosis of tight junction membrane proteins and how it functions with the host factor. The outcome of these studies may have implications for vaccine design and therapy for patients infected with WNV.

REFERENCES

- Afonso, P.V., Ozden, S., Prevost, M.C., Schmitt, C., Seilhean, D., Weksler, B., Couraud, P.O., Gessain, A., Romero, I.A., Ceccaldi, P.E., 2007. Human blood-brain barrier disruption by retroviral-infected lymphocytes: role of myosin light chain kinase in endothelial tight-junction disorganization. *J Immunol* 179, 2576-2583.
- Ahlquist, P., Noueiry, A.O., Lee, W.M., Kushner, D.B., Dye, B.T., 2003. Host factors in positive-strand RNA virus genome replication. *Journal of virology* 77, 8181-8186.
- Ait-Goughoulte, M., Banerjee, A., Meyer, K., Mazumdar, B., Saito, K., Ray, R.B., Ray, R., 2010. Hepatitis C virus core protein interacts with fibrinogen-beta and attenuates cytokine stimulated acute-phase response. *Hepatology* 51, 1505-1513.
- Al-Murrani, S.W., Woodgett, J.R., Damuni, Z., 1999. Expression of I2PP2A, an inhibitor of protein phosphatase 2A, induces c-Jun and AP-1 activity. *The Biochemical journal* 341 (Pt 2), 293-298.
- Al-Sadi, R., Boivin, M., Ma, T., 2009. Mechanism of cytokine modulation of epithelial tight junction barrier. *Front Biosci* 14, 2765-2778.
- Al-Sadi, R.M., Ma, T.Y., 2007. IL-1beta causes an increase in intestinal epithelial tight junction permeability. *J Immunol* 178, 4641-4649.
- Alisi, A., Giambartolomei, S., Cupelli, F., Merlo, P., Fontemaggi, G., Spaziani, A., Balsano, C., 2003. Physical and functional interaction between HCV core protein and the different p73 isoforms. *Oncogene* 22, 2573-2580.
- Allison, S.L., Schalich, J., Stiasny, K., Mandl, C.W., Kunz, C., Heinz, F.X., 1995. Oligomeric rearrangement of tick-borne encephalitis virus envelope proteins induced by an acidic pH. *Journal of virology* 69, 695-700.
- Amberg, S.M., Rice, C.M., 1999. Mutagenesis of the NS2B-NS3-mediated cleavage site in the flavivirus capsid protein demonstrates a requirement for coordinated processing. *Journal of virology* 73, 8083-8094.
- Angus, A.G., Dalrymple, D., Boulant, S., McGivern, D.R., Clayton, R.F., Scott, M.J., Adair, R., Graham, S., Owsianka, A.M., Targett-Adams, P., Li, K., Wakita, T., McLauchlan, J., Lemon, S.M., Patel, A.H., 2010. Requirement of cellular DDX3 for hepatitis C virus replication is unrelated to its interaction with the viral core protein. *The Journal of general virology* 91, 122-132.
- Aoki, H., Hayashi, J., Moriyama, M., Arakawa, Y., Hino, O., 2000. Hepatitis C virus core protein interacts with 14-3-3 protein and activates the kinase Raf-1. *Journal of virology* 74, 1736-1741.
- Ariumi, Y., Kuroki, M., Abe, K., Dansako, H., Ikeda, M., Wakita, T., Kato, N., 2007. DDX3 DEAD-box RNA helicase is required for hepatitis C virus RNA replication. *Journal of virology* 81, 13922-13926.
- Arjona, A., Foellmer, H.G., Town, T., Leng, L., McDonald, C., Wang, T., Wong, S.J., Montgomery, R.R., Fikrig, E., Bucala, R., 2007. Abrogation of macrophage migration inhibitory factor decreases West Nile virus lethality by limiting viral neuroinvasion. *The*

Journal of clinical investigation 117, 3059-3066.

Arroyo, J., Miller, C., Catalan, J., Myers, G.A., Ratterree, M.S., Trent, D.W., Monath, T.P., 2004. ChimeriVax-West Nile virus live-attenuated vaccine: preclinical evaluation of safety, immunogenicity, and efficacy. *Journal of virology* 78, 12497-12507.

Bai, F., Kong, K.F., Dai, J., Qian, F., Zhang, L., Brown, C.R., Fikrig, E., Montgomery, R.R., 2010. A paradoxical role for neutrophils in the pathogenesis of West Nile virus. *The Journal of infectious diseases* 202, 1804-1812.

Beasley, D.W., Li, L., Suderman, M.T., Barrett, A.D., 2002. Mouse neuroinvasive phenotype of West Nile virus strains varies depending upon virus genotype. *Virology* 296, 17-23.

Beasley, D.W., Whiteman, M.C., Zhang, S., Huang, C.Y., Schneider, B.S., Smith, D.R., Gromowski, G.D., Higgs, S., Kinney, R.M., Barrett, A.D., 2005. Envelope protein glycosylation status influences mouse neuroinvasion phenotype of genetic lineage 1 West Nile virus strains. *Journal of virology* 79, 8339-8347.

Beatch, M.D., Everitt, J.C., Law, L.J., Hobman, T.C., 2005. Interactions between rubella virus capsid and host protein p32 are important for virus replication. *Journal of virology* 79, 10807-10820.

Benali-Furet, N.L., Chami, M., Houel, L., De Giorgi, F., Vernejoul, F., Lagorce, D., Buscail, L., Bartenschlager, R., Ichas, F., Rizzuto, R., Paterlini-Brechot, P., 2005. Hepatitis C virus core triggers apoptosis in liver cells by inducing ER stress and ER calcium depletion. *Oncogene* 24, 4921-4933.

Bhuvanakantham, R., Cheong, Y.K., Ng, M.L., 2010a. West Nile virus capsid protein interaction with importin and HDM2 protein is regulated by protein kinase C-mediated phosphorylation. *Microbes and infection / Institut Pasteur* 12, 615-625.

Bhuvanakantham, R., Chong, M.K., Ng, M.L., 2009. Specific interaction of capsid protein and importin-alpha/beta influences West Nile virus production. *Biochemical and biophysical research communications* 389, 63-69.

Bhuvanakantham, R., Li, J., Tan, T.T., Ng, M.L., 2010b. Human Sec3 protein is a novel transcriptional and translational repressor of flavivirus. *Cellular microbiology* 12, 453-472.

Biedenbender, R., Bevilacqua, J., Gregg, A.M., Watson, M., Dayan, G., 2011. Phase II, randomized, double-blind, placebo-controlled, multicenter study to investigate the immunogenicity and safety of a West Nile virus vaccine in healthy adults. *The Journal of infectious diseases* 203, 75-84.

Bolinger, C., Sharma, A., Singh, D., Yu, L., Boris-Lawrie, K., 2010. RNA helicase A modulates translation of HIV-1 and infectivity of progeny virions. *Nucleic acids research* 38, 1686-1696.

Boulant, S., Douglas, M.W., Moody, L., Budkowska, A., Targett-Adams, P., McLauchlan, J., 2008. Hepatitis C virus core protein induces lipid droplet redistribution

in a microtubule- and dynein-dependent manner. *Traffic* 9, 1268-1282.

Boulant, S., Targett-Adams, P., McLauchlan, J., 2007. Disrupting the association of hepatitis C virus core protein with lipid droplets correlates with a loss in production of infectious virus. *The Journal of general virology* 88, 2204-2213.

Boven, L.A., Middel, J., Verhoef, J., De Groot, C.J., Nottet, H.S., 2000. Monocyte infiltration is highly associated with loss of the tight junction protein zonula occludens in HIV-1-associated dementia. *Neuropathology and applied neurobiology* 26, 356-360.

Brinton, M.A., 2002. The molecular biology of West Nile Virus: a new invader of the western hemisphere. *Annual review of microbiology* 56, 371-402.

Bulich, R., Aaskov, J.G., 1992. Nuclear localization of dengue 2 virus core protein detected with monoclonal antibodies. *The Journal of general virology* 73 (Pt 11), 2999-3003.

Byrne, S.N., Halliday, G.M., Johnston, L.J., King, N.J., 2001. Interleukin-1beta but not tumor necrosis factor is involved in West Nile virus-induced Langerhans cell migration from the skin in C57BL/6 mice. *The Journal of investigative dermatology* 117, 702-709.

Calisher, C.H., Gould, E.A., 2003. Taxonomy of the virus family Flaviviridae. *Advances in virus research* 59, 1-19.

Carvalho, F.A., Carneiro, F.A., Martins, I.C., Assuncao-Miranda, I., Faustino, A.F., Pereira, R.M., Bozza, P.T., Castanho, M.A., Mohana-Borges, R., Da Poian, A.T., Santos, N.C., 2012. Dengue virus capsid protein binding to hepatic lipid droplets (LD) is potassium ion dependent and is mediated by LD surface proteins. *Journal of virology* 86, 2096-2108.

Caviston, J.P., Holzbaur, E.L., 2006. Microtubule motors at the intersection of trafficking and transport. *Trends in cell biology* 16, 530-537.

Chambers, T.J., Nestorowicz, A., Amberg, S.M., Rice, C.M., 1993. Mutagenesis of the yellow fever virus NS2B protein: effects on proteolytic processing, NS2B-NS3 complex formation, and viral replication. *Journal of virology* 67, 6797-6807.

Chambers, T.J., Weir, R.C., Grakoui, A., McCourt, D.W., Bazan, J.F., Fletterick, R.J., Rice, C.M., 1990. Evidence that the N-terminal domain of nonstructural protein NS3 from yellow fever virus is a serine protease responsible for site-specific cleavages in the viral polyprotein. *Proceedings of the National Academy of Sciences of the United States of America* 87, 8898-8902.

Chang, C.J., Luh, H.W., Wang, S.H., Lin, H.J., Lee, S.C., Hu, S.T., 2001. The heterogeneous nuclear ribonucleoprotein K (hnRNP K) interacts with dengue virus core protein. *DNA and cell biology* 20, 569-577.

Chang, P.C., Chi, C.W., Chau, G.Y., Li, F.Y., Tsai, Y.H., Wu, J.C., Wu Lee, Y.H., 2006. DDX3, a DEAD box RNA helicase, is deregulated in hepatitis virus-associated hepatocellular carcinoma and is involved in cell growth control. *Oncogene* 25, 1991-2003.

- Chen, C.M., You, L.R., Hwang, L.H., Lee, Y.H., 1997. Direct interaction of hepatitis C virus core protein with the cellular lymphotoxin-beta receptor modulates the signal pathway of the lymphotoxin-beta receptor. *Journal of virology* 71, 9417-9426.
- Chen, Y.R., Chen, T.Y., Zhang, S.L., Lin, S.M., Zhao, Y.R., Ye, F., Zhang, X., Shi, L., Dang, S.S., Liu, M., 2009. Identification of a novel protein binding to hepatitis C virus core protein. *Journal of gastroenterology and hepatology* 24, 1300-1304.
- Cheng, P.L., Chang, M.H., Chao, C.H., Lee, Y.H., 2004. Hepatitis C viral proteins interact with Smad3 and differentially regulate TGF-beta/Smad3-mediated transcriptional activation. *Oncogene* 23, 7821-7838.
- Chu, J.H., Chiang, C.C., Ng, M.L., 2007. Immunization of flavivirus West Nile recombinant envelope domain III protein induced specific immune response and protection against West Nile virus infection. *J Immunol* 178, 2699-2705.
- Chu, J.J., Ng, M.L., 2004a. Infectious entry of West Nile virus occurs through a clathrin-mediated endocytic pathway. *Journal of virology* 78, 10543-10555.
- Chu, J.J., Ng, M.L., 2004b. Interaction of West Nile virus with alpha v beta 3 integrin mediates virus entry into cells. *The Journal of biological chemistry* 279, 54533-54541.
- Chu, P.W., Westaway, E.G., 1992. Molecular and ultrastructural analysis of heavy membrane fractions associated with the replication of Kunjin virus RNA. *Archives of virology* 125, 177-191.
- Chua, J.J., Ng, M.M., Chow, V.T., 2004. The non-structural 3 (NS3) protein of dengue virus type 2 interacts with human nuclear receptor binding protein and is associated with alterations in membrane structure. *Virus research* 102, 151-163.
- Chuang, Y.C., Lei, H.Y., Liu, H.S., Lin, Y.S., Fu, T.F., Yeh, T.M., 2011. Macrophage migration inhibitory factor induced by dengue virus infection increases vascular permeability. *Cytokine* 54, 222-231.
- Chung, K.M., Liszewski, M.K., Nybakken, G., Davis, A.E., Townsend, R.R., Fremont, D.H., Atkinson, J.P., Diamond, M.S., 2006. West Nile virus nonstructural protein NS1 inhibits complement activation by binding the regulatory protein factor H. *Proceedings of the National Academy of Sciences of the United States of America* 103, 19111-19116.
- Colpitts, T.M., Barthel, S., Wang, P., Fikrig, E., 2011. Dengue virus capsid protein binds core histones and inhibits nucleosome formation in human liver cells. *PloS one* 6, e24365.
- Cordin, O., Banroques, J., Tanner, N.K., Linder, P., 2006. The DEAD-box protein family of RNA helicases. *Gene* 367, 17-37.
- Cosby, S.L., Brankin, B., 1995. Measles virus infection of cerebral endothelial cells and effect on their adhesive properties. *Veterinary microbiology* 44, 135-139.
- Cuadras, M.A., Feigelstock, D.A., An, S., Greenberg, H.B., 2002. Gene expression pattern in Caco-2 cells following rotavirus infection. *J Virol* 76, 4467-4482.

Cui, T., Sugrue, R.J., Xu, Q., Lee, A.K., Chan, Y.C., Fu, J., 1998. Recombinant dengue virus type 1 NS3 protein exhibits specific viral RNA binding and NTPase activity regulated by the NS5 protein. *Virology* 246, 409-417.

Dai, J., Wang, P., Bai, F., Town, T., Fikrig, E., 2008. Icam-1 participates in the entry of west nile virus into the central nervous system. *Journal of virology* 82, 4164-4168.

Dallasta, L.M., Pizarov, L.A., Esplen, J.E., Werley, J.V., Moses, A.V., Nelson, J.A., Achim, C.L., 1999. Blood-brain barrier tight junction disruption in human immunodeficiency virus-1 encephalitis. *The American journal of pathology* 155, 1915-1927.

Das, S., Chakraborty, S., Basu, A., 2010. Critical role of lipid rafts in virus entry and activation of phosphoinositide 3' kinase/Akt signaling during early stages of Japanese encephalitis virus infection in neural stem/progenitor cells. *Journal of neurochemistry* 115, 537-549.

Daugherty, B.L., Mateescu, M., Patel, A.S., Wade, K., Kimura, S., Gonzales, L.W., Guttentag, S., Ballard, P.L., Koval, M., 2004. Developmental regulation of claudin localization by fetal alveolar epithelial cells. *American journal of physiology. Lung cellular and molecular physiology* 287, L1266-1273.

Davis, B.S., Chang, G.J., Cropp, B., Roehrig, J.T., Martin, D.A., Mitchell, C.J., Bowen, R., Bunning, M.L., 2001. West Nile virus recombinant DNA vaccine protects mouse and horse from virus challenge and expresses in vitro a noninfectious recombinant antigen that can be used in enzyme-linked immunosorbent assays. *Journal of virology* 75, 4040-4047.

Davis, C.W., Nguyen, H.Y., Hanna, S.L., Sanchez, M.D., Doms, R.W., Pierson, T.C., 2006a. West Nile virus discriminates between DC-SIGN and DC-SIGNR for cellular attachment and infection. *Journal of virology* 80, 1290-1301.

Davis, L.E., DeBiasi, R., Goade, D.E., Haaland, K.Y., Harrington, J.A., Harnar, J.B., Pergam, S.A., King, M.K., DeMasters, B.K., Tyler, K.L., 2006b. West Nile virus neuroinvasive disease. *Annals of neurology* 60, 286-300.

Deas, T.S., Bennett, C.J., Jones, S.A., Tilgner, M., Ren, P., Behr, M.J., Stein, D.A., Iversen, P.L., Kramer, L.D., Bernard, K.A., Shi, P.Y., 2007. In vitro resistance selection and in vivo efficacy of morpholino oligomers against West Nile virus. *Antimicrobial agents and chemotherapy* 51, 2470-2482.

DeBiasi, R.L., Parsons, J.A., Grabert, B.E., 2005. West Nile virus meningoencephalitis in an immunocompetent adolescent. *Pediatric neurology* 33, 217-219.

Diamond, M.S., 2009. Progress on the development of therapeutics against West Nile virus. *Antiviral research* 83, 214-227.

Diamond, M.S., Klein, R.S., 2004. West Nile virus: crossing the blood-brain barrier. *Nature medicine* 10, 1294-1295.

Dietrich, J.B., 2002. The adhesion molecule ICAM-1 and its regulation in relation with

the blood-brain barrier. *Journal of neuroimmunology* 128, 58-68.

Dominguez-Villar, M., Munoz-Suano, A., Anaya-Baz, B., Aguilar, S., Novalbos, J.P., Giron, J.A., Rodriguez-Iglesias, M., Garcia-Cozar, F., 2007. Hepatitis C virus core protein up-regulates energy-related genes and a new set of genes, which affects T cell homeostasis. *Journal of leukocyte biology* 82, 1301-1310.

Dubuisson, J., Penin, F., Moradpour, D., 2002. Interaction of hepatitis C virus proteins with host cell membranes and lipids. *Trends in cell biology* 12, 517-523.

Duong, F.H., Filipowicz, M., Tripodi, M., La Monica, N., Heim, M.H., 2004. Hepatitis C virus inhibits interferon signaling through up-regulation of protein phosphatase 2A. *Gastroenterology* 126, 263-277.

Edgcomb, S.P., Carmel, A.B., Naji, S., Ambrus-Aikelin, G., Reyes, J.R., Saphire, A.C., Gerace, L., Williamson, J.R., 2012. DDX1 is an RNA-dependent ATPase involved in HIV-1 Rev function and virus replication. *Journal of molecular biology* 415, 61-74.

Egloff, M.P., Benarroch, D., Selisko, B., Romette, J.L., Canard, B., 2002. An RNA cap (nucleoside-2'-O-)-methyltransferase in the flavivirus RNA polymerase NS5: crystal structure and functional characterization. *The EMBO journal* 21, 2757-2768.

Elshuber, S., Allison, S.L., Heinz, F.X., Mandl, C.W., 2003. Cleavage of protein prM is necessary for infection of BHK-21 cells by tick-borne encephalitis virus. *The Journal of general virology* 84, 183-191.

Emig, M., Apple, D.J., 2004. Severe West Nile virus disease in healthy adults. *Clinical infectious diseases : an official publication of the Infectious Diseases Society of America* 38, 289-292.

Evans, J.D., Seeger, C., 2007. Differential effects of mutations in NS4B on West Nile virus replication and inhibition of interferon signaling. *Journal of virology* 81, 11809-11816.

Falgout, B., Miller, R.H., Lai, C.J., 1993. Deletion analysis of dengue virus type 4 nonstructural protein NS2B: identification of a domain required for NS2B-NS3 protease activity. *Journal of virology* 67, 2034-2042.

Fang, J., Acheampong, E., Dave, R., Wang, F., Mukhtar, M., Pomerantz, R.J., 2005. The RNA helicase DDX1 is involved in restricted HIV-1 Rev function in human astrocytes. *Virology* 336, 299-307.

Fang, J., Kubota, S., Yang, B., Zhou, N., Zhang, H., Godbout, R., Pomerantz, R.J., 2004. A DEAD box protein facilitates HIV-1 replication as a cellular co-factor of Rev. *Virology* 330, 471-480.

Fischer, S.A., 2008. Emerging viruses in transplantation: there is more to infection after transplant than CMV and EBV. *Transplantation* 86, 1327-1339.

Friebe, P., Harris, E., 2010. Interplay of RNA elements in the dengue virus 5' and 3' ends required for viral RNA replication. *Journal of virology* 84, 6103-6118.

Friedrich, M.L., Cui, M., Hernandez, J.B., Weist, B.M., Andersen, H.M., Zhang, X., Huang, L., Walsh, C.M., 2007. Modulation of DRAK2 autophosphorylation by antigen receptor signaling in primary lymphocytes. *The Journal of biological chemistry* 282, 4573-4584.

Fukuda, M., Asano, S., Nakamura, T., Adachi, M., Yoshida, M., Yanagida, M., Nishida, E., 1997. CRM1 is responsible for intracellular transport mediated by the nuclear export signal. *Nature* 390, 308-311.

Gadaleta, P., Perfetti, X., Mersich, S., Coulombie, F., 2005. Early activation of the mitochondrial apoptotic pathway in Vesicular Stomatitis virus-infected cells. *Virus research* 109, 65-69.

Geiss, B.J., Stahla, H., Hannah, A.M., Gari, A.M., Keenan, S.M., 2009. Focus on flaviviruses: current and future drug targets. *Future Med Chem* 1, 327-344.

Getts, D.R., Terry, R.L., Getts, M.T., Muller, M., Rana, S., Shrestha, B., Radford, J., Van Rooijen, N., Campbell, I.L., King, N.J., 2008. Ly6c+ "inflammatory monocytes" are microglial precursors recruited in a pathogenic manner in West Nile virus encephalitis. *The Journal of experimental medicine* 205, 2319-2337.

Glass, W.G., Lim, J.K., Cholera, R., Pletnev, A.G., Gao, J.L., Murphy, P.M., 2005. Chemokine receptor CCR5 promotes leukocyte trafficking to the brain and survival in West Nile virus infection. *The Journal of experimental medicine* 202, 1087-1098.

Goh, P.Y., Tan, Y.J., Lim, S.P., Tan, Y.H., Lim, S.G., Fuller-Pace, F., Hong, W., 2004. Cellular RNA helicase p68 relocalization and interaction with the hepatitis C virus (HCV) NS5B protein and the potential role of p68 in HCV RNA replication. *Journal of virology* 78, 5288-5298.

Golebiewski, L., Liu, H., Javier, R.T., Rice, A.P., 2011. The avian influenza virus NS1 ESEV PDZ binding motif associates with Dlg1 and Scribble to disrupt cellular tight junctions. *Journal of virology* 85, 10639-10648.

Gollins, S.W., Porterfield, J.S., 1986. The uncoating and infectivity of the flavivirus West Nile on interaction with cells: effects of pH and ammonium chloride. *The Journal of general virology* 67 (Pt 9), 1941-1950.

Gorbalenya, A.E., Donchenko, A.P., Koonin, E.V., Blinov, V.M., 1989. N-terminal domains of putative helicases of flavi- and pestiviruses may be serine proteases. *Nucleic acids research* 17, 3889-3897.

Granwehr, B.P., Lillibridge, K.M., Higgs, S., Mason, P.W., Aronson, J.F., Campbell, G.A., Barrett, A.D., 2004. West Nile virus: where are we now? *The Lancet infectious diseases* 4, 547-556.

Gravitz, L., 2011. Introduction: a smouldering public-health crisis. *Nature* 474, S2-4.

Greenwood, J., Etienne-Manneville, S., Adamson, P., Couraud, P.O., 2002. Lymphocyte migration into the central nervous system: implication of ICAM-1 signalling at the blood-brain barrier. *Vascular pharmacology* 38, 315-322.

- Grone, A., Fonfara, S., Baumgartner, W., 2002. Cell type-dependent cytokine expression after canine distemper virus infection. *Viral Immunol* 15, 493-505.
- Gubler, D.J., 2007. The continuing spread of West Nile virus in the western hemisphere. *Clinical infectious diseases : an official publication of the Infectious Diseases Society of America* 45, 1039-1046.
- Hartman, T.R., Qian, S., Bolinger, C., Fernandez, S., Schoenberg, D.R., Boris-Lawrie, K., 2006. RNA helicase A is necessary for translation of selected messenger RNAs. *Nature structural & molecular biology* 13, 509-516.
- Hayes, C.G., 2001. West Nile virus: Uganda, 1937, to New York City, 1999. *Annals of the New York Academy of Sciences* 951, 25-37.
- Hayes, E.B., Sejvar, J.J., Zaki, S.R., Lanciotti, R.S., Bode, A.V., Campbell, G.L., 2005. Virology, pathology, and clinical manifestations of West Nile virus disease. *Emerging infectious diseases* 11, 1174-1179.
- He, Q.S., Tang, H., Zhang, J., Truong, K., Wong-Staal, F., Zhou, D., 2008. Comparisons of RNAi approaches for validation of human RNA helicase A as an essential factor in hepatitis C virus replication. *Journal of virological methods* 154, 216-219.
- Heinz, F.X., Stiasny, K., 2012. Flaviviruses and flavivirus vaccines. *Vaccine* 30, 4301-4306.
- Hinshaw, J.E., Schmid, S.L., 1995. Dynamin self-assembles into rings suggesting a mechanism for coated vesicle budding. *Nature* 374, 190-192.
- Hiscox, J.A., 2003. The interaction of animal cytoplasmic RNA viruses with the nucleus to facilitate replication. *Virus research* 95, 13-22.
- Hosui, A., Ohkawa, K., Ishida, H., Sato, A., Nakanishi, F., Ueda, K., Takehara, T., Kasahara, A., Sasaki, Y., Hori, M., Hayashi, N., 2003. Hepatitis C virus core protein differently regulates the JAK-STAT signaling pathway under interleukin-6 and interferon-gamma stimuli. *The Journal of biological chemistry* 278, 28562-28571.
- Hsieh, T.Y., Matsumoto, M., Chou, H.C., Schneider, R., Hwang, S.B., Lee, A.S., Lai, M.M., 1998. Hepatitis C virus core protein interacts with heterogeneous nuclear ribonucleoprotein K. *The Journal of biological chemistry* 273, 17651-17659.
- Hsu, S.C., Hazuka, C.D., Foletti, D.L., Scheller, R.H., 1999. Targeting vesicles to specific sites on the plasma membrane: the role of the sec6/8 complex. *Trends in cell biology* 9, 150-153.
- Hunt, T.A., Urbanowski, M.D., Kakani, K., Law, L.M., Brinton, M.A., Hobman, T.C., 2007. Interactions between the West Nile virus capsid protein and the host cell-encoded phosphatase inhibitor, I2PP2A. *Cellular microbiology* 9, 2756-2766.
- Ishaq, M., Hu, J., Wu, X., Fu, Q., Yang, Y., Liu, Q., Guo, D., 2008. Knockdown of cellular RNA helicase DDX3 by short hairpin RNAs suppresses HIV-1 viral replication without inducing apoptosis. *Molecular biotechnology* 39, 231-238.

Ivanov, A.I., Nusrat, A., Parkos, C.A., 2004. Endocytosis of epithelial apical junctional proteins by a clathrin-mediated pathway into a unique storage compartment. *Molecular biology of the cell* 15, 176-188.

Jackson, A.C., 2004. Therapy of West Nile virus infection. *The Canadian journal of neurological sciences. Le journal canadien des sciences neurologiques* 31, 131-134.

Jangra, R.K., Yi, M., Lemon, S.M., 2010. DDX6 (Rck/p54) is required for efficient hepatitis C virus replication but not for internal ribosome entry site-directed translation. *Journal of virology* 84, 6810-6824.

Jankowsky, E., Jankowsky, A., 2000. The DExH/D protein family database. *Nucleic acids research* 28, 333-334.

Jin, M., Snider, M.D., 1993. Role of microtubules in transferrin receptor transport from the cell surface to endosomes and the Golgi complex. *The Journal of biological chemistry* 268, 18390-18397.

Johnston, L.J., Halliday, G.M., King, N.J., 2000. Langerhans cells migrate to local lymph nodes following cutaneous infection with an arbovirus. *The Journal of investigative dermatology* 114, 560-568.

Jones, S.M., Howell, K.E., Henley, J.R., Cao, H., McNiven, M.A., 1998. Role of dynamin in the formation of transport vesicles from the trans-Golgi network. *Science* 279, 573-577.

Kanai, R., Kar, K., Anthony, K., Gould, L.H., Ledizet, M., Fikrig, E., Marasco, W.A., Koski, R.A., Modis, Y., 2006. Crystal structure of west nile virus envelope glycoprotein reveals viral surface epitopes. *Journal of virology* 80, 11000-11008.

Kang, S.M., Kim, S.J., Kim, J.H., Lee, W., Kim, G.W., Lee, K.H., Choi, K.Y., Oh, J.W., 2009. Interaction of hepatitis C virus core protein with Hsp60 triggers the production of reactive oxygen species and enhances TNF-alpha-mediated apoptosis. *Cancer letters* 279, 230-237.

Kapoor, M., Zhang, L., Ramachandra, M., Kusakawa, J., Ebner, K.E., Padmanabhan, R., 1995. Association between NS3 and NS5 proteins of dengue virus type 2 in the putative RNA replicase is linked to differential phosphorylation of NS5. *The Journal of biological chemistry* 270, 19100-19106.

Katoh, H., Okamoto, T., Fukuhara, T., Kambara, H., Morita, E., Mori, Y., Kamitani, W., Matsuura, Y., 2013. Japanese encephalitis virus core protein inhibits stress granule formation through an interaction with Caprin-1 and facilitates viral propagation. *Journal of virology* 87, 489-502.

Khadka, S., Vangeloff, A.D., Zhang, C., Siddavatam, P., Heaton, N.S., Wang, L., Sengupta, R., Sahasrabudhe, S., Randall, G., Gribskov, M., Kuhn, R.J., Perera, R., LaCount, D.J., 2011. A physical interaction network of dengue virus and human proteins. *Molecular & cellular proteomics : MCP* 10, M111 012187.

Khromykh, A.A., Kenney, M.T., Westaway, E.G., 1998. trans-Complementation of

flavivirus RNA polymerase gene NS5 by using Kunjin virus replicon-expressing BHK cells. *Journal of virology* 72, 7270-7279.

Khromykh, A.A., Meka, H., Guyatt, K.J., Westaway, E.G., 2001a. Essential role of cyclization sequences in flavivirus RNA replication. *Journal of virology* 75, 6719-6728.

Khromykh, A.A., Sedlak, P.L., Guyatt, K.J., Hall, R.A., Westaway, E.G., 1999. Efficient trans-complementation of the flavivirus kunjin NS5 protein but not of the NS1 protein requires its coexpression with other components of the viral replicase. *Journal of virology* 73, 10272-10280.

Khromykh, A.A., Varnavski, A.N., Sedlak, P.L., Westaway, E.G., 2001b. Coupling between replication and packaging of flavivirus RNA: evidence derived from the use of DNA-based full-length cDNA clones of Kunjin virus. *Journal of virology* 75, 4633-4640.

King, N.J., Getts, D.R., Getts, M.T., Rana, S., Shrestha, B., Kesson, A.M., 2007. Immunopathology of flavivirus infections. *Immunology and cell biology* 85, 33-42.

Kittlesen, D.J., Chianese-Bullock, K.A., Yao, Z.Q., Braciale, T.J., Hahn, Y.S., 2000. Interaction between complement receptor gC1qR and hepatitis C virus core protein inhibits T-lymphocyte proliferation. *The Journal of clinical investigation* 106, 1239-1249.

Klein, R.S., Lin, E., Zhang, B., Luster, A.D., Tollett, J., Samuel, M.A., Engle, M., Diamond, M.S., 2005. Neuronal CXCL10 directs CD8+ T-cell recruitment and control of West Nile virus encephalitis. *Journal of virology* 79, 11457-11466.

Kleinschmidt, M.C., Michaelis, M., Ogbomo, H., Doerr, H.W., Cinatl, J., Jr., 2007. Inhibition of apoptosis prevents West Nile virus induced cell death. *BMC microbiology* 7, 49.

Ko, A., Lee, E.W., Yeh, J.Y., Yang, M.R., Oh, W., Moon, J.S., Song, J., 2010. MKRN1 induces degradation of West Nile virus capsid protein by functioning as an E3 ligase. *Journal of virology* 84, 426-436.

Kobayashi, S., Orba, Y., Yamaguchi, H., Kimura, T., Sawa, H., 2012. Accumulation of ubiquitinated proteins is related to West Nile virus-induced neuronal apoptosis. *Neuropathology : official journal of the Japanese Society of Neuropathology* 32, 398-405.

Kogel, D., Prehn, J.H., Scheidtmann, K.H., 2001. The DAP kinase family of pro-apoptotic proteins: novel players in the apoptotic game. *BioEssays : news and reviews in molecular, cellular and developmental biology* 23, 352-358.

Krishnan, M.N., Ng, A., Sukumaran, B., Gilfoy, F.D., Uchil, P.D., Sultana, H., Brass, A.L., Adametz, R., Tsui, M., Qian, F., Montgomery, R.R., Lev, S., Mason, P.W., Koski, R.A., Elledge, S.J., Xavier, R.J., Agaisse, H., Fikrig, E., 2008. RNA interference screen for human genes associated with West Nile virus infection. *Nature* 455, 242-245.

Krishnan, M.N., Sukumaran, B., Pal, U., Agaisse, H., Murray, J.L., Hodge, T.W., Fikrig, E., 2007. Rab 5 is required for the cellular entry of dengue and West Nile viruses. *Journal of virology* 81, 4881-4885.

Kubota, N., Inayoshi, Y., Satoh, N., Fukuda, T., Iwai, K., Tomoda, H., Kohara, M., Kataoka, K., Shimamoto, A., Furuichi, Y., Nomoto, A., Naganuma, A., Kuge, S., 2012. HSC90 is required for nascent hepatitis C virus core protein stability in yeast cells. *FEBS letters* 586, 2318-2325.

Kuhn, R.J., Zhang, W., Rossmann, M.G., Pletnev, S.V., Corver, J., Lenches, E., Jones, C.T., Mukhopadhyay, S., Chipman, P.R., Strauss, E.G., Baker, T.S., Strauss, J.H., 2002. Structure of dengue virus: implications for flavivirus organization, maturation, and fusion. *Cell* 108, 717-725.

Kumar, M., Verma, S., Nerurkar, V.R., 2010. Pro-inflammatory cytokines derived from West Nile virus (WNV)-infected SK-N-SH cells mediate neuroinflammatory markers and neuronal death. *Journal of neuroinflammation* 7, 73.

Kuno, G., Chang, G.J., Tsuchiya, K.R., Karabatsos, N., Cropp, C.B., 1998. Phylogeny of the genus *Flavivirus*. *Journal of virology* 72, 73-83.

Kwong, A.D., Rao, B.G., Jeang, K.T., 2005. Viral and cellular RNA helicases as antiviral targets. *Nat Rev Drug Discov* 4, 845-853.

Lanciotti, R.S., Roehrig, J.T., Deubel, V., Smith, J., Parker, M., Steele, K., Crise, B., Volpe, K.E., Crabtree, M.B., Scherret, J.H., Hall, R.A., MacKenzie, J.S., Cropp, C.B., Panigrahy, B., Ostlund, E., Schmitt, B., Malkinson, M., Banet, C., Weissman, J., Komar, N., Savage, H.M., Stone, W., McNamara, T., Gubler, D.J., 1999. Origin of the West Nile virus responsible for an outbreak of encephalitis in the northeastern United States. *Science* 286, 2333-2337.

Ledizet, M., Kar, K., Foellmer, H.G., Wang, T., Bushmich, S.L., Anderson, J.F., Fikrig, E., Koski, R.A., 2005. A recombinant envelope protein vaccine against West Nile virus. *Vaccine* 23, 3915-3924.

Lee, C.J., Liao, C.L., Lin, Y.L., 2005. Flavivirus activates phosphatidylinositol 3-kinase signaling to block caspase-dependent apoptotic cell death at the early stage of virus infection. *Journal of virology* 79, 8388-8399.

Lee, E., Hall, R.A., Lobigs, M., 2004. Common E protein determinants for attenuation of glycosaminoglycan-binding variants of Japanese encephalitis and West Nile viruses. *Journal of virology* 78, 8271-8280.

Lee, J.W., Liao, P.C., Young, K.C., Chang, C.L., Chen, S.S., Chang, T.T., Lai, M.D., Wang, S.W., 2011. Identification of hnRNP1, NF45, and C14orf166 as novel host interacting partners of the mature hepatitis C virus core protein. *Journal of proteome research* 10, 4522-4534.

Leung, J.Y., Pijlman, G.P., Kondratieva, N., Hyde, J., Mackenzie, J.M., Khromykh, A.A., 2008. Role of nonstructural protein NS2A in flavivirus assembly. *Journal of virology* 82, 4731-4741.

Li, J., Tang, H., Mullen, T.M., Westberg, C., Reddy, T.R., Rose, D.W., Wong-Staal, F., 1999. A role for RNA helicase A in post-transcriptional regulation of HIV type 1. *Proceedings of the National Academy of Sciences of the United States of America* 96,

709-714.

Lieberman, M.M., Clements, D.E., Ogata, S., Wang, G., Corpuz, G., Wong, T., Martyak, T., Gilson, L., Collier, B.A., Leung, J., Watts, D.M., Tesh, R.B., Siirin, M., Travassos da Rosa, A., Humphreys, T., Weeks-Levy, C., 2007. Preparation and immunogenic properties of a recombinant West Nile subunit vaccine. *Vaccine* 25, 414-423.

Lim, P.Y., Behr, M.J., Chadwick, C.M., Shi, P.Y., Bernard, K.A., 2011. Keratinocytes are cell targets of West Nile virus in vivo. *Journal of virology* 85, 5197-5201.

Limjindaporn, T., Netsawang, J., Noisakran, S., Thiemmecca, S., Wongwiwat, W., Sudsaward, S., Avirutnan, P., Puttikhunt, C., Kasinrerak, W., Sriburi, R., Sittisombut, N., Yenchitsomanus, P.T., Malasit, P., 2007. Sensitization to Fas-mediated apoptosis by dengue virus capsid protein. *Biochemical and biophysical research communications* 362, 334-339.

Lin, L., Li, Y., Pyo, H.M., Lu, X., Raman, S.N., Liu, Q., Brown, E.G., Zhou, Y., 2012. Identification of RNA helicase A as a cellular factor that interacts with influenza A virus NS1 protein and its role in the virus life cycle. *Journal of virology* 86, 1942-1954.

Lindenbach, B.D., Evans, M.J., Syder, A.J., Wolk, B., Tellinghuisen, T.L., Liu, C.C., Maruyama, T., Hynes, R.O., Burton, D.R., McKeating, J.A., Rice, C.M., 2005. Complete replication of hepatitis C virus in cell culture. *Science* 309, 623-626.

Lindenbach, B.D., Rice, C.M., 2003. Molecular biology of flaviviruses. *Advances in virus research* 59, 23-61.

Lipschutz, J.H., Mostov, K.E., 2002. Exocytosis: the many masters of the exocyst. *Current biology* : CB 12, R212-214.

Liu, W.J., Chen, H.B., Wang, X.J., Huang, H., Khromykh, A.A., 2004. Analysis of adaptive mutations in Kunjin virus replicon RNA reveals a novel role for the flavivirus nonstructural protein NS2A in inhibition of beta interferon promoter-driven transcription. *Journal of virology* 78, 12225-12235.

Liu, W.J., Sedlak, P.L., Kondratieva, N., Khromykh, A.A., 2002. Complementation analysis of the flavivirus Kunjin NS3 and NS5 proteins defines the minimal regions essential for formation of a replication complex and shows a requirement of NS3 in cis for virus assembly. *Journal of virology* 76, 10766-10775.

Liu, W.J., Wang, X.J., Clark, D.C., Lobigs, M., Hall, R.A., Khromykh, A.A., 2006. A single amino acid substitution in the West Nile virus nonstructural protein NS2A disables its ability to inhibit alpha/beta interferon induction and attenuates virus virulence in mice. *Journal of virology* 80, 2396-2404.

Liu, W.J., Wang, X.J., Mokhonov, V.V., Shi, P.Y., Randall, R., Khromykh, A.A., 2005. Inhibition of interferon signaling by the New York 99 strain and Kunjin subtype of West Nile virus involves blockage of STAT1 and STAT2 activation by nonstructural proteins. *Journal of virology* 79, 1934-1942.

Livak, K.J., Schmittgen, T.D., 2001. Analysis of relative gene expression data using real-

time quantitative PCR and the 2(-Delta Delta C(T)) Method. *Methods* 25, 402-408.

Lobigs, M., 1993. Flavivirus premembrane protein cleavage and spike heterodimer secretion require the function of the viral proteinase NS3. *Proceedings of the National Academy of Sciences of the United States of America* 90, 6218-6222.

Lobigs, M., Lee, E., Ng, M.L., Pavy, M., Lobigs, P., 2010. A flavivirus signal peptide balances the catalytic activity of two proteases and thereby facilitates virus morphogenesis. *Virology* 401, 80-89.

Lopez-Herrera, A., Ruiz-Saenz, J., Goetz, Y.P., Zapata, W., Velilla, P.A., Arango, A.E., Urcuqui-Inchima, S., 2009. Apoptosis as pathogenic mechanism of infection with vesicular stomatitis virus. Evidence in primary bovine fibroblast cultures. *Biocell : official journal of the Sociedades Latinoamericanas de Microscopia Electronica ... et. al* 33, 121-132.

Lossinsky, A.S., Shivers, R.R., 2004. Structural pathways for macromolecular and cellular transport across the blood-brain barrier during inflammatory conditions. Review. *Histology and histopathology* 19, 535-564.

Luabeya, M.K., Dallasta, L.M., Achim, C.L., Pauza, C.D., Hamilton, R.L., 2000. Blood-brain barrier disruption in simian immunodeficiency virus encephalitis. *Neuropathology and applied neurobiology* 26, 454-462.

Ludwig, S., Ehrhardt, C., Neumeier, E.R., Kracht, M., Rapp, U.R., Pleschka, S., 2001. Influenza virus-induced AP-1-dependent gene expression requires activation of the JNK signaling pathway. *The Journal of biological chemistry* 276, 10990-10998.

Ma, J., Rong, L., Zhou, Y., Roy, B.B., Lu, J., Abrahamyan, L., Mouland, A.J., Pan, Q., Liang, C., 2008a. The requirement of the DEAD-box protein DDX24 for the packaging of human immunodeficiency virus type 1 RNA. *Virology* 375, 253-264.

Ma, Y., Yates, J., Liang, Y., Lemon, S.M., Yi, M., 2008b. NS3 helicase domains involved in infectious intracellular hepatitis C virus particle assembly. *Journal of virology* 82, 7624-7639.

Macdonald, J., Tonry, J., Hall, R.A., Williams, B., Palacios, G., Ashok, M.S., Jabado, O., Clark, D., Tesh, R.B., Briese, T., Lipkin, W.I., 2005. NS1 protein secretion during the acute phase of West Nile virus infection. *Journal of virology* 79, 13924-13933.

Macia, E., Ehrlich, M., Massol, R., Boucrot, E., Brunner, C., Kirchhausen, T., 2006. Dynasore, a cell-permeable inhibitor of dynamin. *Developmental cell* 10, 839-850.

Mackenzie, J., 2005. Wrapping things up about virus RNA replication. *Traffic* 6, 967-977.

Mackenzie, J.M., Khromykh, A.A., Jones, M.K., Westaway, E.G., 1998. Subcellular localization and some biochemical properties of the flavivirus Kunjin nonstructural proteins NS2A and NS4A. *Virology* 245, 203-215.

Mackenzie, J.M., Westaway, E.G., 2001. Assembly and maturation of the flavivirus

Kunjin virus appear to occur in the rough endoplasmic reticulum and along the secretory pathway, respectively. *Journal of virology* 75, 10787-10799.

Maga, G., Falchi, F., Garbelli, A., Belfiore, A., Witvrouw, M., Manetti, F., Botta, M., 2008. Pharmacophore modeling and molecular docking led to the discovery of inhibitors of human immunodeficiency virus-1 replication targeting the human cellular aspartic acid-glutamic acid-alanine-aspartic acid box polypeptide 3. *Journal of medicinal chemistry* 51, 6635-6638.

Maga, G., Falchi, F., Radi, M., Botta, L., Casaluze, G., Bernardini, M., Irannejad, H., Manetti, F., Garbelli, A., Samuele, A., Zanolli, S., Este, J.A., Gonzalez, E., Zucca, E., Paolucci, S., Baldanti, F., De Rijck, J., Debyser, Z., Botta, M., 2011. Toward the discovery of novel anti-HIV drugs. Second-generation inhibitors of the cellular ATPase DDX3 with improved anti-HIV activity: synthesis, structure-activity relationship analysis, cytotoxicity studies, and target validation. *ChemMedChem* 6, 1371-1389.

Makino, Y., Tadano, M., Anzai, T., Ma, S.P., Yasuda, S., Fukunaga, T., 1989. Detection of dengue 4 virus core protein in the nucleus. II. Antibody against dengue 4 core protein produced by a recombinant baculovirus reacts with the antigen in the nucleus. *The Journal of general virology* 70 (Pt 6), 1417-1425.

Mamiya, N., Worman, H.J., 1999. Hepatitis C virus core protein binds to a DEAD box RNA helicase. *The Journal of biological chemistry* 274, 15751-15756.

Marchiando, A.M., Shen, L., Graham, W.V., Weber, C.R., Schwarz, B.T., Austin, J.R., 2nd, Raleigh, D.R., Guan, Y., Watson, A.J., Montrose, M.H., Turner, J.R., 2010. Caveolin-1-dependent occludin endocytosis is required for TNF-induced tight junction regulation in vivo. *J Cell Biol* 189, 111-126.

Marianneau, P., Cardona, A., Edelman, L., Deubel, V., Despres, P., 1997. Dengue virus replication in human hepatoma cells activates NF-kappaB which in turn induces apoptotic cell death. *Journal of virology* 71, 3244-3249.

McCandless, E.E., Zhang, B., Diamond, M.S., Klein, R.S., 2008. CXCR4 antagonism increases T cell trafficking in the central nervous system and improves survival from West Nile virus encephalitis. *Proceedings of the National Academy of Sciences of the United States of America* 105, 11270-11275.

McGargill, M.A., Wen, B.G., Walsh, C.M., Hedrick, S.M., 2004. A deficiency in Drak2 results in a T cell hypersensitivity and an unexpected resistance to autoimmunity. *Immunity* 21, 781-791.

McLauchlan, J., 2000. Properties of the hepatitis C virus core protein: a structural protein that modulates cellular processes. *Journal of viral hepatitis* 7, 2-14.

McLauchlan, J., Lemberg, M.K., Hope, G., Martoglio, B., 2002. Intramembrane proteolysis promotes trafficking of hepatitis C virus core protein to lipid droplets. *The EMBO journal* 21, 3980-3988.

McMinn, P.C., 1997. The molecular basis of virulence of the encephalitogenic flaviviruses. *The Journal of general virology* 78 (Pt 11), 2711-2722.

Medigeshi, G.R., Hirsch, A.J., Brien, J.D., Uhrlaub, J.L., Mason, P.W., Wiley, C., Nikolich-Zugich, J., Nelson, J.A., 2009. West Nile virus capsid degradation of claudin proteins disrupts epithelial barrier function. *Journal of virology* 83, 6125-6134.

Medigeshi, G.R., Hirsch, A.J., Streblow, D.N., Nikolich-Zugich, J., Nelson, J.A., 2008. West Nile virus entry requires cholesterol-rich membrane microdomains and is independent of alphavbeta3 integrin. *Journal of virology* 82, 5212-5219.

Medigeshi, G.R., Lancaster, A.M., Hirsch, A.J., Briese, T., Lipkin, W.I., Defilippis, V., Fruh, K., Mason, P.W., Nikolich-Zugich, J., Nelson, J.A., 2007. West Nile virus infection activates the unfolded protein response, leading to CHOP induction and apoptosis. *Journal of virology* 81, 10849-10860.

Menard, J., Patchett, A.A., 2001. Angiotensin-converting enzyme inhibitors. *Advances in protein chemistry* 56, 13-75.

Miller, K., McArdle, S., Gale, M.J., Jr., Geller, D.A., Tenoever, B., Hiscott, J., Gretsch, D.R., Polyak, S.J., 2004. Effects of the hepatitis C virus core protein on innate cellular defense pathways. *Journal of interferon & cytokine research : the official journal of the International Society for Interferon and Cytokine Research* 24, 391-402.

Mishra, M.K., Dutta, K., Saheb, S.K., Basu, A., 2009. Understanding the molecular mechanism of blood-brain barrier damage in an experimental model of Japanese encephalitis: correlation with minocycline administration as a therapeutic agent. *Neurochemistry international* 55, 717-723.

Modis, Y., Ogata, S., Clements, D., Harrison, S.C., 2003. A ligand-binding pocket in the dengue virus envelope glycoprotein. *Proceedings of the National Academy of Sciences of the United States of America* 100, 6986-6991.

Modis, Y., Ogata, S., Clements, D., Harrison, S.C., 2004. Structure of the dengue virus envelope protein after membrane fusion. *Nature* 427, 313-319.

Mohd-Ismail, N.K., Deng, L., Sukumaran, S.K., Yu, V.C., Hotta, H., Tan, Y.J., 2009. The hepatitis C virus core protein contains a BH3 domain that regulates apoptosis through specific interaction with human Mcl-1. *Journal of virology* 83, 9993-10006.

Mori, Y., Okabayashi, T., Yamashita, T., Zhao, Z., Wakita, T., Yasui, K., Hasebe, F., Tadano, M., Konishi, E., Moriishi, K., Matsuura, Y., 2005. Nuclear localization of Japanese encephalitis virus core protein enhances viral replication. *Journal of virology* 79, 3448-3458.

Mori, Y., Yamashita, T., Tanaka, Y., Tsuda, Y., Abe, T., Moriishi, K., Matsuura, Y., 2007. Processing of capsid protein by cathepsin L plays a crucial role in replication of Japanese encephalitis virus in neural and macrophage cells. *Journal of virology* 81, 8477-8487.

Moriishi, K., Okabayashi, T., Nakai, K., Moriya, K., Koike, K., Murata, S., Chiba, T., Tanaka, K., Suzuki, R., Suzuki, T., Miyamura, T., Matsuura, Y., 2003. Proteasome activator PA28gamma-dependent nuclear retention and degradation of hepatitis C virus core protein. *Journal of virology* 77, 10237-10249.

Morrey, J.D., Olsen, A.L., Siddharthan, V., Motter, N.E., Wang, H., Taro, B.S., Chen, D., Ruffner, D., Hall, J.O., 2008. Increased blood-brain barrier permeability is not a primary determinant for lethality of West Nile virus infection in rodents. *The Journal of general virology* 89, 467-473.

Moskowitz, D.W., Johnson, F.E., 2004. The central role of angiotensin I-converting enzyme in vertebrate pathophysiology. *Current topics in medicinal chemistry* 4, 1433-1454.

Mukhopadhyay, S., Kim, B.S., Chipman, P.R., Rossmann, M.G., Kuhn, R.J., 2003. Structure of West Nile virus. *Science* 302, 248.

Mulhern, O., Bowie, A.G., 2010. Unexpected roles for DEAD-box protein 3 in viral RNA sensing pathways. *European journal of immunology* 40, 933-935.

Munoz-Jordan, J.L., Laurent-Rolle, M., Ashour, J., Martinez-Sobrido, L., Ashok, M., Lipkin, W.I., Garcia-Sastre, A., 2005. Inhibition of alpha/beta interferon signaling by the NS4B protein of flaviviruses. *Journal of virology* 79, 8004-8013.

Nakajima, T., Uchida, C., Anderson, S.F., Lee, C.G., Hurwitz, J., Parvin, J.D., Montminy, M., 1997. RNA helicase A mediates association of CBP with RNA polymerase II. *Cell* 90, 1107-1112.

Nash, D., Mostashari, F., Fine, A., Miller, J., O'Leary, D., Murray, K., Huang, A., Rosenberg, A., Greenberg, A., Sherman, M., Wong, S., Layton, M., 2001. The outbreak of West Nile virus infection in the New York City area in 1999. *The New England journal of medicine* 344, 1807-1814.

Netsawang, J., Noisakran, S., Puttikhunt, C., Kasinrerak, W., Wongwiwat, W., Malasit, P., Yenchitsomanus, P.T., Limjindaporn, T., 2010. Nuclear localization of dengue virus capsid protein is required for DAXX interaction and apoptosis. *Virus research* 147, 275-283.

Neveu, G., Barouch-Bentov, R., Ziv-Av, A., Gerber, D., Jacob, Y., Einav, S., 2012. Identification and targeting of an interaction between a tyrosine motif within hepatitis C virus core protein and AP2M1 essential for viral assembly. *PLoS pathogens* 8, e1002845.

Ng, T., Hathaway, D., Jennings, N., Champ, D., Chiang, Y.W., Chu, H.J., 2003. Equine vaccine for West Nile virus. *Developments in biologicals* 114, 221-227.

Ngo, H.T., Pham, L.V., Kim, J.W., Lim, Y.S., Hwang, S.B., 2013. Modulation of mitogen-activated protein kinase-activated protein kinase 3 by hepatitis C virus core protein. *Journal of virology* 87, 5718-5731.

Nguyen, H., Sankaran, S., Dandekar, S., 2006. Hepatitis C virus core protein induces expression of genes regulating immune evasion and anti-apoptosis in hepatocytes. *Virology* 354, 58-68.

Nusbaum, K.E., Wright, J.C., Johnston, W.B., Allison, A.B., Hilton, C.D., Staggs, L.A., Stallknecht, D.E., Shelnett, J.L., 2003. Absence of humoral response in flamingos and red-tailed hawks to experimental vaccination with a killed West Nile virus vaccine. *Avian*

diseases 47, 750-752.

Nybakken, G.E., Nelson, C.A., Chen, B.R., Diamond, M.S., Fremont, D.H., 2006. Crystal structure of the West Nile virus envelope glycoprotein. *Journal of virology* 80, 11467-11474.

Oda, S., Schroder, M., Khan, A.R., 2009. Structural basis for targeting of human RNA helicase DDX3 by poxvirus protein K7. *Structure* 17, 1528-1537.

Oh, W., Yang, M.R., Lee, E.W., Park, K.M., Pyo, S., Yang, J.S., Lee, H.W., Song, J., 2006. Jab1 mediates cytoplasmic localization and degradation of West Nile virus capsid protein. *The Journal of biological chemistry* 281, 30166-30174.

Oh, W.K., Song, J., 2006. Hsp70 functions as a negative regulator of West Nile virus capsid protein through direct interaction. *Biochemical and biophysical research communications* 347, 994-1000.

Ohkawa, K., Ishida, H., Nakanishi, F., Hosui, A., Ueda, K., Takehara, T., Hori, M., Hayashi, N., 2004. Hepatitis C virus core functions as a suppressor of cyclin-dependent kinase-activating kinase and impairs cell cycle progression. *The Journal of biological chemistry* 279, 11719-11726.

Ossareh-Nazari, B., Bachelierie, F., Dargemont, C., 1997. Evidence for a role of CRM1 in signal-mediated nuclear protein export. *Science* 278, 141-144.

Otsuka, M., Kato, N., Lan, K., Yoshida, H., Kato, J., Goto, T., Shiratori, Y., Omata, M., 2000. Hepatitis C virus core protein enhances p53 function through augmentation of DNA binding affinity and transcriptional ability. *The Journal of biological chemistry* 275, 34122-34130.

Owsianka, A.M., Patel, A.H., 1999. Hepatitis C virus core protein interacts with a human DEAD box protein DDX3. *Virology* 257, 330-340.

Parquet, M.C., Kumatori, A., Hasebe, F., Morita, K., Igarashi, A., 2001. West Nile virus-induced bax-dependent apoptosis. *FEBS letters* 500, 17-24.

Patkar, C.G., Kuhn, R.J., 2008. Yellow Fever virus NS3 plays an essential role in virus assembly independent of its known enzymatic functions. *Journal of virology* 82, 3342-3352.

Pause, A., Sonenberg, N., 1992. Mutational analysis of a DEAD box RNA helicase: the mammalian translation initiation factor eIF-4A. *EMBO J* 11, 2643-2654.

Pearce, A.F., Lyles, D.S., 2009. Vesicular stomatitis virus induces apoptosis primarily through Bak rather than Bax by inactivating Mcl-1 and Bcl-XL. *Journal of virology* 83, 9102-9112.

Pletnev, A.G., Claire, M.S., Elkins, R., Speicher, J., Murphy, B.R., Chanock, R.M., 2003. Molecularly engineered live-attenuated chimeric West Nile/dengue virus vaccines protect rhesus monkeys from West Nile virus. *Virology* 314, 190-195.

- Qiao, M., Ashok, M., Bernard, K.A., Palacios, G., Zhou, Z.H., Lipkin, W.I., Liang, T.J., 2004. Induction of sterilizing immunity against West Nile Virus (WNV), by immunization with WNV-like particles produced in insect cells. *The Journal of infectious diseases* 190, 2104-2108.
- Radi, M., Falchi, F., Garbelli, A., Samuele, A., Bernardo, V., Paolucci, S., Baldanti, F., Schenone, S., Manetti, F., Maga, G., Botta, M., 2012. Discovery of the first small molecule inhibitor of human DDX3 specifically designed to target the RNA binding site: towards the next generation HIV-1 inhibitors. *Bioorganic & medicinal chemistry letters* 22, 2094-2098.
- Raghavan, B., Ng, M.L., 2013. West Nile virus and Dengue virus capsid protein negates the antiviral activity of human Sec3 protein Through The Proteasome Pathway. *Cellular microbiology*.
- Ranji, A., Boris-Lawrie, K., 2010. RNA helicases: emerging roles in viral replication and the host innate response. *RNA biology* 7, 775-787.
- Reddy, T.R., Tang, H., Xu, W., Wong-Staal, F., 2000. Sam68, RNA helicase A and Tap cooperate in the post-transcriptional regulation of human immunodeficiency virus and type D retroviral mRNA. *Oncogene* 19, 3570-3575.
- Reed, J.C., Molter, B., Geary, C.D., McNevin, J., McElrath, J., Giri, S., Klein, K.C., Lingappa, J.R., 2012. HIV-1 Gag co-opts a cellular complex containing DDX6, a helicase that facilitates capsid assembly. *The Journal of cell biology* 198, 439-456.
- Rey, F.A., 2003. Dengue virus envelope glycoprotein structure: new insight into its interactions during viral entry. *Proceedings of the National Academy of Sciences of the United States of America* 100, 6899-6901.
- Rey, F.A., Heinz, F.X., Mandl, C., Kunz, C., Harrison, S.C., 1995. The envelope glycoprotein from tick-borne encephalitis virus at 2 Å resolution. *Nature* 375, 291-298.
- Rios, M., Zhang, M.J., Grinev, A., Srinivasan, K., Daniel, S., Wood, O., Hewlett, I.K., Dayton, A.I., 2006. Monocytes-macrophages are a potential target in human infection with West Nile virus through blood transfusion. *Transfusion* 46, 659-667.
- Robertson-Anderson, R.M., Wang, J., Edgcomb, S.P., Carmel, A.B., Williamson, J.R., Millar, D.P., 2011. Single-molecule studies reveal that DEAD box protein DDX1 promotes oligomerization of HIV-1 Rev on the Rev response element. *Journal of molecular biology* 410, 959-971.
- Roeth, J.F., Williams, M., Kasper, M.R., Filzen, T.M., Collins, K.L., 2004. HIV-1 Nef disrupts MHC-I trafficking by recruiting AP-1 to the MHC-I cytoplasmic tail. *The Journal of cell biology* 167, 903-913.
- Roosendaal, J., Westaway, E.G., Khromykh, A., Mackenzie, J.M., 2006. Regulated cleavages at the West Nile virus NS4A-2K-NS4B junctions play a major role in rearranging cytoplasmic membranes and Golgi trafficking of the NS4A protein. *Journal of virology* 80, 4623-4632.

Rosenberg, G.A., 2002. Matrix metalloproteinases in neuroinflammation. *Glia* 39, 279-291.

Rossi, S.L., Ross, T.M., Evans, J.D., 2010. West Nile virus. *Clinics in laboratory medicine* 30, 47-65.

Rouille, Y., Helle, F., Delgrange, D., Roingeard, P., Voisset, C., Blanchard, E., Belouzard, S., McKeating, J., Patel, A.H., Maertens, G., Wakita, T., Wychowski, C., Dubuisson, J., 2006. Subcellular localization of hepatitis C virus structural proteins in a cell culture system that efficiently replicates the virus. *Journal of virology* 80, 2832-2841.

Roy, B.B., Hu, J., Guo, X., Russell, R.S., Guo, F., Kleiman, L., Liang, C., 2006. Association of RNA helicase a with human immunodeficiency virus type 1 particles. *The Journal of biological chemistry* 281, 12625-12635.

Sabile, A., Perlemuter, G., Bono, F., Kohara, K., Demaugre, F., Kohara, M., Matsuura, Y., Miyamura, T., Brechot, C., Barba, G., 1999. Hepatitis C virus core protein binds to apolipoprotein AII and its secretion is modulated by fibrates. *Hepatology* 30, 1064-1076.

Sampath, A., Padmanabhan, R., 2009. Molecular targets for flavivirus drug discovery. *Antiviral research* 81, 6-15.

Samsa, M.M., Mondotte, J.A., Iglesias, N.G., Assuncao-Miranda, I., Barbosa-Lima, G., Da Poian, A.T., Bozza, P.T., Gamarnik, A.V., 2009. Dengue virus capsid protein usurps lipid droplets for viral particle formation. *PLoS pathogens* 5, e1000632.

Samuel, M.A., Diamond, M.S., 2005. Alpha/beta interferon protects against lethal West Nile virus infection by restricting cellular tropism and enhancing neuronal survival. *Journal of virology* 79, 13350-13361.

Samuel, M.A., Diamond, M.S., 2006. Pathogenesis of West Nile Virus infection: a balance between virulence, innate and adaptive immunity, and viral evasion. *Journal of virology* 80, 9349-9360.

Samuel, M.A., Morrey, J.D., Diamond, M.S., 2007a. Caspase 3-dependent cell death of neurons contributes to the pathogenesis of West Nile virus encephalitis. *Journal of virology* 81, 2614-2623.

Samuel, M.A., Wang, H., Siddharthan, V., Morrey, J.D., Diamond, M.S., 2007b. Axonal transport mediates West Nile virus entry into the central nervous system and induces acute flaccid paralysis. *Proceedings of the National Academy of Sciences of the United States of America* 104, 17140-17145.

Samuel, M.A., Whitby, K., Keller, B.C., Marri, A., Barchet, W., Williams, B.R., Silverman, R.H., Gale, M., Jr., Diamond, M.S., 2006. PKR and RNase L contribute to protection against lethal West Nile Virus infection by controlling early viral spread in the periphery and replication in neurons. *Journal of virology* 80, 7009-7019.

Sangiambut, S., Keelapang, P., Aaskov, J., Puttikhunt, C., Kasinrerk, W., Malasit, P., Sittisombut, N., 2008. Multiple regions in dengue virus capsid protein contribute to nuclear localization during virus infection. *The Journal of general virology* 89, 1254-

1264.

Santolini, E., Migliaccio, G., La Monica, N., 1994. Biosynthesis and biochemical properties of the hepatitis C virus core protein. *Journal of virology* 68, 3631-3641.

Savage, H.M., Ceianu, C., Nicolescu, G., Karabatsos, N., Lanciotti, R., Vladimirescu, A., Laiv, L., Ungureanu, A., Romanca, C., Tsai, T.F., 1999. Entomologic and avian investigations of an epidemic of West Nile fever in Romania in 1996, with serologic and molecular characterization of a virus isolate from mosquitoes. *The American journal of tropical medicine and hygiene* 61, 600-611.

Scheel, J., Matteoni, R., Ludwig, T., Hoflack, B., Kreis, T.E., 1990. Microtubule depolymerization inhibits transport of cathepsin D from the Golgi apparatus to lysosomes. *Journal of cell science* 96 (Pt 4), 711-720.

Scheller, N., Mina, L.B., Galao, R.P., Chari, A., Gimenez-Barcons, M., Noueir, A., Fischer, U., Meyerhans, A., Diez, J., 2009. Translation and replication of hepatitis C virus genomic RNA depends on ancient cellular proteins that control mRNA fates. *Proceedings of the National Academy of Sciences of the United States of America* 106, 13517-13522.

Scherbik, S.V., Brinton, M.A., 2010. Virus-induced Ca²⁺ influx extends survival of west nile virus-infected cells. *Journal of virology* 84, 8721-8731.

Schmid, S.R., Linder, P., 1992. D-E-A-D protein family of putative RNA helicases. *Mol Microbiol* 6, 283-291.

Schoggins, J.W., Wilson, S.J., Panis, M., Murphy, M.Y., Jones, C.T., Bieniasz, P., Rice, C.M., 2011. A diverse range of gene products are effectors of the type I interferon antiviral response. *Nature* 472, 481-485.

Schwer, B., Ren, S., Pietschmann, T., Kartenbeck, J., Kaehlcke, K., Bartenschlager, R., Yen, T.S., Ott, M., 2004. Targeting of hepatitis C virus core protein to mitochondria through a novel C-terminal localization motif. *Journal of virology* 78, 7958-7968.

Shen, L., Weber, C.R., Raleigh, D.R., Yu, D., Turner, J.R., 2011. Tight junction pore and leak pathways: a dynamic duo. *Annual review of physiology* 73, 283-309.

Shi, P.-Y., 2012. *Molecular virology and control of flaviviruses*. Caister Academic Press, Norfolk, UK.

Shi, P.Y., Brinton, M.A., Veal, J.M., Zhong, Y.Y., Wilson, W.D., 1996. Evidence for the existence of a pseudoknot structure at the 3' terminus of the flavivirus genomic RNA. *Biochemistry* 35, 4222-4230.

Shi, S.T., Polyak, S.J., Tu, H., Taylor, D.R., Gretch, D.R., Lai, M.M., 2002. Hepatitis C virus NS5A colocalizes with the core protein on lipid droplets and interacts with apolipoproteins. *Virology* 292, 198-210.

Singleton, M.R., Dillingham, M.S., Wigley, D.B., 2007. Structure and mechanism of helicases and nucleic acid translocases. *Annual review of biochemistry* 76, 23-50.

Sips, G.J., Wilschut, J., Smit, J.M., 2011. Neuroinvasive flavivirus infections. *Rev Med Virol*.

Sips, G.J., Wilschut, J., Smit, J.M., 2012. Neuroinvasive flavivirus infections. *Reviews in medical virology* 22, 69-87.

Sitati, E., McCandless, E.E., Klein, R.S., Diamond, M.S., 2007. CD40-CD40 ligand interactions promote trafficking of CD8⁺ T cells into the brain and protection against West Nile virus encephalitis. *Journal of virology* 81, 9801-9811.

Smith, J.L., Grey, F.E., Uhrlaub, J.L., Nikolich-Zugich, J., Hirsch, A.J., 2012. Induction of the cellular microRNA, Hs_154, by West Nile virus contributes to virus-mediated apoptosis through repression of antiapoptotic factors. *Journal of virology* 86, 5278-5287.

Speight, G., Coia, G., Parker, M.D., Westaway, E.G., 1988. Gene mapping and positive identification of the non-structural proteins NS2A, NS2B, NS3, NS4B and NS5 of the flavivirus Kunjin and their cleavage sites. *The Journal of general virology* 69 (Pt 1), 23-34.

Stadler, K., Allison, S.L., Schalich, J., Heinz, F.X., 1997. Proteolytic activation of tick-borne encephalitis virus by furin. *Journal of virology* 71, 8475-8481.

Stankiewicz-Drogon, A., Dorner, B., Erker, T., Boguszevska-Chachulska, A.M., 2010. Synthesis of new acridone derivatives, inhibitors of NS3 helicase, which efficiently and specifically inhibit subgenomic HCV replication. *J Med Chem* 53, 3117-3126.

Stocks, C.E., Lobigs, M., 1998. Signal peptidase cleavage at the flavivirus C-prM junction: dependence on the viral NS2B-3 protease for efficient processing requires determinants in C, the signal peptide, and prM. *Journal of virology* 72, 2141-2149.

Sun, C., Payer, C.T., Luo, G., Sarnow, P., Cate, J.H., 2010. Hepatitis C virus core-derived peptides inhibit genotype 1b viral genome replication via interaction with DDX3X. *PLoS one* 5.

Tadano, M., Makino, Y., Fukunaga, T., Okuno, Y., Fukai, K., 1989. Detection of dengue 4 virus core protein in the nucleus. I. A monoclonal antibody to dengue 4 virus reacts with the antigen in the nucleus and cytoplasm. *The Journal of general virology* 70 (Pt 6), 1409-1415.

Takahashi, S., Iwamoto, N., Sasaki, H., Ohashi, M., Oda, Y., Tsukita, S., Furuse, M., 2009. The E3 ubiquitin ligase LNX1p80 promotes the removal of claudins from tight junctions in MDCK cells. *Journal of cell science* 122, 985-994.

Targett-Adams, P., Hope, G., Boulant, S., McLauchlan, J., 2008. Maturation of hepatitis C virus core protein by signal peptide peptidase is required for virus production. *The Journal of biological chemistry* 283, 16850-16859.

Teoh, K.T., Siu, Y.L., Chan, W.L., Schluter, M.A., Liu, C.J., Peiris, J.S., Bruzzone, R., Margolis, B., Nal, B., 2010. The SARS coronavirus E protein interacts with PALS1 and alters tight junction formation and epithelial morphogenesis. *Molecular biology of the cell* 21, 3838-3852.

TerBush, D.R., Maurice, T., Roth, D., Novick, P., 1996. The Exocyst is a multiprotein complex required for exocytosis in *Saccharomyces cerevisiae*. *The EMBO journal* 15, 6483-6494.

Tetsuka, T., Uranishi, H., Sanda, T., Asamitsu, K., Yang, J.P., Wong-Staal, F., Okamoto, T., 2004. RNA helicase A interacts with nuclear factor kappaB p65 and functions as a transcriptional coactivator. *European journal of biochemistry / FEBS* 271, 3741-3751.

Tsai, T.F., Popovici, F., Cernescu, C., Campbell, G.L., Nedelcu, N.I., 1998. West Nile encephalitis epidemic in southeastern Romania. *Lancet* 352, 767-771.

Tsuda, Y., Mori, Y., Abe, T., Yamashita, T., Okamoto, T., Ichimura, T., Moriishi, K., Matsuura, Y., 2006. Nucleolar protein B23 interacts with Japanese encephalitis virus core protein and participates in viral replication. *Microbiology and immunology* 50, 225-234.

Tsutsumi, T., Suzuki, T., Shimoike, T., Suzuki, R., Moriya, K., Shintani, Y., Fujie, H., Matsuura, Y., Koike, K., Miyamura, T., 2002. Interaction of hepatitis C virus core protein with retinoid X receptor alpha modulates its transcriptional activity. *Hepatology* 35, 937-946.

Turell, M.J., Bunning, M., Ludwig, G.V., Ortman, B., Chang, J., Speaker, T., Spielman, A., McLean, R., Komar, N., Gates, R., McNamara, T., Creekmore, T., Farley, L., Mitchell, C.J., 2003. DNA vaccine for West Nile virus infection in fish crows (*Corvus ossifragus*). *Emerging infectious diseases* 9, 1077-1081.

Turtle, L., Griffiths, M.J., Solomon, T., 2012. Encephalitis caused by flaviviruses. *QJM : monthly journal of the Association of Physicians* 105, 219-223.

Urbanowski, M.D., Hobman, T.C., 2013. The West Nile virus capsid protein blocks apoptosis through a phosphatidylinositol 3-kinase-dependent mechanism. *Journal of virology* 87, 872-881.

Urbanowski, M.D., Ilkow, C.S., Hobman, T.C., 2008. Modulation of signaling pathways by RNA virus capsid proteins. *Cellular signalling* 20, 1227-1236.

van Marle, G., Antony, J., Ostermann, H., Dunham, C., Hunt, T., Halliday, W., Maingat, F., Urbanowski, M.D., Hobman, T., Peeling, J., Power, C., 2007. West Nile virus-induced neuroinflammation: glial infection and capsid protein-mediated neurovirulence. *Journal of virology* 81, 10933-10949.

Verma, S., Kumar, M., Gurjav, U., Lum, S., Nerurkar, V.R., 2010. Reversal of West Nile virus-induced blood-brain barrier disruption and tight junction proteins degradation by matrix metalloproteinases inhibitor. *Virology* 397, 130-138.

Verma, S., Lo, Y., Chapagain, M., Lum, S., Kumar, M., Gurjav, U., Luo, H., Nakatsuka, A., Nerurkar, V.R., 2009. West Nile virus infection modulates human brain microvascular endothelial cells tight junction proteins and cell adhesion molecules: Transmigration across the in vitro blood-brain barrier. *Virology* 385, 425-433.

Wahl-Jensen, V.M., Afanasieva, T.A., Seebach, J., Stroher, U., Feldmann, H., Schnittler,

- H.J., 2005. Effects of Ebola virus glycoproteins on endothelial cell activation and barrier function. *Journal of virology* 79, 10442-10450.
- Wakita, T., Pietschmann, T., Kato, T., Date, T., Miyamoto, M., Zhao, Z., Murthy, K., Habermann, A., Krausslich, H.G., Mizokami, M., Bartenschlager, R., Liang, T.J., 2005. Production of infectious hepatitis C virus in tissue culture from a cloned viral genome. *Nature medicine* 11, 791-796.
- Wang, H., Kim, S., Ryu, W.S., 2009. DDX3 DEAD-Box RNA helicase inhibits hepatitis B virus reverse transcription by incorporation into nucleocapsids. *Journal of virology* 83, 5815-5824.
- Wang, P., Dai, J., Bai, F., Kong, K.F., Wong, S.J., Montgomery, R.R., Madri, J.A., Fikrig, E., 2008a. Matrix metalloproteinase 9 facilitates West Nile virus entry into the brain. *Journal of virology* 82, 8978-8985.
- Wang, S., Welte, T., McGargill, M., Town, T., Thompson, J., Anderson, J.F., Flavell, R.A., Fikrig, E., Hedrick, S.M., Wang, T., 2008b. Drak2 contributes to West Nile virus entry into the brain and lethal encephalitis. *J Immunol* 181, 2084-2091.
- Wang, S.H., Syu, W.J., Huang, K.J., Lei, H.Y., Yao, C.W., King, C.C., Hu, S.T., 2002. Intracellular localization and determination of a nuclear localization signal of the core protein of dengue virus. *The Journal of general virology* 83, 3093-3102.
- Wang, T., Town, T., Alexopoulou, L., Anderson, J.F., Fikrig, E., Flavell, R.A., 2004. Toll-like receptor 3 mediates West Nile virus entry into the brain causing lethal encephalitis. *Nature medicine* 10, 1366-1373.
- Ward, A.M., Bidet, K., Yinglin, A., Ler, S.G., Hogue, K., Blackstock, W., Gunaratne, J., Garcia-Blanco, M.A., 2011. Quantitative mass spectrometry of DENV-2 RNA-interacting proteins reveals that the DEAD-box RNA helicase DDX6 binds the DB1 and DB2 3' UTR structures. *RNA biology* 8, 1173-1186.
- Watashi, K., Hijikata, M., Tagawa, A., Doi, T., Marusawa, H., Shimotohno, K., 2003. Modulation of retinoid signaling by a cytoplasmic viral protein via sequestration of Sp110b, a potent transcriptional corepressor of retinoic acid receptor, from the nucleus. *Molecular and cellular biology* 23, 7498-7509.
- Wengler, G., Wengler, G., 1991. The carboxy-terminal part of the NS 3 protein of the West Nile flavivirus can be isolated as a soluble protein after proteolytic cleavage and represents an RNA-stimulated NTPase. *Virology* 184, 707-715.
- Westaway, E.G., Khromykh, A.A., Kenney, M.T., Mackenzie, J.M., Jones, M.K., 1997a. Proteins C and NS4B of the flavivirus Kunjin translocate independently into the nucleus. *Virology* 234, 31-41.
- Westaway, E.G., Khromykh, A.A., Mackenzie, J.M., 1999. Nascent flavivirus RNA colocalized in situ with double-stranded RNA in stable replication complexes. *Virology* 258, 108-117.
- Westaway, E.G., Mackenzie, J.M., Kenney, M.T., Jones, M.K., Khromykh, A.A., 1997b.

Ultrastructure of Kunjin virus-infected cells: colocalization of NS1 and NS3 with double-stranded RNA, and of NS2B with NS3, in virus-induced membrane structures. *Journal of virology* 71, 6650-6661.

Westaway, E.G., Mackenzie, J.M., Khromykh, A.A., 2002. Replication and gene function in Kunjin virus. *Current topics in microbiology and immunology* 267, 323-351.

Weston, A., Sommerville, J., 2006. Xp54 and related (DDX6-like) RNA helicases: roles in messenger RNP assembly, translation regulation and RNA degradation. *Nucleic acids research* 34, 3082-3094.

Wilder-Smith, A., Schwartz, E., 2005. Dengue in travelers. *The New England journal of medicine* 353, 924-932.

Wong, M.L., Medrano, J.F., 2005. Real-time PCR for mRNA quantitation. *BioTechniques* 39, 75-85.

Xu, L., Khadijah, S., Fang, S., Wang, L., Tay, F.P., Liu, D.X., 2010. The cellular RNA helicase DDX1 interacts with coronavirus nonstructural protein 14 and enhances viral replication. *Journal of virology* 84, 8571-8583.

Xu, Z., Anderson, R., Hobman, T.C., 2011. The capsid-binding nucleolar helicase DDX56 is important for infectivity of West Nile virus. *Journal of virology* 85, 5571-5580.

Xu, Z., Hobman, T.C., 2012. The helicase activity of DDX56 is required for its role in assembly of infectious West Nile virus particles. *Virology* 433, 226-235.

Yamshchikov, V.F., Compans, R.W., 1993. Regulation of the late events in flavivirus protein processing and maturation. *Virology* 192, 38-51.

Yang, C.M., Lin, C.C., Lee, I.T., Lin, Y.H., Yang, C.M., Chen, W.J., Jou, M.J., Hsiao, L.D., 2012. Japanese encephalitis virus induces matrix metalloproteinase-9 expression via a ROS/c-Src/PDGFR/PI3K/Akt/MAPKs-dependent AP-1 pathway in rat brain astrocytes. *Journal of neuroinflammation* 9, 12.

Yang, J.S., Ramanathan, M.P., Muthumani, K., Choo, A.Y., Jin, S.H., Yu, Q.C., Hwang, D.S., Choo, D.K., Lee, M.D., Dang, K., Tang, W., Kim, J.J., Weiner, D.B., 2002. Induction of inflammation by West Nile virus capsid through the caspase-9 apoptotic pathway. *Emerging infectious diseases* 8, 1379-1384.

Yang, M.R., Lee, S.R., Oh, W., Lee, E.W., Yeh, J.Y., Nah, J.J., Joo, Y.S., Shin, J., Lee, H.W., Pyo, S., Song, J., 2008. West Nile virus capsid protein induces p53-mediated apoptosis via the sequestration of HDM2 to the nucleolus. *Cellular microbiology* 10, 165-176.

Yang, X., Khosravi-Far, R., Chang, H.Y., Baltimore, D., 1997. Daxx, a novel Fas-binding protein that activates JNK and apoptosis. *Cell* 89, 1067-1076.

Yasuda-Inoue, M., Kuroki, M., Ariumi, Y., 2013. Distinct DDX DEAD-box RNA helicases cooperate to modulate the HIV-1 Rev function. *Biochemical and biophysical*

research communications 434, 803-808.

Yasui, K., Wakita, T., Tsukiyama-Kohara, K., Funahashi, S.I., Ichikawa, M., Kajita, T., Moradpour, D., Wands, J.R., Kohara, M., 1998. The native form and maturation process of hepatitis C virus core protein. *Journal of virology* 72, 6048-6055.

Yeaman, C., Grindstaff, K.K., Wright, J.R., Nelson, W.J., 2001. Sec6/8 complexes on trans-Golgi network and plasma membrane regulate late stages of exocytosis in mammalian cells. *The Journal of cell biology* 155, 593-604.

Yedavalli, V.S., Neuveut, C., Chi, Y.H., Kleiman, L., Jeang, K.T., 2004. Requirement of DDX3 DEAD box RNA helicase for HIV-1 Rev-RRE export function. *Cell* 119, 381-392.

Yedavalli, V.S., Zhang, N., Cai, H., Zhang, P., Starost, M.F., Hosmane, R.S., Jeang, K.T., 2008. Ring expanded nucleoside analogues inhibit RNA helicase and intracellular human immunodeficiency virus type 1 replication. *Journal of medicinal chemistry* 51, 5043-5051.

Yoshida, T., Hanada, T., Tokuhisa, T., Kosai, K., Sata, M., Kohara, M., Yoshimura, A., 2002. Activation of STAT3 by the hepatitis C virus core protein leads to cellular transformation. *The Journal of experimental medicine* 196, 641-653.

You, L.R., Chen, C.M., Lee, Y.H.W., 1999a. Hepatitis C virus core protein enhances NF-kappaB signal pathway triggering by lymphotoxin-beta receptor ligand and tumor necrosis factor alpha. *J Virol* 73, 1672-1681.

You, L.R., Chen, C.M., Yeh, T.S., Tsai, T.Y., Mai, R.T., Lin, C.H., Lee, Y.H., 1999b. Hepatitis C virus core protein interacts with cellular putative RNA helicase. *Journal of virology* 73, 2841-2853.

Yu, S.F., Lujan, P., Jackson, D.L., Emerman, M., Linial, M.L., 2011. The DEAD-box RNA helicase DDX6 is required for efficient encapsidation of a retroviral genome. *PLoS pathogens* 7, e1002303.

Zeller, H.G., Schuffenecker, I., 2004. West Nile virus: an overview of its spread in Europe and the Mediterranean basin in contrast to its spread in the Americas. *European journal of clinical microbiology & infectious diseases* : official publication of the European Society of Clinical Microbiology 23, 147-156.

Zhang, W., Chipman, P.R., Corver, J., Johnson, P.R., Zhang, Y., Mukhopadhyay, S., Baker, T.S., Strauss, J.H., Rossmann, M.G., Kuhn, R.J., 2003a. Visualization of membrane protein domains by cryo-electron microscopy of dengue virus. *Nature structural biology* 10, 907-912.

Zhang, X., Orlando, K., He, B., Xi, F., Zhang, J., Zajac, A., Guo, W., 2008. Membrane association and functional regulation of Sec3 by phospholipids and Cdc42. *The Journal of cell biology* 180, 145-158.

Zhang, Y., Corver, J., Chipman, P.R., Zhang, W., Pletnev, S.V., Sedlak, D., Baker, T.S., Strauss, J.H., Kuhn, R.J., Rossmann, M.G., 2003b. Structures of immature flavivirus

particles. *The EMBO journal* 22, 2604-2613.

Zhang, Y., Zhang, W., Ogata, S., Clements, D., Strauss, J.H., Baker, T.S., Kuhn, R.J., Rossmann, M.G., 2004. Conformational changes of the flavivirus E glycoprotein. *Structure* 12, 1607-1618.

Zhong, J., Gastaminza, P., Cheng, G., Kapadia, S., Kato, T., Burton, D.R., Wieland, S.F., Uprichard, S.L., Wakita, T., Chisari, F.V., 2005. Robust hepatitis C virus infection in vitro. *Proceedings of the National Academy of Sciences of the United States of America* 102, 9294-9299.

Zhu, N., Ware, C.F., Lai, M.M., 2001. Hepatitis C virus core protein enhances FADD-mediated apoptosis and suppresses TRADD signaling of tumor necrosis factor receptor. *Virology* 283, 178-187.

Zirwes, R.F., Eilbracht, J., Kneissel, S., Schmidt-Zachmann, M.S., 2000. A novel helicase-type protein in the nucleolus: protein NOH61. *Molecular biology of the cell* 11, 1153-1167.